

THE REACTIONS OF ACTIVE NITROGEN
WITH MOLECULAR OXYGEN, ATOMIC OXYGEN AND HYDROGEN

by

Constantine Mavroyannis

A thesis submitted to the Faculty of Graduate
Studies and Research of McGill University
in partial fulfilment of the requirements
for the degree of Doctor of Philosophy

From the Physical Chemistry Laboratory under
the supervision of Prof. C. A. Winkler

McGill University
Montreal, Canada

July 1961

ACKNOWLEDGEMENTS

The author wishes to express his appreciation

to

the Consolidated Mining and Smelting Company
of Canada Limited for the award of a "Cominco" Fellowship;

to

the National Research Council of Canada
for financial assistance in the form of a Fellowship.

TABLE OF CONTENTS

INTRODUCTION

ACTIVE NITROGEN.....	1
ELECTRICAL PROPERTIES OF ACTIVE NITROGEN.....	3
EXCITATION OF SPECTRA AND ENERGY MEASUREMENTS.....	4
EMISSION SPECTRUM OF THE AFTERGLOW.....	5
THEORIES OF ACTIVE NITROGEN.....	11
The Rayleigh-Sponer Theory.....	11
The Cario-Kaplan Theory.....	14
The Mitra Theory.....	15
The Pre-association Theory of Nitrogen Afterglow....	16
ACTIVE NITROGEN AT LOW TEMPERATURES.....	23
Mechanism of Nitrogen Afterglow in the Solid.....	25
KINETICS OF NITROGEN ATOM RECOMBINATION.....	28
CHEMICAL REACTIVITY OF ACTIVE NITROGEN.....	30
The Reactions with Organic Compounds.....	31
The Reactions with Inorganic Compounds.....	35
Ammonia.....	35
Phosphine.....	37
Hydrogen Halides.....	37
Oxides of Nitrogen.....	39
Molecular Oxygen.....	42
OXYGEN ATOMS.....	44
REACTIONS OF OXYGEN ATOMS.....	47
RECOMBINATION OF OXYGEN ATOMS.....	52

TABLE OF CONTENTS (continued)

THE NITROGEN ATOM-OXYGEN ATOM REACTION.....53
HYDROGEN ATOMS.....55
THE RECOMBINATION OF HYDROGEN ATOMS.....58
SOME REACTIONS OF HYDROGEN ATOMS.....60
NITROGEN ATOM-HYDROGEN ATOM REACTIONS.....63

PART I

THE REACTION OF ACTIVE NITROGEN WITH MOLECULAR OXYGEN.....69
EXPERIMENTAL.....70
 Materials.....70
 Apparatus.....71
 Procedure for a Typical Experiment.....74
 Analysis.....75
RESULTS.....78
DISCUSSION.....109
 Approximate Calculation of the Pre-exponential
 Factor for the Reaction of Atomic Nitrogen with
 Molecular Oxygen.....113

PART II

THE REACTION OF NITROGEN ATOMS WITH OXYGEN ATOMS IN
THE ABSENCE OF OXYGEN MOLECULES AND THE HOMOGENEOUS
AND HETEROGENEOUS RECOMBINATION OF NITROGEN ATOMS.....123
EXPERIMENTAL.....124
 Materials.....124
 Procedure.....124

TABLE OF CONTENTS (continued)

RESULTS AND DISCUSSION.....127

 The Decay Processes of Nitrogen Atoms.....127

 The Reaction of Nitrogen Atoms with Oxygen Atoms...136

PART III

THE REACTION OF NITROGEN ATOMS WITH HYDROGEN ATOMS.....144

 EXPERIMENTAL.....145

 Materials.....145

 Procedure.....145

 RESULTS AND DISCUSSION.....148

 The Reaction of Hydrogen Atoms with
 Hydrogen Bromide.....148

 The Reaction of Active Nitrogen with
 Molecular Hydrogen.....153

 The Reaction of Nitrogen Atoms with
 Hydrogen Atoms.....154

 COMPARISON WITH THEORY OF ASSOCIATION REACTIONS.....166

 Collision Model.....166

 Wigner's Theory.....169

SUMMARY AND CONTRIBUTIONS TO KNOWLEDGE.....173

BIBLIOGRAPHY.....176

LIST OF FIGURES

Figure 1.	Electronic Levels of the Nitrogen Molecule.....	7
2.	Apparent Distribution of Molecules in the different Vibrational Levels of the $B^3\Pi_g$ State.....	8
3.	Summary of N---N Interactions.....	18
4.	Potential Energy Curves of the Nitrogen Molecule.....	20
5.	Morse Potential Energy Curves for the Nitrogen Molecule indicating the different Group Bands observed in the Afterglow Spectrum.....	24
6.	Potential Energy Curves of the Observed States of the O_2 Molecule.....	48
7.	Energy Level Diagram of the O_2 Molecule.....	49
8.	Molecular Orbitals for O_2 , showing the Triplet Nature of the Ground State.....	50
9.	Energy Level Diagram of NO.....	56
10.	Potential Energy Curves of the two Lowest States of the H_2 Molecule.....	59
11.	Potential Energy Curves of the Observed Electronic States of NH.....	68
12.	Diagram of Apparatus.....	72
13.	Plot of Ozone produced <u>vs</u> Oxygen Flow Rate.....	82
14.	Plot of Maximum Yield of HCN <u>vs</u> Ethylene Flow Rate.....	85
15.	Plot of Maximum Yield of HCN and Oxygen Atoms from the Reactions of Active	

LIST OF FIGURES (continued)

Nitrogen with Ethylene and Oxygen,
respectively, vs Total Pressure.....88

16. Arrhenius Plot of $\text{Log } k_1$ vs $1/T$107

17. Plot of $\text{Log } k_1$ vs $(\frac{1}{2} \log T - E/2.3 RT)$108

18. Plot of k_{13} , calculated from equation
[1], vs Total Pressure.....133

19. Plot of $1/(N)(M)$ vs Reaction Time at a
Total Pressure of 2.5 mm.....134

20. Plot of the Average Slopes (sec^{-1}) vs
 $(M) \times 10^7$ (mole cc^{-1}).....135

21. Plot of HBr Consumed vs Flow Rate.....152

THE REACTIONS OF ACTIVE NITROGEN
WITH MOLECULAR OXYGEN, ATOMIC OXYGEN AND HYDROGEN

ABSTRACT

For the reaction of nitrogen atoms with molecular oxygen, the nitrogen and oxygen atom concentrations were estimated, at different temperatures and pressures, by addition of excess NO_2 and measurement of N_2O and NO produced. The rate constant was given by $2.3 \times 10^{12} \exp(-5,900/RT)$ $\text{cc mole}^{-1} \text{sec}^{-1}$. The maximum production of oxygen atoms was found to correspond to the maximum amount of HCN produced in the active nitrogen-ethylene reaction.

A rate constant of $1.83(^{+} 0.2) \times 10^{15} \text{cc}^2 \text{mole}^{-2} \text{sec}^{-1}$ was determined for the reaction of nitrogen atoms with oxygen atoms, in the absence of molecular oxygen, at pressures of 3, 3.5 and 4 mm, in an unheated reaction tube. The nitrogen atom consumption was estimated by titrating active nitrogen with NO at different positions along the reaction tube. Using the same titration method, the rate constant for the decay of nitrogen atoms, in an unheated vessel, was found to have the value of $5.2 \times 10^{15} \text{cc}^2 \text{mole}^{-2} \text{sec}^{-1}$, with $\gamma = 7.5 (^{+} 0.6) \times 10^{-5}$, in the pressure range from 0.5 to 4 mm.

Under similar conditions, and by similar methods, a value of $4.87(^{+} 0.8) \times 10^{14} \text{cc}^2 \text{mole}^{-2} \text{sec}^{-1}$ was obtained for the rate constant of the reaction between nitrogen atoms and hydrogen atoms, over the pressure range from 2.5 mm to 4.5 mm.

INTRODUCTION

ACTIVE NITROGEN

When nitrogen is subjected to a condensed or high frequency electrodeless electric discharge, a bright golden-yellow glow is produced which persists for a considerable time after the exciting voltage has been cut off. This so-called afterglow of nitrogen was first noticed by Warburg (1) and systematically studied by Lewis (2). In 1911 Strutt (3) named the glowing gas "active nitrogen" and suggested that many of its properties could be attributed to the presence of atomic nitrogen. Many workers have since investigated the phenomenon in its various aspects, e.g., duration of the afterglow, its spectrum, its laws of decay, special methods of excitation, energy of the glowing gas, etc.

Several theories have been put forward, in which excited atoms and molecules, and even ions, have been invoked to explain the afterglow, but recent applications of modern experimental techniques have shown that the main reactive component in active nitrogen is the nitrogen atom in the ground state. A summary of experimental work up to 1945 is given in a short book by Mitra (4), and two recent reviews by Jennings and Linnett (5), and Edwards (6), outline the results of recent studies, with many of references to the original literature on the subject.

Active nitrogen can be produced by a condensed electrode discharge or by a high frequency electrodeless discharge. Kently and Turner (7) produced active nitrogen by bombarding the gas with electrons of energy greater than 16.3 ev, and Stanley (8) used an arc discharge to produce active nitrogen at pressures as high as 20 cm Hg.

Lewis (9) found that absolutely pure nitrogen in a baked-out vessel appeared not to give the afterglow, and this was attributed to the rapid removal of nitrogen atoms from the gas by recombination at the walls. Strutt (10) showed that small admixtures of many foreign gases markedly increased the intensity of the afterglow, although argon, helium and nitrogen itself, were without effect. On the other hand, many impurities, at higher concentrations, inhibited the production of the afterglow, owing to their chemical reaction with active nitrogen.

Herzberg (11) found that a silica discharge vessel, when strongly heated, was changed so that the glow could not be obtained in it. He suggested that a trace of ammonia on the surface might induce favourable conditions for the glow, since he was able to restore it by introducing a trace of hydrogen into the electric discharge. Similarly, Rayleigh (12) found that the glow could be enhanced by coating the vessel wall with sulphuric or metaphosphoric acid. He made the now classical observation that, in a large vessel, poison-

ed with metaphosphoric acid, the glow of active nitrogen remained visible for some six hours in a darkened room.

ELECTRICAL PROPERTIES OF ACTIVE NITROGEN

If the stream of glowing gas from the discharge tube is passed between two auxiliary electrodes, it is found that the gas has a high electrical conductivity. Constantinides (13) found that, by increasing the applied voltage, a saturation current was obtained, of a magnitude proportional to the area of the negative electrode. He concluded that electrons were emitted from the cathode as a result of atomic or molecular bombardment.

Rayleigh (14) studied the rates of decay of both the ionization and the afterglow, using electrodes of metaphosphoric acid smeared on glass, and found that the saturation current decreased, rather than increased, and suggested that positive ions in the gas phase were responsible for the conductivity.

Benson (15) has made measurements of the electron density in active nitrogen, using microwaves in a resonant cavity. He found that the charged particles were electrons, at a concentration less than 10^{-6} of the concentration of the chemically active species in active nitrogen, and that the glowing stream of active nitrogen showed no response to magnetic fields transverse to the stream. He also pointed

out that the removal of ions from active nitrogen had no effect on the intensity or spectral distribution of the afterglow. Several workers have shown that, if the glowing gas is passed through an ion trap, the glow is not affected, and it seems improbable, therefore, that charged particles play any part in the production of the afterglow.

EXCITATION OF SPECTRA AND ENERGY MEASUREMENTS

When substances are introduced into the stream of active nitrogen, a luminous zone is often observed at the point of mixing. The spectra excited in these flames are either those of the unchanged substance, or those of radicals or molecules formed by chemical reaction. Summaries of the many systems investigated are given by Strutt (3), Strutt and Fowler (16) and Willey and Rideal (17). Metallic vapours usually give rise to spectra consisting of atomic lines of the metal, accompanied by the formation of the nitride.

Knauss (18) attempted to determine the amount of energy available for the excitation of spectra, by looking for emission spectra between 1000 and 2500 Å when H₂, O₂, CO and NO were mixed with active nitrogen in a flow system. In addition to the β and γ bands of NO, characteristic of the afterglow when NO is present, he found a new system corresponding to 6.4 eV excitation above the ground state.

Rayleigh (19) observed the temperature rise when

active nitrogen was destroyed on a copper oxide probe, and compared it with the temperature rise recorded when the active nitrogen was made to react with nitric oxide before it reached the probe. He concluded that active nitrogen did not contain an abnormally high amount of energy. From the temperature attained by a metal foil exposed to active nitrogen, Rayleigh calculated (20) that the energy available in active nitrogen might be as high as 12.9 ev/mole of total nitrogen. However, Benson (15) found that much of this heating effect was due to electron bombardment from the discharge.

Jackson and Broadway (21) applied the Stern-Gerlach method to a study of active nitrogen. They observed deflection of a narrow beam of active nitrogen when it was passed through an inhomogeneous magnetic field to measure the magnetic moment of the active particles. They suggested that excited atoms in the $^2P_{\frac{1}{2}}$ state were responsible for the deflection, but Herbert et al. (22) found no absorption in the region of 1400-1800 Å, in which both 2P and 2D atoms would absorb, and suggested that any atoms present were in the ground state.

EMISSION SPECTRUM OF THE AFTERGLOW

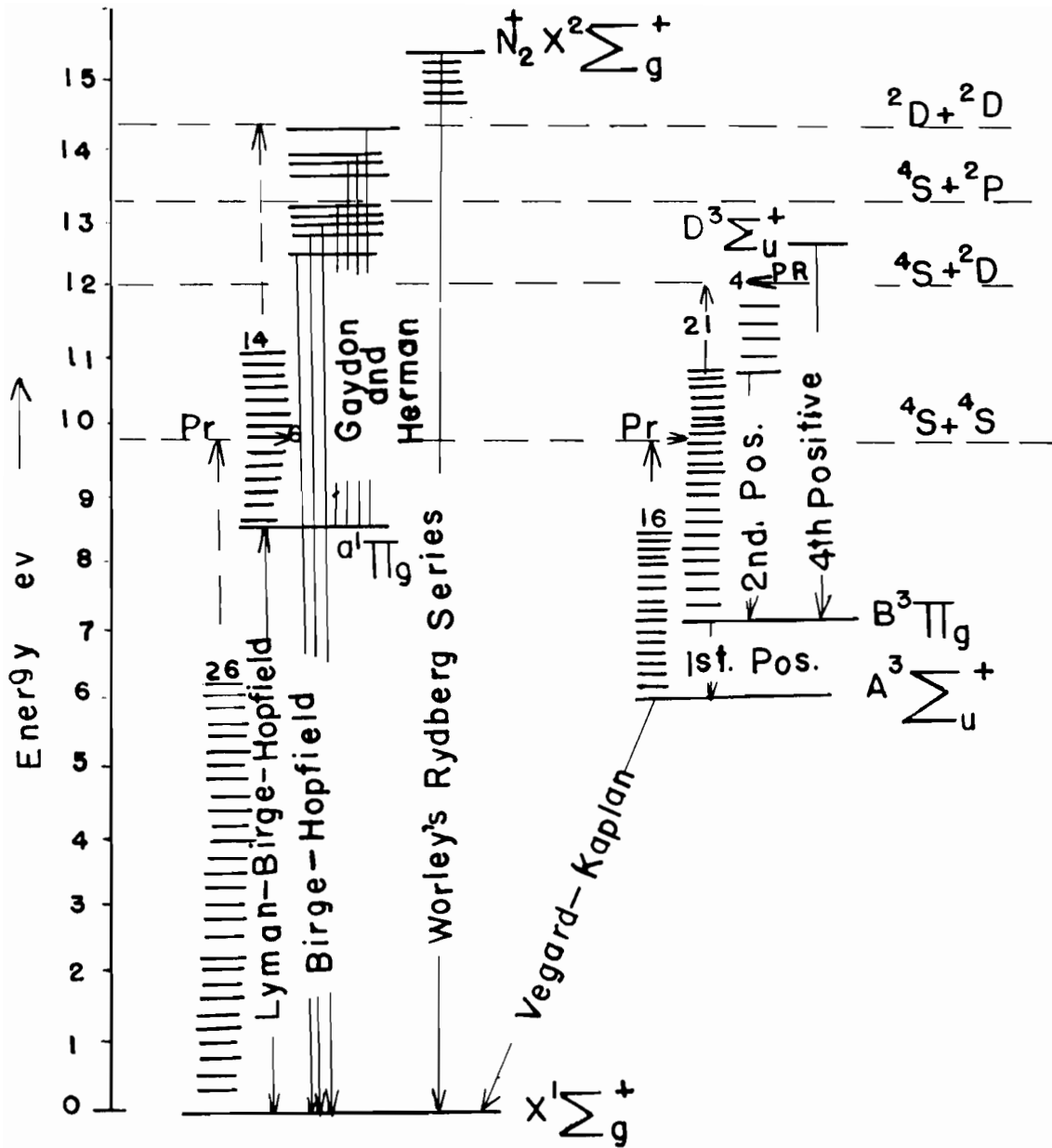
In the discharge region, the glow of the discharged nitrogen is pink and is found to emit strongly the N_2 first positive ($B^3\Pi_g \rightarrow A^3\Sigma_u^+$), N_2 second positive ($C^3\Pi_u \rightarrow B^3\Pi_g$) and N_2^+ first negative ($B^2\Sigma_u^- \rightarrow X^2\Sigma_g^+$) bands. After the discharged region, the glow appears yellow, and emits only the

N_2 first positive ($B^3\Pi_g \rightarrow A^3\Sigma_u^+$) band system (23, 24, 25, 26, 27). These bands are due to an allowed transition from a more highly excited state (the $B^3\Pi_g$ state) to a lower excited state (the $A^3\Sigma_u^+$ state) from which the molecules reach the ground state (the $X^1\Sigma_g^+$ state) by losing their excess energy in collisions with other molecules and with the wall of the vessel (Fig. 1). The radiation has a long lifetime (~ 0.1 sec), compared with the radiative lifetime of the $B^3\Pi_g$ state ($\sim 10^{-8}$ sec), and thus requires that the mechanism producing that state be present in the afterglow.

From the intensity distribution of the vibrational bands, the enhanced bands appear to originate mainly in the 12th, 11th and 10th vibrational levels of the $B^3\Pi_g$ state, but bands originating in the 6th, 4th, 3rd and 2nd vibrational levels appear to be enhanced to a smaller extent (25, 27). Rayleigh (23) has shown that an admixture of inert gases shifts the intensity maximum to bands corresponding to lower vibrational levels ($v' = 9$ and 10), while Herzberg (28) has found that cooling the afterglow results in preferentially populating the 12th level.

Kistiakowsky and Warneck (29) suggested that the weaker bands are not members of the first positive system, but form a new system arising from transitions between unknown states of the nitrogen molecule. The position of the 12-11-10 peak (Fig. 2) shifts to lower energies with rising temperature,

Figure 1
Electronic Levels of the Nitrogen Molecule

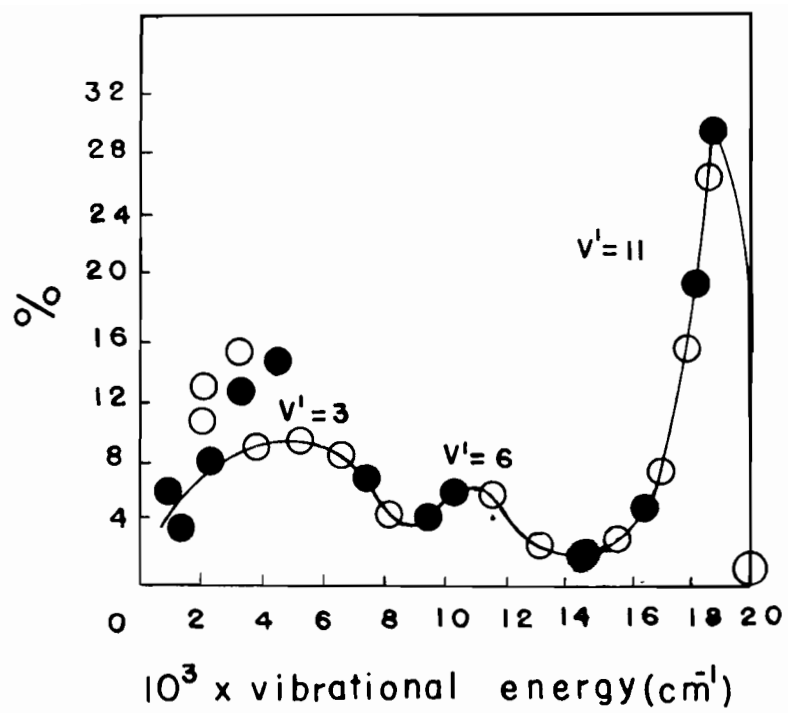


Energy Level Diagram of the N_2 Molecule

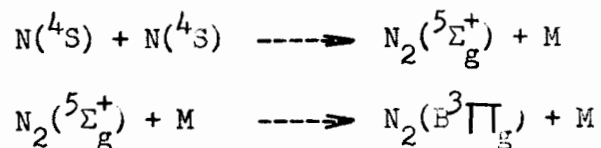
Figure 2

Apparent distribution of molecules in the
different vibrational levels of the $B^3\Pi_g$ state,
as indicated by the intensity distribution
in the afterglow (ref.-29)

● $^{14}_N$ $^{14}_N$
○ $^{15}_N$ $^{15}_N$



or addition of helium, and it becomes broader. Extrapolated to 0° K., its position is found to coincide with the energy of the ${}^5\Sigma_g^+$ state. This is definite proof for a two step mechanism of the afterglow:



The shifting and broadening of the peak indicates that the second step is accompanied by loss of vibrational energy by the nitrogen molecule undergoing the collision induced electronic transition. The lower peaks behave differently; evidence that they are not part of the first positive system is as follows: (a) the population distributions of the two isotopes disagree at lower v' levels to an extent which depends upon the conditions; (b) the ratio of intensities of bands originating in the same v' level varies with conditions; (c) the spectrum includes at least three bands which fit poorly into the first positive system; (d) the isotopic shift observed is inconsistent with that expected from the first positive system assignment. Hence, neither the B nor the A state appears to be involved.

The ratio of the total intensities in the two parts of the population-distribution curve does not vary with pressure, and varies only slightly with temperature. This suggests that the molecules in each of the upper states involved in these

transitions are formed from nitrogen atoms via the $^5\Sigma_g^+$ state, through a collision-induced radiationless transition to a state "Y", in competition with the process leading to the $B^3\Pi_g$ state.

LeBlanc, Tanaka and Jursa (30) have accurately measured frequencies of many band heads in the afterglow spectrum, and they have demonstrated the existence of another band system, for which $B^3\Pi_g$ is the lower state. According to Mulliken's (31, 32) theoretical prediction, there are two electronic states, $^3\Sigma_u^-$ and $^3\Delta_u$, which could account for the upper state of the bands. The data of LeBlanc et al. (30) for the upper state are midway between the data for the $^3\Sigma_u^-$ and $^3\Delta_u$ state predicted by Mulliken, although they favour the interpretation that the upper state is $^3\Delta_u$.

Berkowitz, Chupka and Kistiakowsky (33) showed that the intensity of the afterglow was proportional to the square of the concentration of nitrogen atoms in the ground state. The ratio of the intensity to the square of the atom concentration did not alter when oxygen was added to the system, which indicates that oxygen plays no part in the production of the afterglow. Since the ratio increased when helium or argon was added to the nitrogen, these gases were apparently more efficient than nitrogen as third bodies for the recombination of nitrogen atoms.

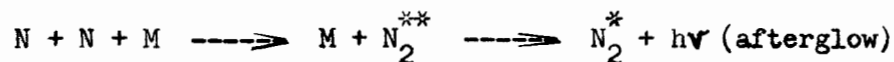
In the spectrum of the afterglow, bands of the Lyman-Hopfield system, due to the transition $\alpha^1\Pi_g \rightarrow X^1\Sigma_g^+$, have been observed (34) weakly in the vacuum ultraviolet region. No bands due to transitions from levels higher than $v' = 6$ are observed.

THEORIES OF ACTIVE NITROGEN

Explanations of the behaviour of active nitrogen have differed depending upon the value assumed for its energy content and for the dissociation energy of the N_2 molecule, both of which have been uncertain until quite recently. In addition, the number and complexity of the excited levels of the N_2 molecule have made a detailed interpretation difficult.

The Rayleigh-Sponer Theory

Rayleigh (3) attributed the chemical reactivity of active nitrogen to nitrogen atoms and Sponer (35) suggested a two-step mechanism for production of the afterglow:

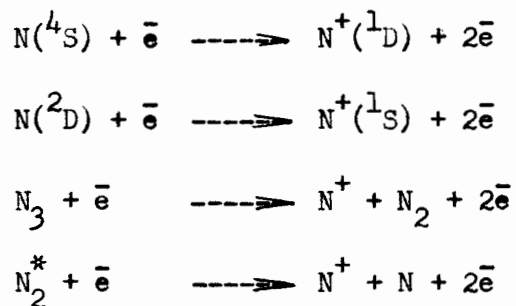


This sufficed to explain the long life of the afterglow, since three-body collisions are rare in the gas phase at low pressures, and it served also explain the kinetics of the decay. Also, on the basis of a dissociation energy for the N_2 molecule of 9.76 ev, as found by Gaydon (36), it was possible to account

for all the observations on the energy content of active nitrogen (except Rayleigh's invalid metal foil experiments). The theory, that active nitrogen contains appreciable quantities of ground state atoms, was supported by measurements with a diffusion gauge (37), and by studies of the vacuum ultra-violet absorption spectrum (22). However, it explains neither the selective enhancement of certain vibrational bands in the spectrum of the afterglow, nor the electrical properties of active nitrogen.

The most direct evidence for the presence of ground-state nitrogen atoms (4S) in the afterglow was recently obtained from mass spectroscopic studies of appearance potentials by Jackson and Schiff (38) and by Berkowitz et al. (33). Jackson and Schiff (38) obtained atom concentrations from 0.1% to 1% for nitrogen dissociated in a Wood's tube. The ionization efficiency curve, for mass 14 in the discharge gas, showed two breaks indicative of three sources of mass 14. Of these, one would be the dissociative ionization of ground state molecular nitrogen, as observed in the absence of the electrical discharge. The appearance potentials observed for the latter two processes were $14.7^{+0.2}$ ev and $16.1^{+0.3}$ ev. Berkowitz et al. (33) obtained a value of 14.8 ev, in agreement with the lower value of Jackson and Schiff, but they did not observe a higher value. Both the 14.7 and 14.8 ev values are within the experimental error of the ionization potential of ground state (4S) atomic nitrogen, i.e., 14.54 ev (39).

The mass 14 appearance potential of 16.1 ev is of interest since it might reflect the presence, in active nitrogen, of some species other than atomic nitrogen. Jackson and Schiff (38) proposed the following mechanism to account for this higher value:



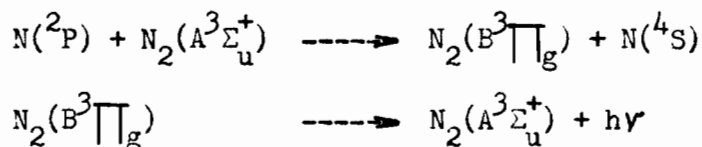
in which N_2^* represents an excited metastable molecule. The failure of Berkowitz et al. (33) to observe the higher value might have been due to an unfavourable sampling arrangement into the mass spectrometer, associated with possible slow removal of products from the ion source. Such a combination could lead to removal of excess energy from the $\text{N}(^2\text{D})$ and N_2^* and to decomposition of N_3 if it were initially present (40). On the other hand, this would not affect the first reaction above, and since Berkowitz et al. (33) obtained no indication of a second species, it seems likely that this reaction probably does not occur, even if it be conceded that a second species is present.

The presence of excited nitrogen atoms in the afterglow has been reported by Tanaka et al. (41), based on obser-

vation of ultra-violet absorption by 2D and 2P nitrogen atoms. The concentration of both $N(^2D)$ and $N(^2P)$ was found to be approximately 500 times less than that of $N(^4S)$.

The Cario-Kaplan Theory

Cario and Kaplan (42) have suggested that active nitrogen is a mixture of metastable atoms and molecules, which produce the afterglow as follows:



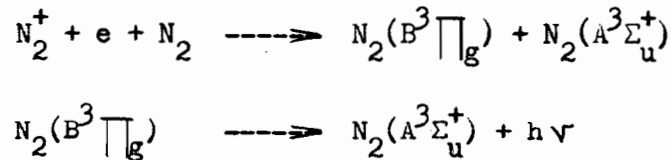
This theory was preferred to the atomic theory at a time when the dissociation energy of N_2 molecule was thought to be 7.37 ev. It gained support from the results of the Stern-Gerlach experiment (21), but not from the vacuum-ultra-violet absorption spectrum (22).

This theory requires that the glowing gas should contain appreciable concentrations of excited atoms in the 2P and 2D states, and excited molecules in the A state. The absence from the afterglow of the Vegard-Kaplan bands, due to the transition $A^3\Sigma_u^+ \text{ -----} X^1\Sigma_g^+$, suggests a very low concentration of molecules in this state (43). The lifetime for radiation of the $A^3\Sigma_u^+$ state of nitrogen was found (44) to be 10^{-3} to 10^{-4} sec. However, Lichten (45) redetermined the lifetime of $A^3\Sigma_u^+$ and $\alpha^1\Pi_g$ states, and concluded that the former

workers had obtained the lifetime of the $\alpha^1 \Pi_g$ state, instead of the A state, and that the true lifetime of the A state molecules is probably greater than 10^{-2} sec. Nevertheless, even this lifetime for these molecules is very short to account for an afterglow which may last for several hours (46). In any case, recent evidence supports the presence of 4S , rather 2P or 2D atoms, in active nitrogen, with a dissociation energy for the N_2 molecule of 9.76 ev (36), and the Cario-Kaplan theory has therefore been abandoned.

The Mitra Theory

Mitra (4) suggested that the activity of active nitrogen was due to a mixture of N_2^+ ions and electrons, and proposed the following scheme for the production of the afterglow:



The reaction $N_2^+ + e$ liberates 15.58 ev while 15.85 ev are required to produce one nitrogen molecule in the $v' = 12$ vibrational level of the B state and one in the $v' = 0$ vibrational level of the A state. Mitra suggests that the energy deficiency of 0.27 ev may be derived from kinetic energy. This theory can explain Rayleigh's fallacious metal-foil experiment (20), since it provides for an energy content of 15.5 ev, and

also the long life of the afterglow, since its production is a three-body collision process and consequently slow.

Gaydon (36) did not accept Mitra's theory, since it was unable to explain why an electric field does not quench the afterglow. He attributed the heating effect on a metal foil to be due to the combined effect of cathode rays and active nitrogen. Later, Benson (15) repeated Rayleigh's metal foil experiments, but placed a grounded aluminum elbow in the gas flow to remove electrons from the discharge, and obtained an energy content only 1/400 of that observed by Rayleigh. He showed that the intensity of the glow was unaffected by the removal of charged particles, and that a beam of glowing gas was not affected by a magnetic field. The concentration of electrons in the afterglow was found to be only 10^9 /cc., compared with a concentration of active particles of about 10^{15} /cc., on the assumption of 9.76 ev as the excitation required to produce the afterglow.

Worley (43) also failed to obtain support for Mitra's theory, when he observed no absorption due to N_2^+ in the visible region of the afterglow spectrum with a path length of 13 m. Mitra subsequently abandoned his earlier suggestion (47).

The Pre-association Theory of the Nitrogen Afterglow

The possible products arising from the collision of two 4S nitrogen atoms must be considered. The ground state of

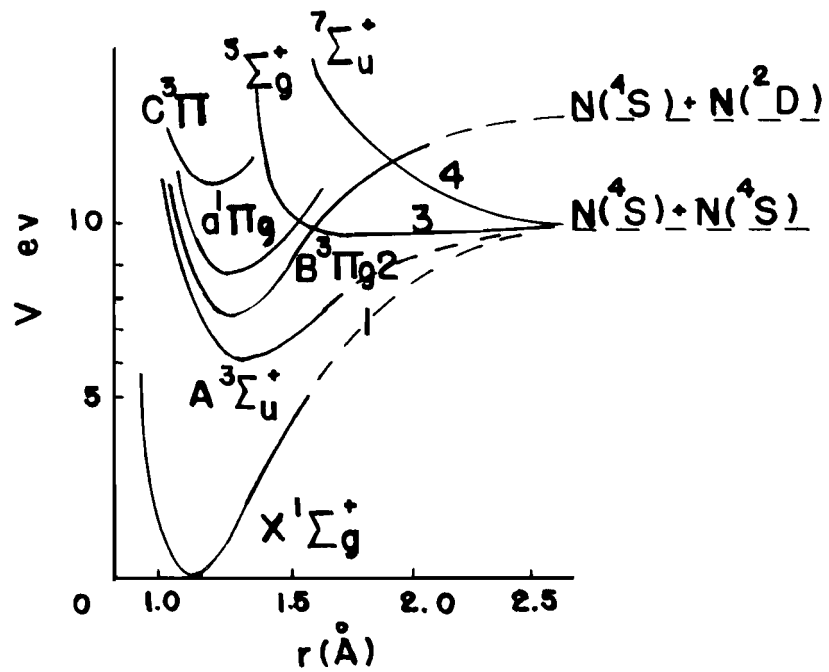
nitrogen atom has the electronic configuration of $1s^2 2s^2 2p_x$
 $2p_y 2p_z$, the three unpaired p electrons having parallel spins.
Two such atoms may approach each other along four different
potential energy curves (48), corresponding to the pairing of
6, 4, 2 and 0 electrons. The possible molecular states correspond-
ing to the four different potential energy curves have the
terms $1_{\Sigma_g^+}$, $3_{\Sigma_u^+}$, $5_{\Sigma_g^+}$ and $7_{\Sigma_u^+}$, and the relative probabilities,
1: 3: 5: 7 (Fig. 3).

The probability of a molecule to lose its excess
energy by radiation is very small. Whichever path the two
atoms follow, they will fly apart again at the end of the
first molecular vibration, unless energy is removed by collision
with a third body. If the atoms follow path 1 or 2 (Fig. 3),
a collision with a third body would remove energy from the
newly-formed N_2 molecules, and stabilize them in the X and
A states. On the other hand, if the atoms follow path 4,
they will fly apart again, even in the presence of a third
body, since no bond is formed between the atoms (the $7_{\Sigma_u^+}$
potential energy curve is strongly repulsive).

The fourth possibility is that the atoms would follow
path 3, and form a very weakly-bound N_2 molecule in the $5_{\Sigma_g^+}$
state. The potential energy curve of the loosely bound quintet
state $5_{\Sigma_g^+}$ for which the binding energy is 0.13 ev (49), crosses
that of the B state. This suggestion has been made by Gaydon

Figure 3

Summary of N--N interactions

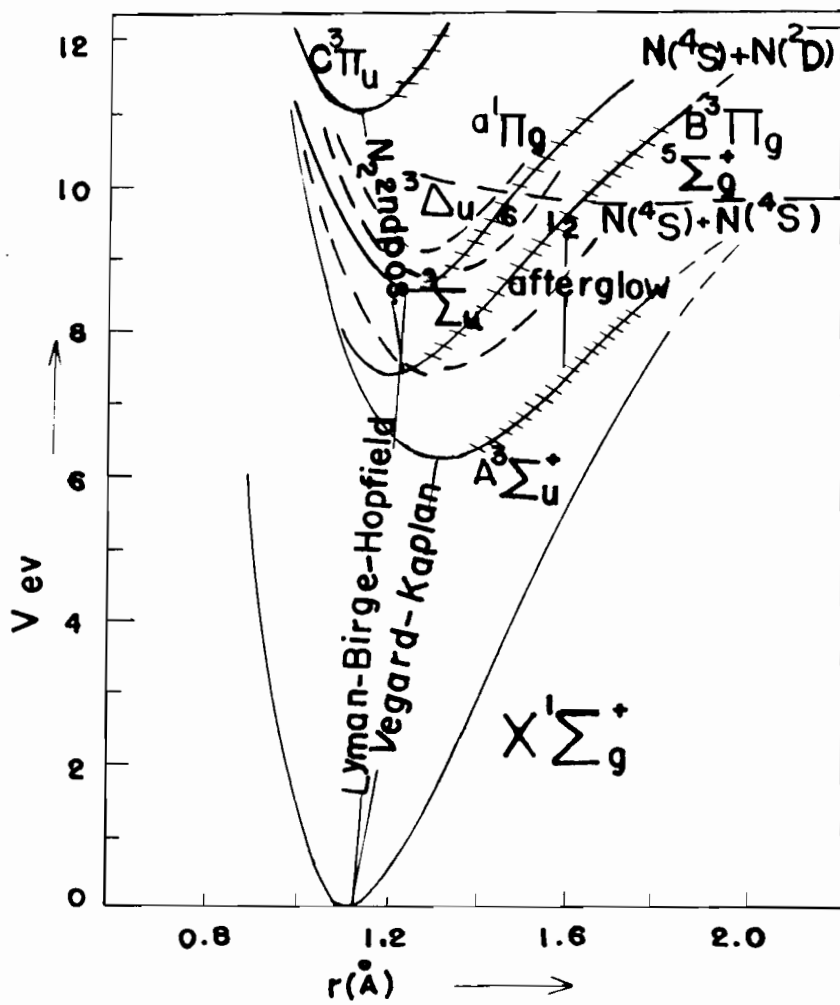


(50), who has found, in the absorption spectrum, that bands due to transitions from $v' = 13$ to the $v' = 16$ level (Fig. 4) have only one head instead of the usual four, and have no fine structure. However, for $v' = 12$ or below, or 17 and above, the bands have the normal structure. This phenomenon is explained by assuming that the molecules in the levels $v' = 13-16$ of the B state can undergo a collision-induced radiationless transition to the ${}^5\Sigma_g^+$ state, which would then dissociate into 4S nitrogen atoms (50).

The reverse of this process enables 4S atoms to produce molecules in the B state, and in the nitrogen afterglow it is postulated that two 4S nitrogen atoms collide on the ${}^5\Sigma_g^+$ potential energy curve, after which a collision with a third body induces a pre-association into the 12th vibrational level of the B state. The ${}^5\Sigma_g^+$ molecule is supposed to undergo many collisions during its lifetime, and a near equilibrium between ground state atoms $N({}^4S)$ and the ${}^5\Sigma_g^+$ molecules is established (36, 51). This accounts satisfactorily for the cut-off of the v' levels above 12.

The Birge-Hopfield bands in the afterglow can be explained similarly. Gaydon (36) has observed a strong forbidden predissociation in the $v' = 6$ level of the $\alpha^1\Pi_g$ state, and suggested that this is due to the process $N_2(\alpha^1\Pi_g) \rightarrow N_2({}^5\Sigma_g^+) \rightarrow N({}^4S) + N({}^4S)$ (Fig. 4). The reverse of this process can give rise to the Lyman-Birge-Hopfield bands in

Figure 4
Potential Energy Curves of the Nitrogen Molecule



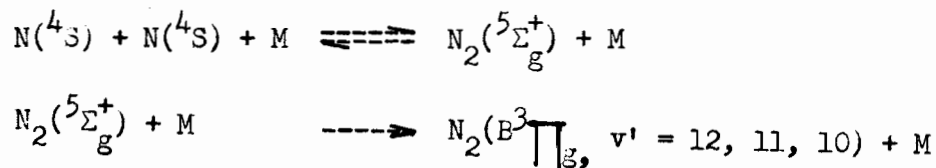
Pot. Energy Curves of the N_2 Molecule

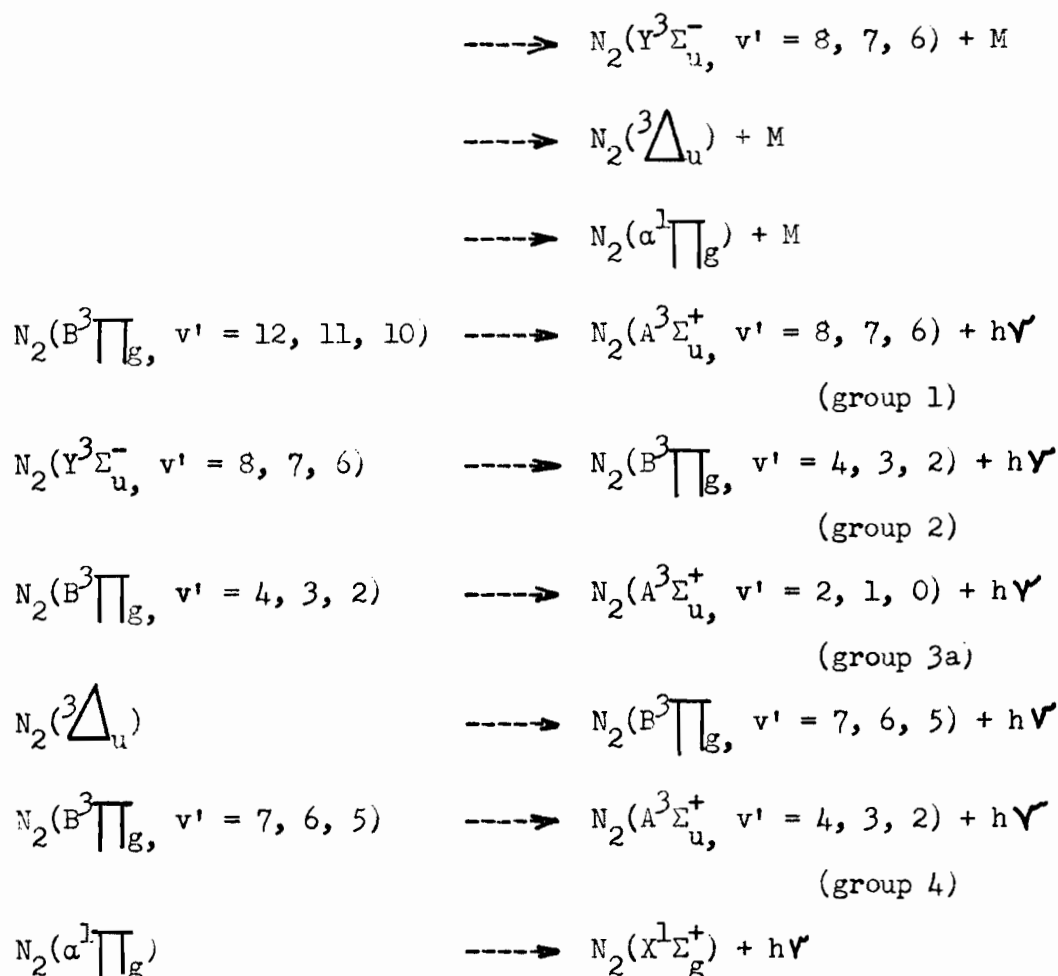
emission, and account for the fact that no bands were observed originating in v' levels above the sixth.

Stanley (52) has shown that vibrational energy transfer from $v' = 11$, of the $B^3\Pi_g$ state, is quite slow in nitrogen, compared with transitions giving rise to the first positive bands. Bayes and Kistiakowsky (53) have found that vibrational relaxation in the $B^3\Pi_g$ state is very pronounced under the experimental conditions used.

The new system could arise in a similar way. A decrease of temperature, or the addition of an inert gas (A, Kr), enhances the new band system relative to the first positive. Changes of temperature also shift the vibrational level populations of the new electronic state in the same manner as that of the $B^3\Pi_g$ ($v' = 9$ to 12) state (29). This analogy supports the idea that the new electronic state is also populated by a collision-induced radiationless transition from the $^5\Sigma_g^+$ state, in competition with the process leading to the population of the high vibrational levels of $B^3\Pi_g$.

Bayes and Kistiakowsky (54) have proposed the following detailed mechanism





This scheme, which has several steps in common with the mechanism postulated by Berkowitz, Chupka and Kistiakowsky (33), and by Kistiakowsky and Warneck (29), accounts for the most of the afterglow emission. It differs from that proposed by Gaydon (36, 50), and Cario and Reinecke (51), in that the $^5\Sigma_g^+$ state is a stable intermediate in the emission of the afterglow, since it has been found (54) that the $^5\Sigma_g^+$ state has a dissociation energy of about 850 cm^{-1} , instead of 350 cm^{-1} and 100 cm^{-1} derived from predissociations from the $\text{B}^3\Pi_g$ and $\alpha^1\Pi_g$ states, respectively. The Morse potential energy curves

of the electronic states of nitrogen, which are thought to be involved in the afterglow, are shown in Fig. 5, in which each group of bands is indicated by a single vertical arrow.

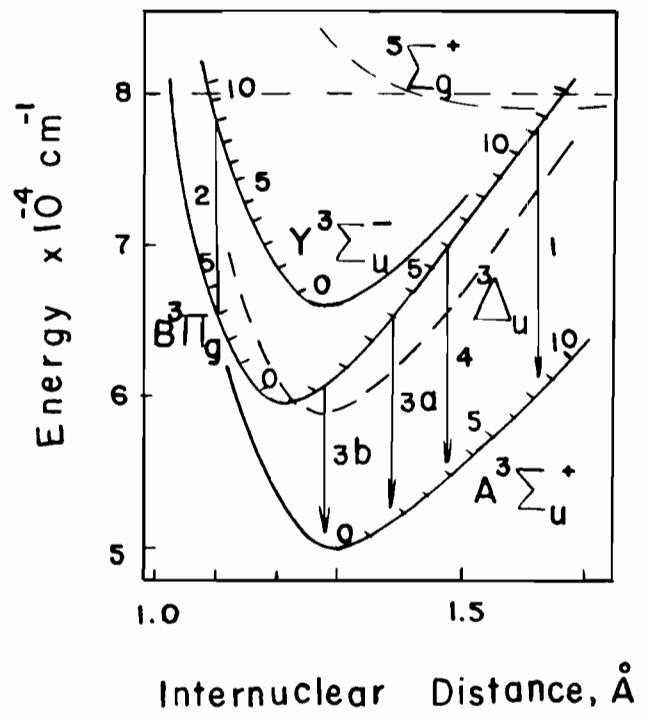
ACTIVE NITROGEN AT LOW TEMPERATURES

Broida and Pellam (55), showed that active nitrogen condensed at 4.2° K emits a bright green glow, and gives off occasional blue flashes, as long as the discharge is maintained. The glow becomes yellow-green at higher flow rates of nitrogen. Brilliant blue flashes, observed on the surface of the vessel, are thought to be due to local warming. If the flow of nitrogen is stopped, and the discharge is turned off, the green glow persists for some minutes, but with gradually diminishing intensity, and then reappears upon warming to 10° K (56, 57).

From measurements of the rate of temperature rise of the collection chamber, Broida and Lutes (58) estimated that the nitrogen atom content of the solid was approximately 0.2%. Minkoff et al. (59) have estimated the nitrogen atom content of the solid to be 4 to 6%, from the heat-released during warm-up, on the assumption that all of the heat resulted from atom recombination. However, some doubt exists about the origin of heat in the experiments with dissociated nitrogen.

Studies of trapped nitrogen atoms have recently been made by Fontana (60, 61) using thermal and magnetic measurements, and correlation of the gross light effects with

Figure 5
Morse Potential Energy Curves for
the Nitrogen Molecule. The numbered
arrows represent the different group
bands observed in the afterglow spectrum (Ref.-54)



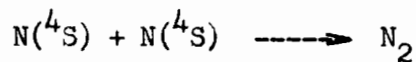
spectral investigations of similarly prepared deposits (56). Magnetic susceptibility measurements were made by Fontana with "high" nitrogen atom concentrations i.e., without passing the nitrogen through a liquid nitrogen trap prior to the discharge. However, no magnetic effects were observed, and it was estimated that not more than 0.04, and possible only 0.01, mole per cent of atoms were present in the solid.

The spectra of the glows at low temperatures have been studied in detail in the region 2200-9000 Å. The main features are: (1) Five sharp blue-green lines, known as the α lines, are found in the region 5214 to 5240 Å. They are due to the transition ${}^2D \rightarrow {}^4S$ of atomic nitrogen. This transition is strongly forbidden in the gaseous state, but it has been observed in the auroral spectrum at 5199 Å (62). (2) Three diffuse yellow-green lines at 5549, 5616 and 5657 Å, the so-called β lines, are thought to be due to the ${}^1S \rightarrow {}^1D$ transition of atomic oxygen. (3) Ten bands stretching from 3572 Å to 6390 Å, known as B bands, are attributed to the transition ${}^5\Sigma_g^+ \rightarrow {}^3\Sigma_u^+$ and are the only bands known which involve the ${}^5\Sigma_g^+$ state of nitrogen. (4) The Vegard-Kaplan bands, which are observed only when very pure nitrogen is used, are enhanced in the presence of argon (57).

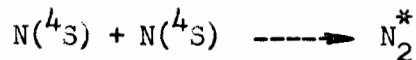
Mechanism of Nitrogen Afterglow in the Solid

The theory is based on the assumption that electro-

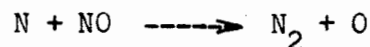
nically excited nitrogen molecules have a radiative lifetime in the solid which is comparable with the half-life for the recombination reaction of nitrogen atoms, and that these molecules can transfer electronic energy to N and O atoms, which subsequently radiate the α and β lines. Thus, it is assumed that the dark solid remaining at 4.2° K contains about 0.01 mole per cent nitrogen atoms (61), and approximately an equal percentage of oxygen, in the form of atoms and oxides of nitrogen. These atoms are stabilized, i.e., unable to move. Diffusion commences when the deposit is warmed up to 9° K, and nitrogen atoms migrate and react to give nitrogen molecules in the ground state, $X^1\Sigma_g^+$, and in the electronically excited states, $A^3\Sigma_u^+$ and $5^5\Sigma_g^+$



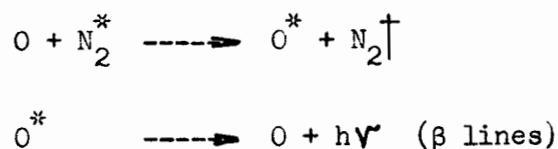
or



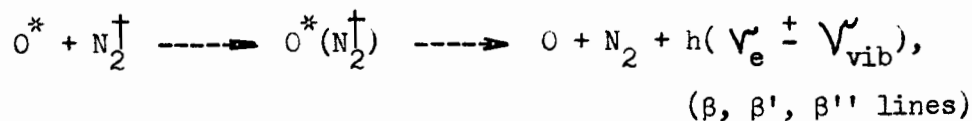
where N_2^* is an electronically excited molecule (63). Heat also is liberated, which causes further warming of the solid, and promotes the above reactions. Nitrogen atoms also react with NO, to liberate oxygen atoms



which may be in electronically excited states, and emit the β lines. Transfer of energy, followed by radiation from an excited atom, O^* , may be possible

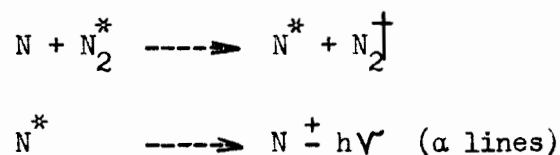


or

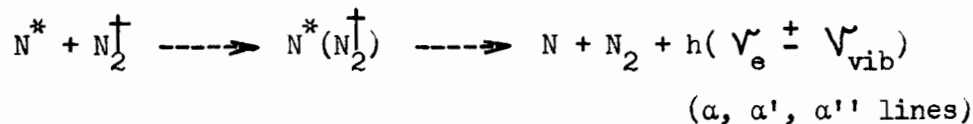


where N_2^\dagger is vibrationally excited N_2 , and $\text{O}^*(\text{N}_2^\dagger)$ signifies an intermediate radiative state, possibly giving rise to the β , β' and β'' lines. The absence of the Vegard-Kaplan bands in the presence of oxygen is attributed to the high efficiency of the oxygen atom for quenching electronic excitation of the nitrogen molecule (63).

The α lines arise in an analogous way to the β lines, that is,



or



The α lines are stronger than the β lines during the thermal peak, while β lines seem to predominate in the catastrophic recombination observed by Fontana (60, 61). (The combined thermal, magnetic, and light-emission effect which occur during the warm-up period of solid nitrogen discharge products,

are attributed by Fontana to catastrophic recombination, because the effects are very vigorous, owing to a high concentration of atoms). Fontana suggests that the B bands are due to the N_2 molecule, while they are attributed doubtfully to nitrogen dioxide by Peyron and Broida (64).

KINETICS OF NITROGEN ATOM RECOMBINATION

Rayleigh (46, 65) showed that the rate of decay of nitrogen atoms was proportional to the square of the concentration of nitrogen atoms, and probably proportional to pressure. The temperature dependence appears to involve a negative temperature coefficient for the glow reaction.

Rabinowitch (66) made a rough estimate of the rate of nitrogen atom recombination, based on Rayleigh's data, from which he approximated the nitrogen atom concentration and the half-lifetime. He found the value for the over-all recombination coefficient to be $1.0 \times 10^{16} \text{ cc}^2 \text{ mole}^{-2} \text{ sec}^{-1}$, assuming that nitrogen atoms disappear by a three-body mechanism.

Berkowitz, Chupka and Kistiakowsky (33) obtained the value of $7.5 \times 10^{15+2} \text{ cc}^2 \text{ mole}^{-2} \text{ sec}^{-1}$ for the over-all recombination coefficient of nitrogen atoms based on approximate estimates of nitrogen atom concentration and afterglow intensity.

Hartek et al. (67) have studied the recombination

of nitrogen atoms by "titrating" the nitrogen atoms with nitric oxide, and measuring the relative decrease in intensity of the afterglow by means of a photomultiplier. The rate constant for the homogeneous recombination of nitrogen atoms was found to be $6.19 \times 10^{15} \text{ cc}^2 \text{ mole}^{-2} \text{ sec}^{-1}$, with $M = \text{N}_2$ or argon. Wall recombination was neglected, since the walls of the reaction tube were coated with orthophosphoric acid.

Herron et al. (68, 69) have studied the recombination of nitrogen atoms, using nitric oxide as a titrant, and determining the nitric oxide content continuously by mass spectrometer. They have found that the reaction is predominantly homogeneous, and third order, at pressures above about 3 mm. They reported a rate constant of $5.7 \times 10^{15} \text{ cc}^2 \text{ mole}^{-2} \text{ sec}^{-1}$, over the range of temperature 195-450° K., for the homogeneous recombination. Below about 3 mm, a pseudo-first order wall recombination becomes important, and recombination coefficient, $\gamma = 1.6 \times 10^{-5}$, was found for a glass wall that undoubtedly was partly poisoned by water.

Wentink et al. (70) used platinum as a detector to measure nitrogen atom concentrations, and a photomultiplier to estimate afterglow intensity. They found the rate coefficient for the gas phase reaction to be $1.2 \times 10^{16} \text{ cc}^2 \text{ mole}^{-2} \text{ sec}^{-1}$ (corresponding to the disappearance of two nitrogen atoms), and $\gamma = 3 \times 10^{-5}$ for the wall reaction on clean pyrex glass.

Kelly and Winkler (71) have studied the surface and homogeneous decay of nitrogen atoms as a function of pressure. They estimated nitrogen atom concentrations from the hydrogen cyanide production from ethylene or ethane, under conditions of complete consumption of nitrogen atoms, and complete initial dissociation of nitrogen. For the surface decay, the recombination coefficient was found to be $\gamma = 2.75 \times 10^{-4}$ on a surface coated by Na_2HPO_4 , and the activation energy $1.0 \text{ kcal mole}^{-1}$ in the range of temperatures from 55° C. , to 400° C. For the homogeneous decay, the rate constants varied from 3.83×10^{13} to $4.75 \times 10^{15} \text{ cc}^2 \text{ mole}^{-2} \text{ sec}^{-1}$, depending on the temperature, and whether or not N_2 and N were considered as third bodies. The homogeneous decay appeared to have a positive temperature coefficient, and to be of only secondary importance below about 2 mm pressure under the conditions that prevailed.

Rate constants for homogeneous recombination of nitrogen atoms, and first or zero order surface decay on surfaces coated with different poisons, have been reported by Back and Winkler (72). A slight positive temperature coefficient for the homogeneous decay was found.

CHEMICAL REACTIVITY OF ACTIVE NITROGEN

The reactivity of active nitrogen towards many reactants has been the subject of investigation by many workers.

It is now generally accepted that the main chemically active species in active nitrogen is the nitrogen atom in the ground state, 4S , although there is some evidence, as will be seen later, that excited nitrogen molecules (73, 74, 75, 76, 77, 78) may participate in at least some of the reactions studied.

Greenblatt and Winkler, in 1949, reported a study of the reaction of active nitrogen with ethylene (79), and the application of diffusion flame technique to this reaction (80). Since then a large number of papers have appeared in the literature by Winkler and his associates, describing the mechanism and kinetic characteristics of the complex reactions of active nitrogen with a large variety of hydrocarbons and their derivatives. Reactions of active nitrogen with saturated and unsaturated paraffin hydrocarbons, cycloparaffins, alkyl halides, methyl cyanide, methylamine and sulphur containing compounds, have been studied.

The Reactions with Organic Compounds

Evans, Freeman and Winkler (81) have given a comprehensive review dealing with the main features of the reactions of active nitrogen with various organic molecules. Nitrogen was activated by a condensed discharge, and introduced into a reaction vessel, where it was mixed with the second reactant, which also entered through a fine jet. Products were trapped, and analysed by appropriate methods.

With hydrocarbons, the reaction zone is marked by a lilac-coloured flame; with halogen compounds, by an orange-coloured flame. The main product from these reactions, with the exception of some chlorinated compounds, is hydrogen cyanide. The yield of this rises more or less linearly with increase in hydrocarbon flow rate, until a maximum is reached, the magnitude of which depends on the rate at which nitrogen atoms reach the reaction zone. This maximum hydrogen cyanide production corresponds to complete removal of nitrogen atoms by the hydrocarbon, and in spherical reaction vessels, at least, it varies with temperature up to 250° C., above which a further increase in temperature has no appreciable effect.

Wrede gauge (82) measurements of atomic nitrogen concentrations are in agreement with those determined by the maximum HCN production from the ethylene reaction at high temperatures. It has been observed that the reactivity of active nitrogen is quite comparable towards a large variety of hydrocarbons and hydrocarbon derivatives, when the reactivity is measured by the maximum amount of HCN produced under given conditions.

A re-investigation of the ethylene reaction (83) has shown that, under conditions of complete removal of nitrogen atoms, the products of this reaction are hydrogen cyanide (75%), ethane (10%), methane (9%), acetylene (3%) and cyanogen

(2%), with material balances in the neighbourhood of 98%.

No significant amount of polymeric material was found.

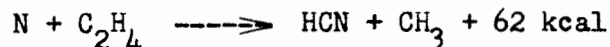
The reaction with acetylene (84) yields HCN as the main product, and a polymer that contained approximately 32% nitrogen. The yield of HCN and polymer increased to constant values with increase of acetylene flow rate. Some cyanogen and methane are also formed.

The reaction with propylene (85) has been found to produce hydrogen cyanide (68%) and ethylene (20%) as the main products, together with small amounts of propane (6%), ethane (2.5%), methane (2%), and traces of acetylene and of a C_4 fraction. An activation energy of less than 2.5 kcal/mole for this reaction has been reported.

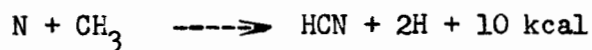
Butene-1, cis-butene-2 and isobutene were found to react with nitrogen atoms (86) to produce HCN, propylene and ethylene as the main products together with smaller amounts of butane, propane, ethane, and methane.

Reactions of active nitrogen with saturated hydrocarbons, such as methane, ethane, (87, 88), propane (89) butanes (90), neopentane (91), and with cycloparaffins and many other substances have been studied. However, detailed discussion of these reactions is irrelevant to the subject of the present thesis.

On the assumption that ground state nitrogen atoms (4S) are responsible for the reactions of active nitrogen with organic molecules, Evans, Freeman and Winkler (81) have proposed as a mechanism for the reaction with ethylene:



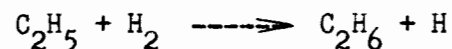
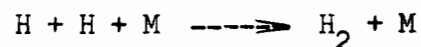
and



Since the first reaction involves a change in spin (73), and the movement of a hydrogen atom from one carbon atom to another, the formation of a relatively long-lived transition complex is quite probable. Theoretically, it is based on the assumption that the repulsion due to exchange forces during the initial approach of the nitrogen atom should be small, since p electrons are involved, and delocalized orbitals embracing the π orbitals of the carbon-carbon bond and the nitrogen atomic orbitals should lead to considerable lowering of the potential energy, particularly after the change in spin has occurred (73). Experimental evidence for the formation of such complexes is the emission of the reaction flame and the formation of cyanogen and acetylene.

The second reaction, above, is spin-allowed for three-eighths of the collisions and must be much more probable than the spin disallowed reaction $N + CH_3 \dashrightarrow HCN + H_2$. Most of the hydrogen atoms formed should recombine, while some of

them may react to form ethane:



This would explain the variation in the production of ethane with the ethylene flow rate.

Mechanisms for the formation of cyanogen and acetylene, and a unified mechanism for most of the hydrocarbon reactions have been discussed in detail in ref. (81), based on the assumption that an intermediate cyclic activated complex is formed. Recombination of nitrogen atoms catalysed by the reactant has been suggested by Forst, Evans and Winkler (92) to be involved in the reactions of active nitrogen with organic molecules.

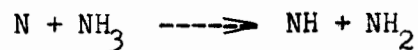
The Reactions with Inorganic Compounds

Many reactions of active nitrogen with inorganic molecules have been studied. Some of them, relevant to the present study, will be discussed briefly.

Ammonia

Freeman and Winkler (74) have shown that the reaction with ammonia is in sharp contrast to the reaction of active

nitrogen with hydrocarbons. They found the maximum destruction of ammonia by active nitrogen to correspond to only about one-sixth of the reactivity of active nitrogen estimated from the maximum HCN production from the ethylene reaction. This maximum destruction of ammonia is found to be temperature independent. After the optimum amount of reaction with ammonia, the gas is still reactive towards hydrocarbons, which indicates that ammonia does not react with nitrogen atoms. It was suggested that the N_3 radical might be a possible second active component. Later, Evans and Winkler (73) postulated that a vibrationally excited ground state nitrogen molecule might be the second reactive species, but this remains doubtful. The reaction



is endothermic to an extent of 19^{+12} kcal/mole (36), while the reaction



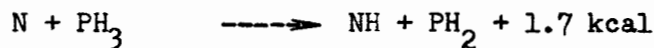
is spin forbidden.

Kistiakowsky and Volpi (75) have studied the ammonia reaction, using the "stirred" reactor technique, and a mass spectrometer for the identification of the products. They have shown that, in the presence of ammonia, the intensity of the afterglow is reduced, while the atomic nitrogen concentration is not affected. They have concluded that ammonia decom-

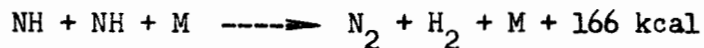
position may be the result of an inelastic collision, in the course of which the nitrogen molecule undergoes a triplet-siglet ($B^3\Pi_g \text{-----} X^1\Sigma_g^+$) transition, and the ammonia molecule of singlet-triplet transition. This would help to explain quenching of the afterglow, but additional effects on the nitrogen atom concentration may be expected to arise from the possible decomposition of the excited ammonia. Kelly and Winkler (93) have postulated that ammonia probably reacts with some species produced from the decay of nitrogen atoms. However, the active species in active nitrogen which causes the decomposition of ammonia is still not known.

Phosphine

Wiles and Winkler (94) studied the reaction with phosphine, and found the main products of this reaction to be molecular hydrogen and the α -form of $(PN)_n$. The postulated mechanism was



followed by



No ammonia was found among the products.

Hydrogen Halides

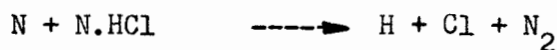
Willey and Rideal (17) showed that hydrogen bromide

and hydrogen iodide were destroyed by active nitrogen, but hydrogen chloride suffered no decomposition. On the contrary, hydrogen chloride was formed when hydrogen-chlorine mixtures were introduced to active nitrogen. Ewart and Rodebush (95) found that the reactions of HBr and HI gave orange and blue flames respectively.

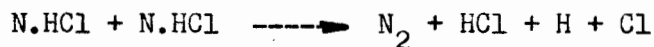
Wiles and Winkler (96) found that hydrogen chloride was apparently destroyed by catalyzing the recombination of nitrogen atoms. The assumed mechanism was



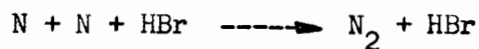
followed either by



or



Dunford and Melanson (97), and Milton and Dunford (98), have recently studied the reaction with hydrogen bromide and bromine. They found that HBr is very efficient as a third body to recombine nitrogen atoms



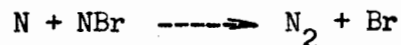
The rate constant for the first step



was found to be $1.68 \times 10^{10} \text{ cc mole}^{-1} \text{ sec}^{-1}$ at 40° C . For the bromine reaction, the postulated mechanism is



and



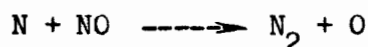
The formation of some excited state of NBr in the reaction



has been observed (98).

Oxides of Nitrogen

The reaction of nitric oxide with active nitrogen has been studied by Spealman and Rodebush (99), Kistiakowsky and Volpi (75, 100), Kaufman and Kelso (101), Harteck and Dondes (102), Verbeke and Winkler (77) and Nelson, Wright and Winkler (78). The addition of a little NO weakens the afterglow by rapidly removing nitrogen atoms by the reaction



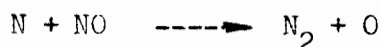
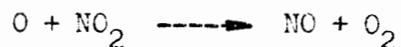
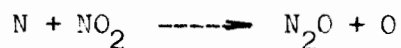
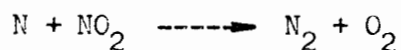
Excited NO molecules may then be formed by the relatively slow combination of a nitrogen atom and an oxygen atom in the presence of a third body, and the emission of these molecules accounts for the range of colours, yellow-pink-blue, i.e.,



The addition of sufficient nitric oxide removes all the nitrogen

atoms, and excess of NO produces the yellow-green NO + O continuum of the air afterglow. The rapidity of this reaction makes it possible to use nitric oxide as a titrating agent for nitrogen atoms (100, 101). When ^{15}NO is added to active nitrogen, only ^{14}NO bands are observed (101), indicating that the excited NO molecules are formed by chemical reaction, and not by excitation of the original NO molecules. The rate constant of this reaction was found by Kistiakowsky and Volpi (75) to be greater than $5 \times 10^{13} \text{ cc mole}^{-1} \text{ sec}^{-1}$, while Clyne and Thrush (103) have recently reported the value of $3 \times 10^{13} \exp(-200/RT) \text{ cc mole}^{-1} \text{ sec}^{-1}$ over the range of temperatures from 476 to 755° K.

The reaction of nitrogen dioxide with nitrogen atoms has been studied by many investigators (99, 100, 75, 102, 77). The mechanism of this reaction appears to be



Verbeke and Winkler (77) have shown that the maximum amount of NO_2 destroyed by active nitrogen is essentially the same

as the maximum HCN produced from the ethylene reaction under comparable conditions. No reaction of active nitrogen with N_2O was detected (100, 77).

However, when N_2O was added (about 2%), a strong decrease in the afterglow intensity occurred and considerable temperature rise was observed (76). No similar effects were observed with He, A, N_2 or O_2 . A mass spectrometer analysis of the gas sampled far down-stream did not detect any loss of N_2O , nor the formation of O_2 or NO. The evolution of heat was determined to be 2 kcal per mole of nitrogen, and was attributed to the efficiency of N_2O for deactivating vibrationally excited nitrogen molecules, while the loss of the afterglow intensity was ascribed to the negative temperature coefficient of the afterglow. N_2O was added at different points along the flow tube and the heat release was estimated. The half life of the activated species is found to be 0.50 sec., corresponding to 3×10^5 collisions at a pressure of 1 mm, which is of the same order of magnitude as the number of collisions required to deactivate vibrationally excited oxygen molecules (104, 105).

In further experiments, by the same authors, active nitrogen was titrated by NO, and, under these conditions, the addition of N_2O downstream caused a greater heat release than without added NO. The heat releasing species is therefore not affected by NO; on the contrary the reaction $N + NO$

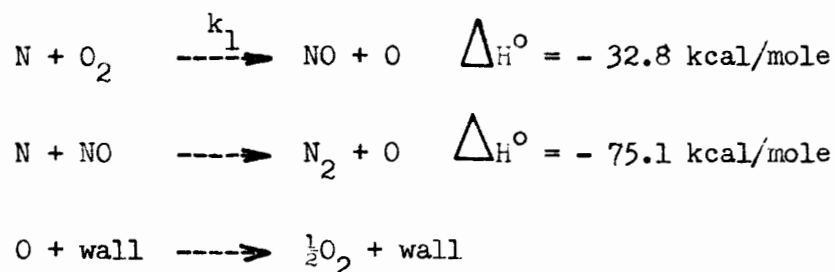
apparently produces more of the heat releasing species, presumably vibrationally excited nitrogen. Similar experiments have been carried out by Nelson, Wright and Winkler (78) but no significant heat release was observed on the addition of N_2O or CO_2 to the active nitrogen. Both nitrous oxide and carbon dioxide were destroyed to a very small extent even at elevated temperatures.

Verbeke and Winkler (77), and Nelson, Wright and Winkler (78), have observed that the maximum amount of NO destroyed by active nitrogen is higher than the maximum production of HCN from the ethylene reaction under similar conditions. The ratio of the amount of NO destroyed to the maximum HCN production, or NO_2 destruction, varied from 1.4 to 2.4 over the pressure range from 1 mm to 16 mm. This discrepancy might be interpreted as further evidence for the existence of a second reactive species in active nitrogen, but further study is required to explain the observations unequivocally.

Molecular Oxygen

Varney (106) has observed that the addition of O_2 to active nitrogen produces small amounts of N_2O , NO and NO_2 . The reaction of active nitrogen with molecular oxygen has been studied by Kistiakowsky and Volpi (100). Using a stirred reactor technique, in conjunction with a mass spectrometer, they detected no reaction at room temperature, but at elevated

temperatures the atomic nitrogen concentration was reduced without change of the oxygen concentration, or generation of a new molecular species. The appearance of the β bands of nitric oxide, in addition to the afterglow, and the absence of any oxides of nitrogen among the products, indicated the mechanism of the reaction to be:



They found the rate constant for the first reaction, the rate-controlling step, to be

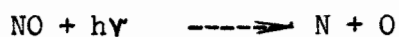
$$k_1 = 2 \times 10^{12} \exp(-6,200/RT) \text{ cc mole}^{-1} \text{ sec}^{-1}$$

From studies on the oxygen-sensitized decomposition of NO, Kaufman (107) found $k_1 = 1.7 \times 10^{13} \exp(-7,500/RT)$, and more recently Clyne and Thrush (103) have obtained the value $k_1 = 8.3 \times 10^{12} \exp(-7,100/RT)$, by measuring the decay of nitrogen atoms with the nitric oxide titration method. The reaction of nitrogen atoms with molecular oxygen has also been assumed by Harteck and Dondes (108) to occur during the fixation of nitrogen by irradiation of nitrogen oxygen mixtures.

OXYGEN ATOMS

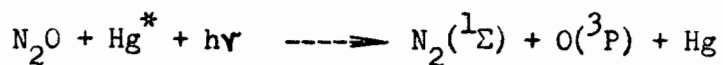
Oxygen atoms may be produced by either photochemical or electrical discharge methods.

Typical of the photochemical production may be mentioned several reactions that are known to occur in the earth's atmosphere, under the influence of sun light:



Kistiakowsky (109) has prepared oxygen atoms in the laboratory by irradiation of molecular oxygen, but this method has not been used elsewhere, owing to the experimental difficulties involved.

The mercury photosensitized decomposition of nitrous oxide has been used by Cvetanovic (110) to produce ground state oxygen atoms, according to the scheme



Ford and Endow (111) have prepared oxygen atoms for kinetic studies by the photolysis of nitrogen dioxide at 3600

O° , but the complexity of the method has been emphasized by the same authors (112). Schumacher (113) has found that ^1D oxygen atoms, produced by the photolysis of nitrogen dioxide, react with H_2 , while ^3P oxygen atoms, produced at a different wave length, do not.

Generally, atomic oxygen is produced in the laboratory by subjecting oxygen, at about 1 mm. pressure, to an electrical discharge. As with active nitrogen, an afterglow, yellow-green in colour is observed to persist for a short time after the discharge is shut off. Strutt (114, 115), in 1911, studied the production of "activated oxygen", and assumed that the glow was a result of the reaction between nitric oxide and ozone, both of which were present in the discharge. Since then, many studies on active oxygen have been made, using improved experimental techniques. The main constituent of active oxygen is found to be the oxygen atom in the ground state (^3P). Other active species such as ions, excited molecules, metastable atoms and ozone have also been sought, and some have been found. The products of oxygen that has been subjected to an electrical discharge may be summarised as follows:

- a) Ions: Harteck and Kopsch (116) and McCarthy (117), found that no ions were present.
- b) Excited atoms: Harteck and Kopsch (116) have shown that

active oxygen does not react with H_2 , which suggests that no appreciable concentration of 1D atoms is present in active oxygen. Experiments made by Kurt and Phipps (118), Rawson and Beringer (119), Rodebush and Troxel (120) and Herron and Schiff (121), are in agreement that 3P oxygen atoms are the main constituent of oxygen subjected to an electrical discharge.

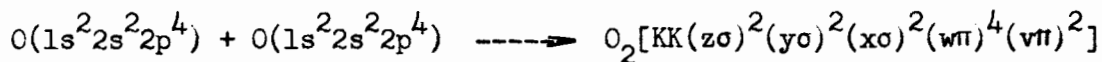
c) Ozone: Although many investigators have reported the existence of small amounts of ozone in active oxygen, Herron and Schiff (121) have shown that the ozone concentration is less than 0.02% at pressures up to 2 mm.

d) Electronically excited molecules: Kaplan (122) and Branscomb (123) have observed transitions due to $^1\Sigma_g^+ \rightarrow ^3\Sigma_g^-$ in emission spectrum, while Broida and Gaydon (124) have found the Herzberg band $^3\Sigma_u^- \rightarrow ^3\Sigma_g^-$, but failed to detect the Schumann-Runge system $^3\Sigma_u^- \rightarrow ^3\Sigma_g^+$ or the low lying $^1\Delta_g \rightarrow ^3\Sigma_g^-$ system.

Recent mass spectrometric studies of active oxygen also indicate that relatively large concentrations of electronically excited oxygen molecules are present. Foner and Hudson (125), using a free radical mass spectrometer, observed a decrease of 0.93 volts in the appearance potential of mass 32, and attributed it to the presence of oxygen molecules in the $^1\Delta_g$ state. Herron and Schiff (121) have shown, from the initial slopes of the ionization curves, that active oxygen contains excited O_2 molecules in the $^1\Delta_g$ state, in concentrations

of about 10%. The potential energy curves for the oxygen molecule, arising from the interaction of two oxygen atoms according to Heitler-London scheme, are shown in Fig. 6, while Fig. 7 shows the energy level diagram of O_2 , with ${}^3\Sigma_g^-$ the ground state.

Lennard-Jones (126) has proved theoretically that the ground state of O_2 has the term ${}^3\Sigma_g^-$. According to the molecular orbital theory, O_2 formed by recombination of two oxygen atoms is represented by

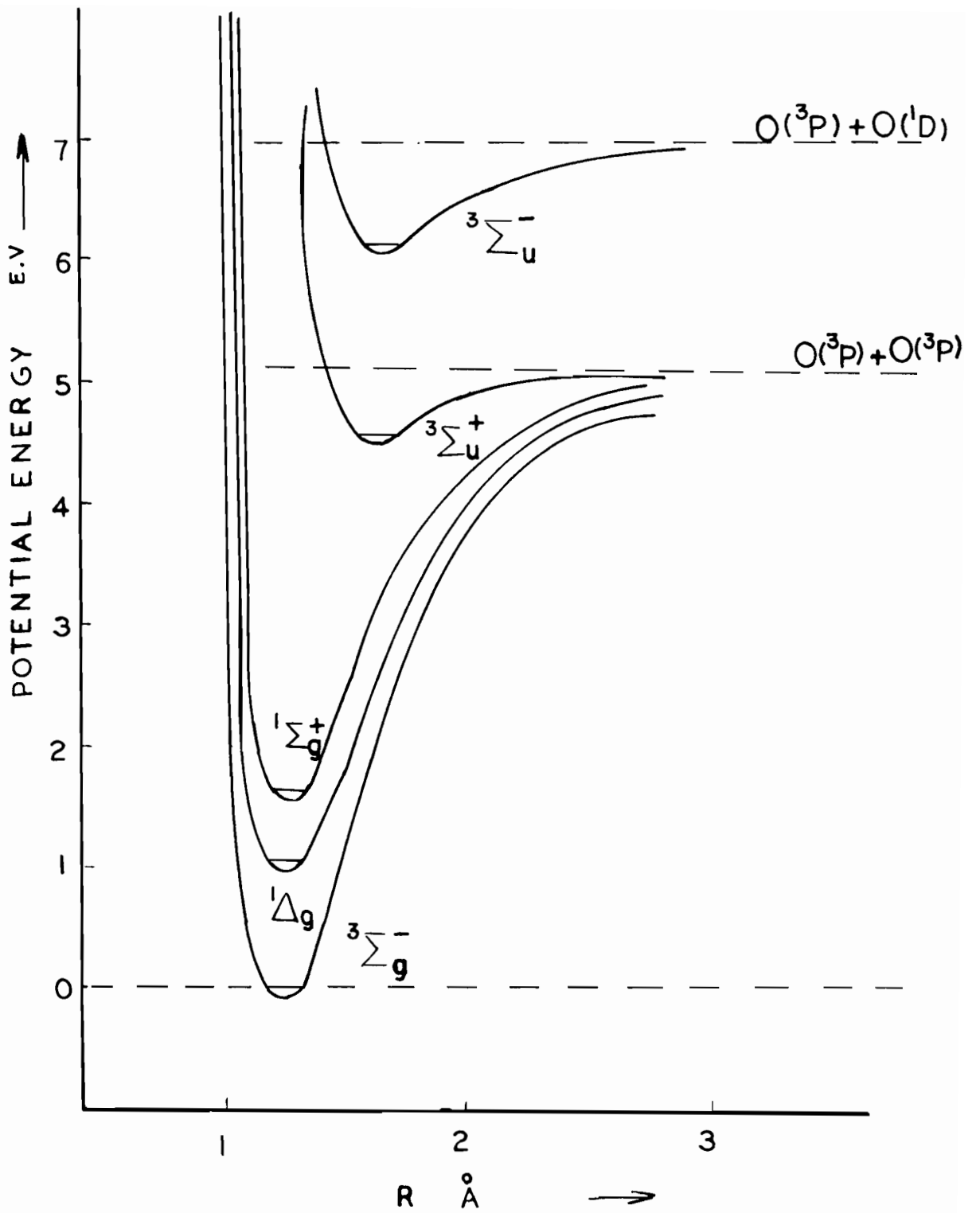


There are four effective bonding electrons, $(x\sigma)^2(\pi\pi)^2$, giving a double bond $O=O$, but the $\pi\pi$ level is degenerate since it contains both $\pi_y^* 2p$ and $\pi_z^* 2p$, and it will therefore accommodate four electrons. Since it is assigned only two in the recombination reaction, the application of Hund's rule indicates that these two electrons will go one each into $\pi_y^* 2p$ and $\pi_z^* 2p$, and will have parallel spins. In this way, the ground state of O_2 should have total spin of unity, that is, a ${}^3\Sigma_g^-$ term, and should show paramagnetism. On the left and right of Fig. 8, the various L-shell levels of the separate atoms are shown, and in the centre there are the allowed molecular levels (127).

REACTIONS OF OXYGEN ATOMS

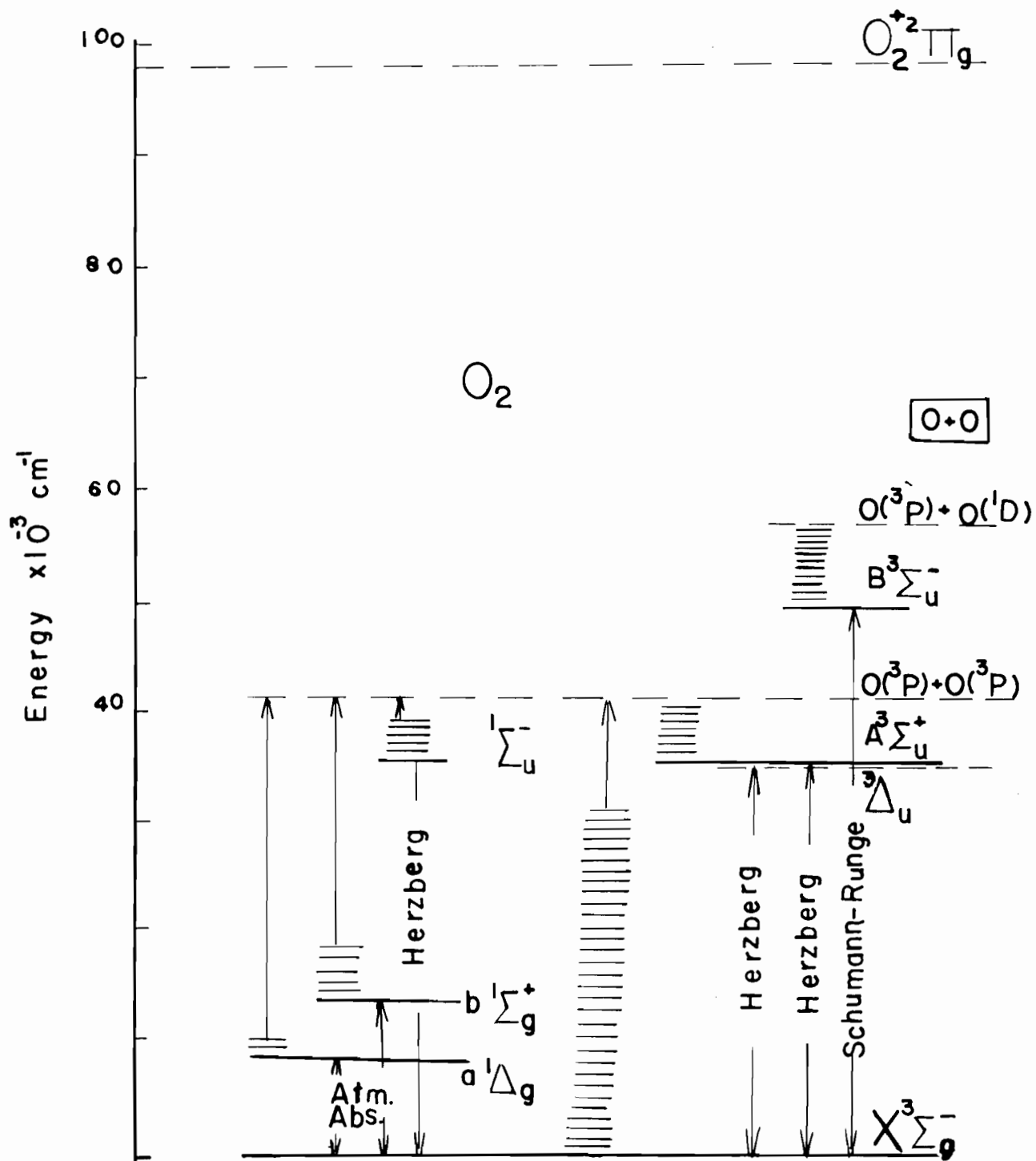
A large part of the work on the reactions of atomic

Figure 6
Potential Energy Curves of the Observed States
of the O_2 Molecule



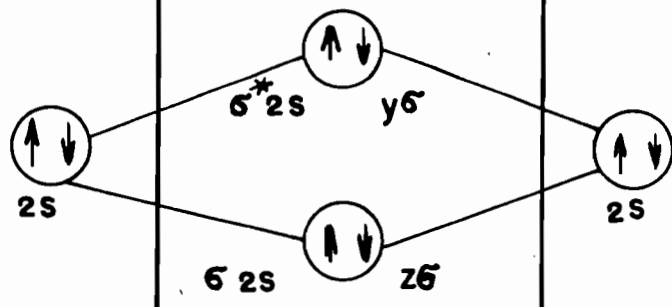
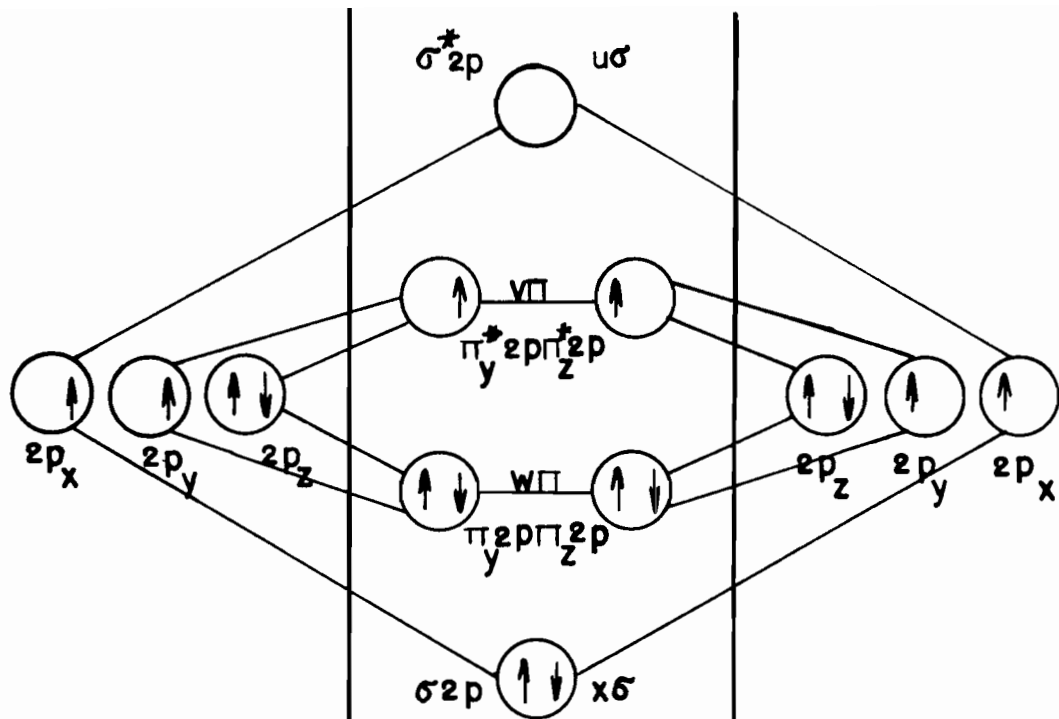
Pot. Energy Curves of the O_2 Molecule

Figure 7
Energy Level Diagram of the
 O_2 Molecule



Energy Level Diagram of O_2

Figure 8
Molecular Orbitals for O_2 , showing
the Triplet Nature of the Ground State



Atomic Orbitals Molecular Orbitals Atomic Orbitals

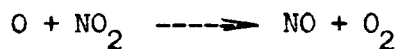
oxygen with hydrocarbons has been due to Harteck and Kopsch (116), Geib and Harteck (128) and Cvetanovic (110).

From studies on the thermal decomposition of nitrous oxide, Kaufman et al. (129), estimated, indirectly, that the rate constant for the reaction



was $6 \times 10^{15} \text{ cc}^2 \text{ mole}^{-2} \text{ sec}^{-1}$. Ford and Endow (111) gave a value of $1.8 \times 10^{16} \text{ cc}^2 \text{ mole}^{-2} \text{ sec}^{-1}$, derived from studies on the photolysis of nitrogen dioxide at 3660 \AA . Kaufman (130) has recently determined the rate constant for this reaction to be $2 \times 10^{16} \text{ cc}^2 \text{ mole}^{-2} \text{ sec}^{-1}$, with argon or molecular nitrogen as the third body, which is in agreement with the value given by Ogryzlo and Schiff (131) of $2.15 \times 10^{16} \text{ cc}^2 \text{ mole}^{-2} \text{ sec}^{-1}$, derived from an isothermal calorimetric method.

The rate constant for the reaction



has been determined by a number of workers. Ford and Endow (111), Kistiakowsky, and Kydd (132), and Kaufman (130) have reported values of 2.1×10^{12} , and lower limits of 10^{12} and $10^{11} \text{ cc mole}^{-1} \text{ sec}^{-1}$, respectively.

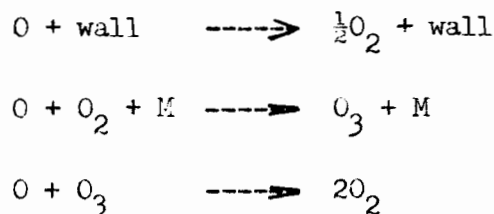
For the rate constant of the reaction



Herron and Schiff (121) gave an upper limit of 3×10^5 cc mole⁻¹ sec⁻¹ at room temperature, while Kaufman (123), from indirect measurements, derived the value of $3 \times 10^{10} \exp(-145/RT)$ cc mole⁻¹ sec⁻¹.

THE RECOMBINATION OF OXYGEN ATOMS

Elias, Ogryzlo and Schiff (133), assumed the mechanism for the recombination of oxygen atoms to be

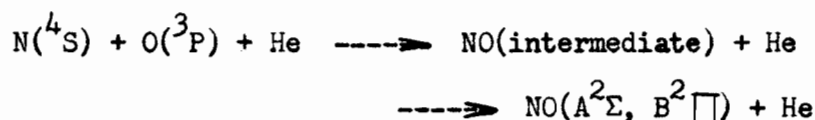


They reported values of 10^{14} cc² mole⁻² sec⁻¹ and $\gamma = 7.7 \times 10^{-5}$ for the rate constant of the gas phase recombination, and the wall reaction respectively. Benson (134) derived, indirectly, the value of $6 \times 10^{13} \exp(600/RT)$ cc² mole⁻² sec⁻¹ for the gas phase recombination of oxygen atoms. Reeves et al. (135), and Matthews (136) have given the values of 9.7×10^{14} and 7.9×10^{14} cc² mole⁻² sec⁻¹, respectively, for the rate constant of the homogeneous recombination, while Morgan and Schiff (137) found the values of 3.2×10^{15} cc² mole⁻² sec⁻¹ for the homogeneous recombination, and $\gamma = 1.65 \times 10^{-5}$ on clean pyrex glass in the absence of oxygen molecules. Linnett and Marsden (138), and Greaves and Linnett (139), have studied the heterogeneous recombination of oxygen atoms on glass surfaces

coated with different salts. They reported the value of $\gamma = 3 \times 10^{-5}$ on pyrex glass.

THE NITROGEN ATOM-OXYGEN ATOM REACTION

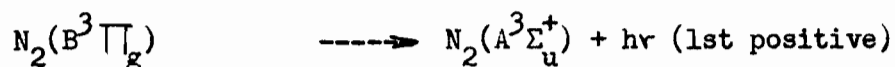
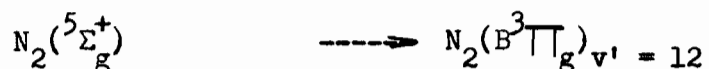
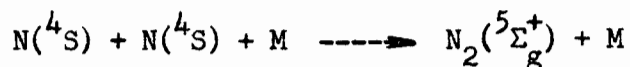
Barth et al. (140) have studied the spectrum of the blue nitric oxide afterglow, and the effect on it of adding rare gases. From the sensitivity of the vibrational intensity distribution of the nitric oxide afterglow emission spectrum to the addition of helium, they concluded that the afterglow emission spectrum arose from the three-body recombination of a ground state oxygen atom and a ground state nitrogen atom, by way of some intermediate state, into the excited upper states of the β , γ and infra-red bands, such as



The intermediate state may, or may not, be long-lived compared with the duration of the collision. By comparing the lifetime of the molecules in $\text{A}^2\Sigma$ and $\text{B}^2\Pi$ states ($\sim 10^{-8}$ sec) with the time of a collision ($\sim 10^{-7}$ sec), they concluded that helium must affect the distribution of vibrational energy during the formation or the lifetime of the intermediate state. Further support for these views was given by Kaufman and Kelso (101).

The surface-catalysed nitrogen and oxygen atom recombination has been studied by Reeves et al. (141, 142). The same band systems were found to be produced by the gas-phase

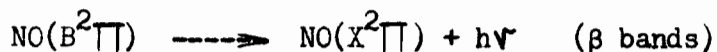
reactions



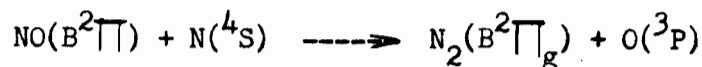
and

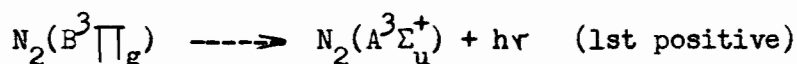


Several important differences were observed in the spectral analysis of the glows produced over metals (Co, Ni or Ag). The radiation from the second reaction in the gas phase showed the strongest transitions to be from $v' = 12, 11, 10..$, while the spectrum of the glow over metals showed the most intense bands to be from $v' = 8$ and 6 . Also, the mixing of N- and O-atom streams is observed to produce the NO γ bands, in addition to the β bands, in the gas phase reactions, but not γ bands were observed in the spectrum of the glows over metals. To account for this difference, it was postulated that the primary molecule formed on the metal surface was the $\text{NO}(\text{B}^2\Pi)$, which diffused into the gas phase and either radiated



or reacted with a $\text{N}(^4\text{S})$ to form an electronically excited N_2 molecule, which then radiated,





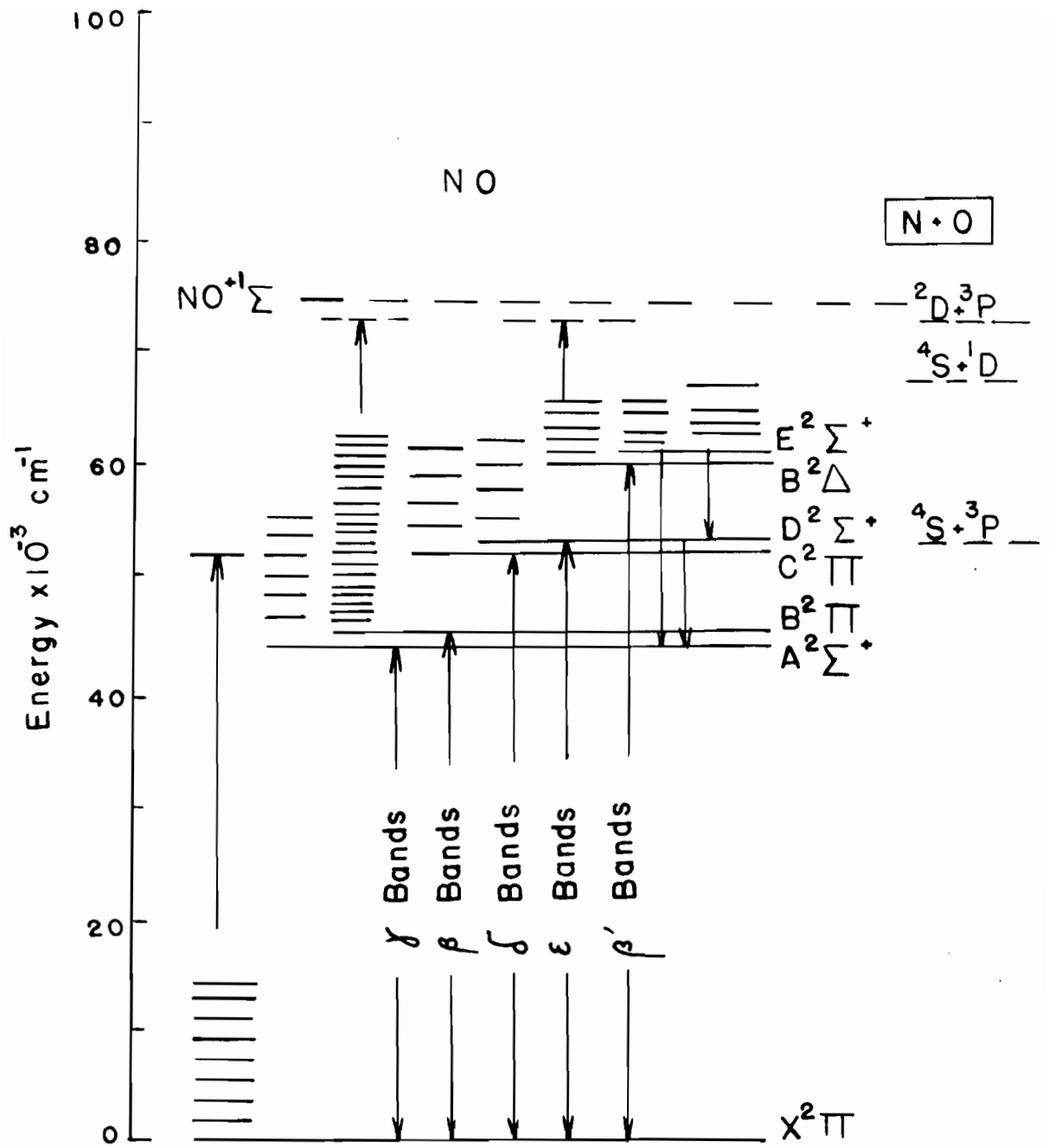
The thickness of the blue radiation was found to be in excellent agreement with the diffusion distance.

To explain the strong radiation from $v' = 8$ and 6 , and the long lifetime of the species responsible for the red glow, the authors (141, 142) assumed that $N_2(A^3\Sigma_u^+)$ is formed on the metal surface. The $N_2(A^3\Sigma_u^+)$ and $N_2(B^3\Pi_g)$ potential energy curves cross at about 8.5-9.0 ev, or $v' = 6-8$. The metastable $N_2(A^3\Sigma_u^+)$ diffuses into the gas phase and, by collision, crosses into the $(B^3\Pi_g)$ state at $v' = 9$ and 6 , and then radiates immediately from the $(B^3\Pi_g)$ back to the $(A^3\Sigma_u^+)$. The lifetime of the species responsible for the red glow was estimated from both the diffusion distances, and the linear velocity of the gas stream, to be about 10^{-3} sec. The time interval 10^{-3} sec is sufficient for the $N_2(A^3\Sigma_u^+)$ (lifetime 10^{-2} sec) to relax vibrationally into the crossing region, and cross, by collision, into the $B^3\Pi_g$ state. When N-atoms alone were passed over a Cu plate, the blue glow of the second positive system of nitrogen was observed ($C^3\Pi_u \longrightarrow B^3\Pi_g$). The energy level diagram of the NO molecule is shown in Fig. 9.

HYDROGEN ATOMS

Langmuir (143) first produced hydrogen atoms by dissociation on a heated filament and Wood (144) has obtained more than 50% dissociation into atoms using a low frequency

Figure 9
Energy Level Diagram of NO



Energy Level Diagram of the NO Molecule

electrode discharge through hydrogen at pressures 0.2 and 1.0 mm. He concluded that gas films adsorbed on the walls of the tube were an important factor in determining the yield of atomic hydrogen that could be obtained from the discharge tube. No atomic hydrogen was obtained with dry hydrogen, and water vapour or oxygen was believed to reduce the ability of the walls to catalyze recombination.

Finch (145) found that dry hydrogen is not dissociated, and that water vapour or oxygen is somehow involved in the dissociation process. Poole (146) concluded that the use of water vapour as an anticatalyst in glass or silica discharge tubes is very unreliable and likely to yield erratic results. Tubes coated with metaphosphoric acid, when used with wet hydrogen, gave reproducible and high yields of atomic hydrogen. Dingle and LeRoy (147) have produced a satisfactory yield of atomic hydrogen by thermal dissociation of dry hydrogen on a hot filament, when the walls of the apparatus were coated with a mixture of orthophosphoric acid and phosphorous pentoxide.

Wittke and Dicke (148) have obtained satisfactory yields of atomic hydrogen in a Wood's tube when the walls of apparatus were coated with Dri-film. This is a mixture of dimethyldichlorosilane and methyltrichlorosilane, which is heat stable, and has a very low vapour pressure.

Shaw (149) found that, when tank hydrogen with less

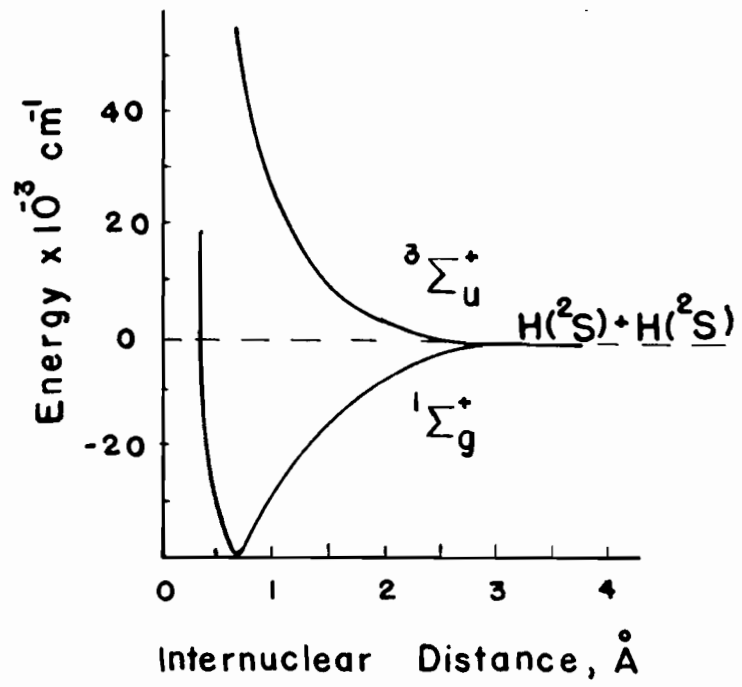
than 0.5% impurities was passed through a deoxo unit and silica gel to remove oxygen and water vapour, and the discharge tube is coated with 12% hydrofluoric acid, the yield of atomic hydrogen was small and variable, while with the discharge tube coated with Dri-film the yield was increased and was stable. When the hydrogen was further dried in a liquid nitrogen trap, the yield of hydrogen atoms was reduced as much as thirtyfold.

Emeleus et al. (150), Lunt and Meck (151) and Lunt et al. (152), have developed a theory for the dissociation of hydrogen in an electrical discharge. According to this theory, the number of electronic excitations leading to the dissociation of molecules into atoms is directly proportional to the number of electrons supplied to the discharge, for conditions such that the density of undissociated molecules is effectively constant. It is assumed that essentially all dissociation of hydrogen occurs by direct excitation of the lowest repulsive state $1\Sigma_g^+ \rightarrow 3\Sigma_u^+$ and to a lesser extent via the process $1\Sigma_g^+ \rightarrow 3\Sigma_g^+$ where, after emission $3\Sigma_g^+$ falls to $3\Sigma_u^+$ and dissociates. The potential energy curves of the hydrogen molecule are shown in Fig. 10.

THE RECOMBINATION OF HYDROGEN ATOMS

The recombination of hydrogen atoms has been studied by a number of workers (153-160), and has been treated theoretically by Schuler and Laidler (161). Steiner and Wicke (155)

Figure 10
Potential Energy Curves of the
Two Lowest States of the H₂ Molecule

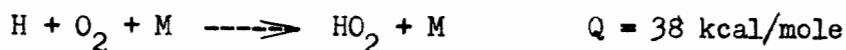


reported the value of $9 \times 10^{15} \text{ cc}^2 \text{ mole}^{-2} \text{ sec}^{-1}$ and later (156) the value of $11 \pm 2 \times 10^{15} \text{ cc}^2 \text{ mole}^{-2} \text{ sec}^{-1}$ for the coefficient of the homogeneous recombination of hydrogen atoms and they concluded that there was a small first order wall reaction and that hydrogen molecules were the most efficient third bodies. Smith (160) studied the recombination of hydrogen atoms on a number of salts, and found the recombination coefficient on pyrex glass poisoned with metaphosphoric acid to be $\gamma = 2.0 \times 10^{-5}$, based on the assumption of a first order wall recombination.

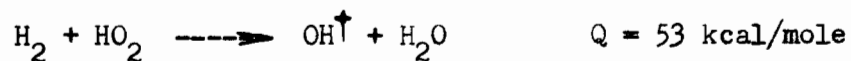
Dingle and LeRoy (162) found the value of γ to be $\gamma = 4.5 \times 10^{-5}$ on glass surface coated with a mixture of orthophosphoric acid and phosphorous pentoxide. In this method, the hydrogen atoms were produced by the dissociation of hydrogen molecules on tungsten filaments and detected by their heat of recombination on platinum.

SOME REACTIONS OF HYDROGEN ATOMS

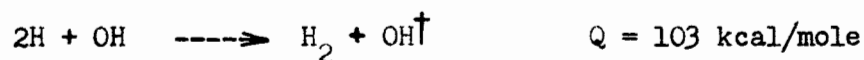
The reaction of hydrogen atoms with oxygen molecules has been studied by Foner and Hudson (163), Robertson (164) and recently by Polanyi et al. (165, 166), who obtained the spectrum of the hydroperoxy radical HO_2 in emission. They postulate the mechanism



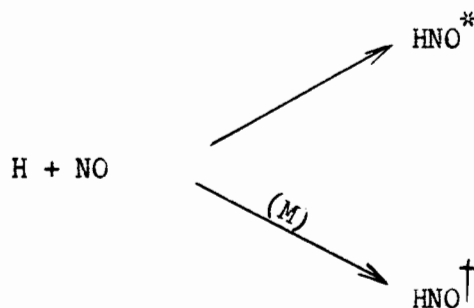
followed by



with a very minor contribution from

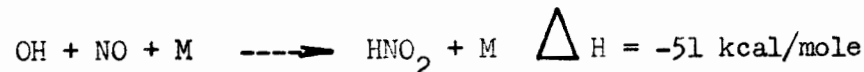
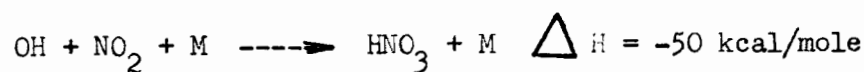
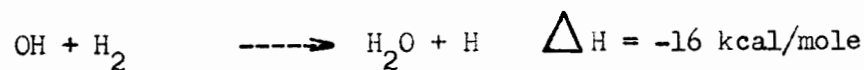
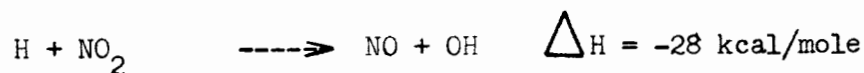
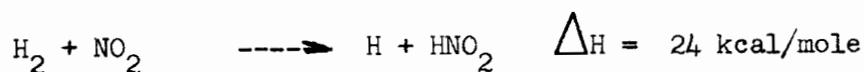


The emission bands in the spectral ranges 0.6-1 μ and 2.7-3.9 μ have been detected in the reaction of atomic hydrogen with nitric oxide by Cashion and Polanyi (167). These are attributed to emission from electronically excited HNO^* , and vibrationally excited HNO^\dagger , i.e.,

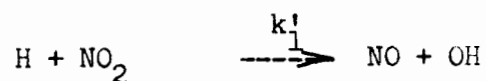


Hoare and Walsh (168) found that this reaction requires a third body.

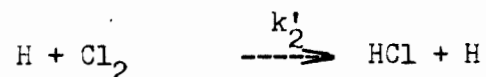
Rosser and Wise (169) have studied the reactions of hydrogen molecules and hydrogen atoms (170) with nitrogen dioxide in the temperature region from 600° to 700° K, and 500° to 540° K, respectively. A five step mechanism has been postulated for the reaction of hydrogen molecules with nitrogen dioxide, i.e.,



The rate constant for the reaction



has been measured relative to that of



by the same investigators (170), in a system containing H_2 , Cl_2 and NO_2 . Hydrogen atoms were produced by the reaction of H_2 with NO_2 and Cl_2 . For long reaction chains resulting from the hydrogen atoms so produced, it was assumed that the ratio k_1'/k_2' might be given by

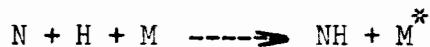
$$k_1'/k_2' = \frac{-d(\text{NO}_2)}{dt} (\text{Cl}_2) / \frac{-d(\text{Cl}_2)}{dt} (\text{NO}_2)$$

Measuring the (NO_2) and (Cl_2) concentrations at measured times by optical means, they found $k_1'/k_2' = 2.63 e^{3130/RT}$. Using the known value of k_2' , k_1' was found to be $k_1' = 10^{13.5}$ cc mole⁻¹ sec⁻¹, which corresponds to a collision efficiency of about 1 in 20.

Nitrogen Atom-Hydrogen Atom Reactions

Willey and Rideal (17) and Lewis (171) have studied the reaction of nitrogen atoms with both molecular and atomic hydrogen. It was found that active nitrogen has no effect on molecular hydrogen, no ammonia being formed. It was also concluded that no ammonia is formed by atomic hydrogen and unexcited molecular nitrogen. Lewis (171) has shown that ammonia is formed only when active nitrogen is mixed with atomic hydrogen.

Steiner (172) has reported the formation of small amounts of NH_3 and hydrazine from the reaction of hydrogen atoms with high active nitrogen concentrations. He also postulated, contrary to the results of Lewis (171), that the reaction with hydrogen molecules yielded hydrazine in small amounts, which varied with the nitrogen atom concentration. A small amount of ammonia was formed, but it was attributed to the diffusion of hydrogen molecules into the discharge tube, where the production of atomic hydrogen made a reaction between nitrogen and hydrogen atoms highly probable. For ammonia formation, he suggested

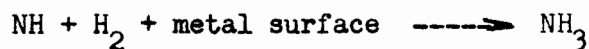


and for hydrazine





Dixon and Steiner (173) found more ammonia and less hydrazine, in the presence of a metallic surface, than that found by Steiner (172). The formation of ammonia was attributed to the reactions



and hydrazine formation to



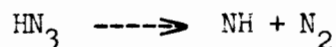
The lower yield of hydrazine was believed to be due to the rapid recombination of hydrogen atoms on the metal surface. They failed to find spectroscopically the existence of the NH radical.

Varney (106) claimed that he observed a reaction with H_2 , the only trapped product being ammonia. Both mass spectrographic and indicator tests were made for hydrazine but results were negative. Diffusion of hydrogen into the discharge seemed to be possible at low nitrogen pressures but at higher nitrogen pressures the backward diffusion was diminished.

More recently, the reaction of active nitrogen

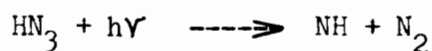
with H_2 has been re-examined by Kistiakowsky and Volpi (75). No detectable reaction was observed at room temperature and $300^\circ C$.

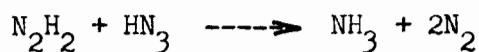
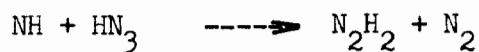
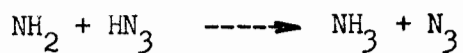
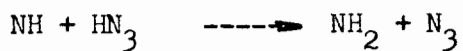
The NH radical has been identified by a number of workers. Rice and Frearno (174) studied the thermal decomposition of hydrazoic acid, HN_3 , at low pressures. A blue paramagnetic solid was trapped at the temperature of liquid nitrogen, but this solid disappeared when it was allowed to warm to $148^\circ K$. They assumed that hydrazoic acid decomposes according to the reaction



and that the blue colour and the paramagnetism of the solid is attributed to condensed NH radicals or to some polymer of NH. The blue solid could be also prepared by freezing the products of an electrical discharge through HN_3 (175).

Mador and Williams (176) made a spectroscopic investigation of the blue solid at $7^\circ K$. In the visible and ultra-violet regions, two broad absorption bands were observed near 3500 and 6500 \AA , due to the presence of NH and NH_2 respectively, in the blue solid. Becker et al. (177) found the existence of NH in the study of the photolysis of hydrazoic acid, in solid nitrogen, argon and xenon matrices at $20^\circ K$. They proposed the following mechanism



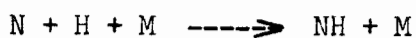


Bands due to NH_3 were identified.

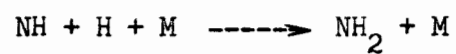
Foner and Hudson (178) made a mass spectroscopic study of the products of electrically dissociated hydrazine. They found the radicals, H, N, NH_2 and N_2H_2 and molecules H_2 , NH_3 , N_2 , H_2 , N_2H_4 and N_3H_3 . Since no NH radical was detected in these experiments, it seemed likely that NH must have a short life-time in this mixture.

Ruehrwein et al. (179) dissociated a mixture of H_2 and N_2 at a distance of only several centimeters from a trap cooled with liquid helium, in which all the gases condensed, and they found only a very small amount of NH_3 . There was no sign of a blue deposit similar to that derived from hydrazoic acid.

The electronic spectra of the NH and NH_2 radicals have been studied in detail by McCarty et al. (180). An argon-ammonia discharge (181) yields a detectable number of trapped NH_2 radicals, which were probably formed by the mechanism

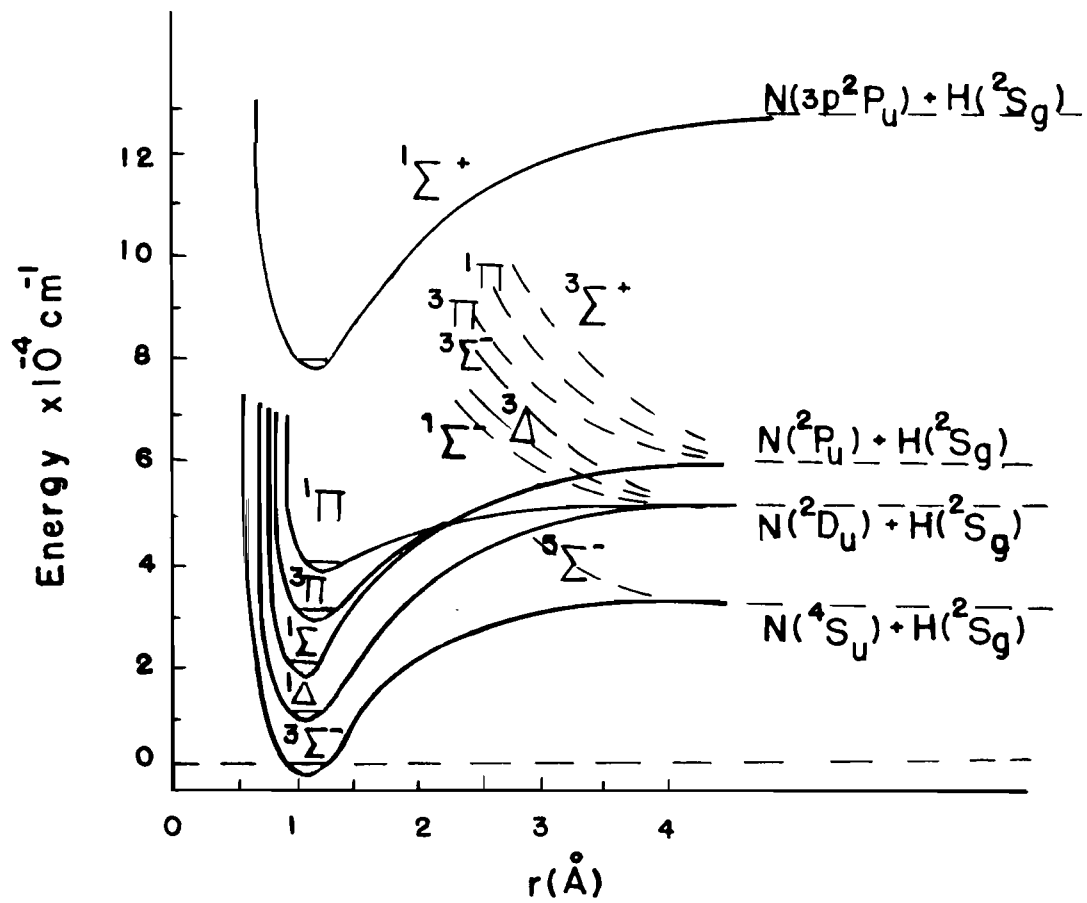


followed by



The potential energy curves of the observed electronic states of NH (48, 182) are shown in Fig. 11.

Figure 11
Potential Energy Curves of the
Observed Electronic States of NH



PART I

THE REACTION OF ACTIVE NITROGEN
WITH MOLECULAR OXYGEN^{*}

As indicated previously, it has been observed in this laboratory, from earlier studies, that the reactivity of active nitrogen is quite comparable towards a rather large variety of hydrocarbons and hydrocarbon derivatives, when the reactivity is measured by the maximum amount of HCN produced under given conditions. A recent study (77) has shown that the maximum HCN production corresponds closely to the maximum destruction of NO₂ but to be much less than the destruction of NO under similar conditions.

In seeking an explanation of the apparent discrepancy, the relative extent of the corresponding reaction of active nitrogen with molecular oxygen immediately became of interest. In addition to the maximum extent of the reaction, its products and kinetic characteristics were studied.

*The results of this study were presented at the symposium "Chemical Reactions in the Lower and Upper Atmosphere" held at San Fransisco, California, April 18-20, 1961, and will be published in the proceedings of the symposium.

EXPERIMENTAL

MATERIALS

Nitrogen, 99.9% pure, was obtained from Linde Company. It was passed through a trap cooled in liquid air to remove water and other impurities that might have been present.

Oxygen, of 99.6% purity (Liquid Carbonic Canadian Corp. Ltd.) was passed through a dry ice-acetone trap to remove water.

Nitrogen dioxide was prepared by treating pure nitric oxide (Matheson Co. Inc.) with an excess of pure oxygen. When the reaction was complete and the blue N_2O_3 was no longer present in the condensed material, the excess oxygen was pumped off. The nitrogen dioxide was normally condensed in a dry ice-acetone trap, when not in use, and KEL F stopcock grease was used in all parts of the apparatus in contact with the nitrogen dioxide. During the experiments, nitrogen dioxide was never allowed to come into contact with mercury. Frequent checks were made for the presence of N_2O_3 and if it was necessary, the oxidation was repeated.

Ethylene, 99% pure, was obtained from the Ohio Chemical Co. It was purified by two bulb-to-bulb distillations, in which only the middle fraction was retained.

APPARATUS

The apparatus was a fast flow system constructed entirely from Pyrex glass, similar to that used previously in this laboratory, and is shown diagrammatically in Figure 12.

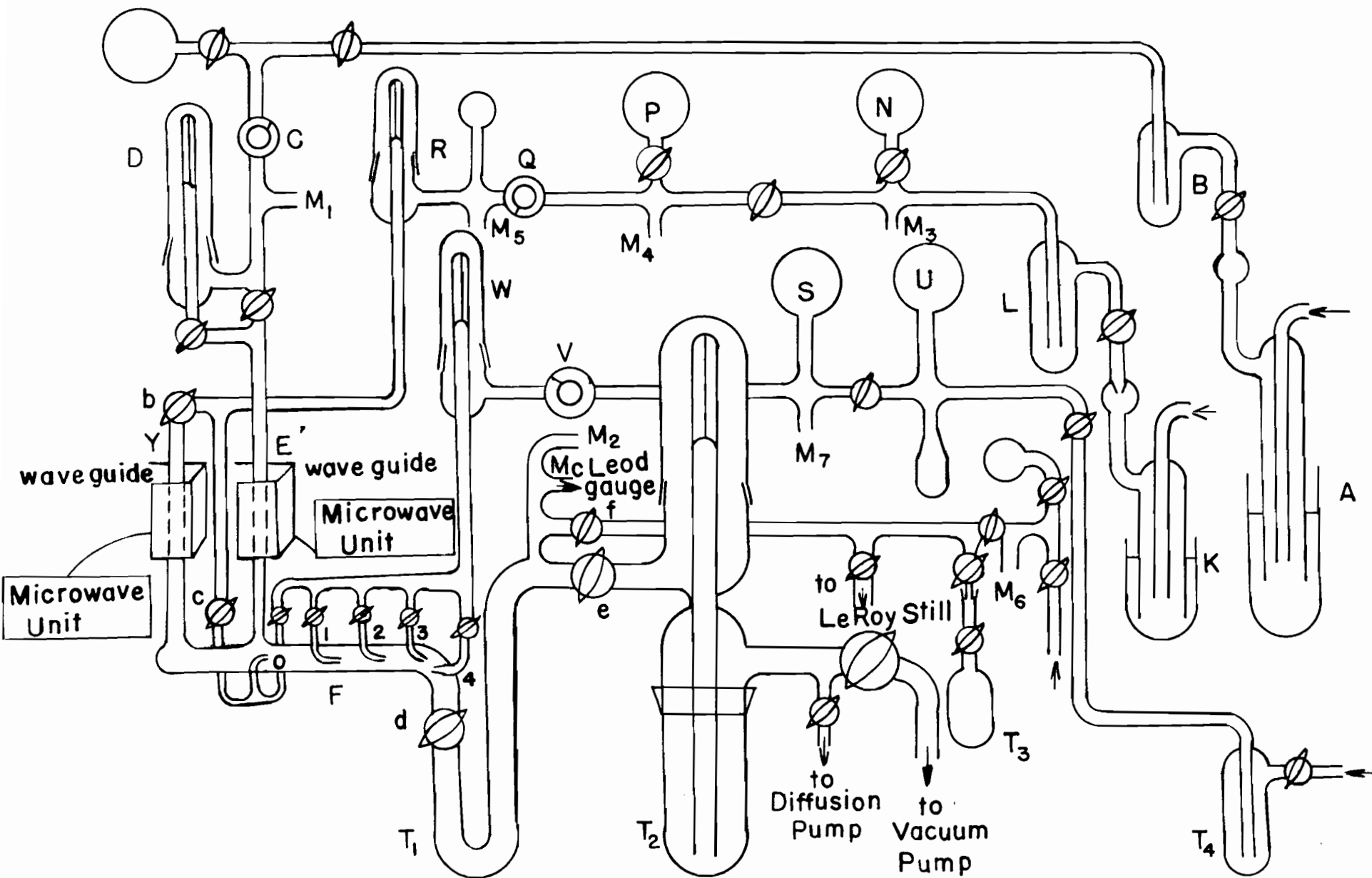
Nitrogen, from a cylinder, passed through a dibutyl phthalate manostat A, and a cold trap B, surrounded by liquid air. It then passed through a needle valve C, and a capillary flowmeter D, and finally entered the discharge tube, E.

The flow rate through the flowmeter D was determined by measuring the rate of evacuation from a known volume. During the experiment the flow rate through the capillary D was kept constant by properly adjusting the needle valve C, and measuring the flow head by the manometer M_1 .

The discharge tube, E, was made from a cylindrical quartz tube of 12 mm i.d., and 10 cm long. The nitrogen was dissociated by a microwave generator. The microwave equipment was a Raytheon 125-watt diathermy unit, operating at a frequency of 2400 Mc (Raytheon Manufacturing Co., Mass. U.S.A), with a rectangular waveguide around the discharge tube.

The reaction vessel, F, consisted of a pyrex tube of 20 mm i.d., and 26 cm long. Five small inlets were placed along the reaction tube at different distances. The reaction tube was heated, as required, with a suitable electric furnace,

Figure 12
DIAGRAM OF APPARATUS



and the temperature measured with a copper-constantan thermocouple. The pressure in the reaction vessel was measured by a McLeod gauge, and a dibutyl phthalate manometer, M_2 . For some experiments, the wall of the reaction tube was poisoned with 10% Na_2HPO_4 . After removal of the solution, the reaction vessel was heated to 300°C ., and the system evacuated for several hours to remove the excess water.

Tank oxygen, after passage through the manostat K, and the cold trap L, was stored in the flasks N and P. During the experiments, oxygen, from the flask P, passed through the needle valve Q, and the capillary flowmeter R, and entered the reaction vessel through the inlet O. The oxygen flow rate was determined from the pressure drop in a calibrated volume over a certain time, assuming the gas to be ideal. Different flow rates were obtained by varying the pressure, measured by manometer M_4 , across the capillary flowmeter R. During the experiment, the flow head of the manometer M_5 was kept constant by leaking in gas from the known volume P through the needle valve Q.

Nitrogen dioxide, was stored, when not in use, in the cold trap T_4 , and expanded in the flasks U and S. During any one experiment, nitrogen dioxide, from flask S was passed through the needle valve V, and the capillary flowmeter W, and entered the reaction vessel through any desired inlet jet located along the reaction tube (jets 1, 2, 3, 4). Since

NO₂ was used in excess in all the experiments, the precise determination of the NO₂ flow rate was not necessary.

For some experiments with ethylene, either the oxygen or the nitrogen dioxide line was used to introduce ethylene as a reactant. The ethylene flow rate was determined by calibration of the flowmeter in the same way as for nitrogen and oxygen.

The pumping system consisted of a Hypervac oil pump, capable of producing an ultimate vacuum in the system of about 4×10^{-3} mm. This was coupled with a mercury diffusion pump for evacuation of the system. Pressures were measured with a McLeod gauge.

PROCEDURE FOR A TYPICAL EXPERIMENT

Before each experiment, the traps B, T₁, T₂ and T₃ were immersed in liquid air, and the system was checked for leaks with the McLeod gauge. For experiments at high temperature, the furnace was turned on, and the experiment started when the desired temperature was achieved, as measured by the thermocouple. The nitrogen flow was then started, and the microwave discharge put into operation. Reaction was initiated by turning on the flow of the reactant, and allowed to proceed for a measured time. The flow rate of the reactant was maintained at the desired value by properly adjusting the needle valve Q, to keep the flow head of the manometer M₅ constant

(Fig. 12).

The reaction was stopped by shutting off the flow of the reactant and the discharge simultaneously. The nitrogen flow was then stopped, and the system was evacuated for several minutes. The trap T_1 was isolated from the system by shutting off the stopcocks d and e (Fig. 12), the stopcock f was turned on, and the liquid air removed to allow the products to distill into the first trap, T_3 , of the analytical system.

To condense ozone or nitric oxide, in a series of experiments with oxygen, the trap T_1 was immersed in liquid nitrogen, which was boiled at a reduced pressure of about 10 cm, to produce a temperature of about -210° C.

In the experiments in which two reactants, in addition to active nitrogen, were used, the only difference in the procedure was that the reaction was started or stopped by turning on or shutting off the flow of both reactants (stopcocks c and one of the four located along the reaction tube, say, 1) simultaneously.

ANALYSIS

When the products consisted of a mixture of small amounts of NO, NO₂ and N₂O, they were analysed by the method developed by Verbeke and Winkler (77). The mixture was condensed in the bulb T_3 , to which was attached a manometer M_6

(Fig. 12). A known pressure of oxygen, P_1 , was introduced to oxidize all the nitric oxide in the mixture, and the pressure P_2 was measured. The mixture was condensed in liquid nitrogen, and the excess oxygen pumped off. On warming up, the pressure P_3 was measured. The partial pressure of nitric oxide could be obtained by

$$P_{NO} = 2(P_1 + P_3 - P_2)$$

The bulb was then immersed on a dry ice-acetone bath, the nitrous oxide was pumped off, and the pressure P_4 , of nitrogen dioxide measured. The partial pressure of nitrous oxide was given by

$$P_{N_2O} = P_3 - P_4$$

where P_4 was the sum of nitrogen dioxide and nitric oxide.

In some experiments, a mixture of ozone and nitrous oxide had to be analyzed, and this was done as follows: The mixture was distilled from the trap T_1 (Fig. 12) into a LeRoy still surrounded with liquid nitrogen. The amount of ozone was determined by distilling it, at -180° C., from the LeRoy still into the bulb T_3 , which contained a 2% solution of neutral potassium iodide frozen in liquid nitrogen, and then warming the solution to absorb the ozone*. The liberated

* A number of explosions occurred during the analysis.

iodine was titrated against 0.1 N thiosulfate solution. The amount of nitrous oxide was estimated by expanding it into a known volume, and applying the ideal gas equation.

The amount of nitric oxide in products containing an excess of nitrogen dioxide, together with small amounts of nitrous oxide, was determined by condensing the mixture in the bulb T_3 (Fig. 12) frozen in liquid air. A known pressure of oxygen, measured by the manometer M_6 , was admitted, after which the stopcock of the bulb, T_3 , was shut off and the liquid air removed to permit oxidation of the nitric oxide. After several minutes, when the oxidation was complete, the bulb was again immersed in liquid air, and the pressure measured. The difference between the two readings gave the pressure of oxygen consumed at liquid air temperature. By calibrating the system at liquid air temperature and 25° C., the amount of oxygen consumed was estimated at 25° C. Multiplication by two gave the amount of nitric oxide present in the mixture at 25° C. The unreacted oxygen was then pumped off, while the products were kept at liquid air temperature, and the pressure of nitrous oxide was determined by allowing it to expand from a dry ice-acetone trap (to retain nitrogen dioxide) into a known volume. "Blank" experiments with known amounts of nitric oxide showed that this method was accurate to within about $\pm 3\%$.

Hydrogen cyanide, produced in the reaction of active

nitrogen with ethylene, was determined by distilling it from the cold trap T_1 into a removable absorber T_3 (Fig. 12) containing 15 ml of distilled water and immersed in liquid air. A layer of carbon tetrachloride was frozen around the trap T_1 after the liquid air had been removed, to prevent rapid warming of the contents, and minimize polymerization of the hydrogen cyanide. The amount of hydrogen cyanide present was determined by titration with silver nitrate, according to the Liebig-Deniges method (183).

RESULTS

When oxygen was introduced into the active nitrogen stream, no change in the colour of the yellow afterglow was observed at room temperature. At elevated temperatures, above about 100° C., and with high oxygen flow rates, the yellow afterglow of active nitrogen was replaced by a blue glow. When the temperature was increased, the blue glow occurred at lower oxygen flow rates, while further increase in the oxygen flow rate at a given temperature left the blue glow unchanged. The change of colour from yellow to blue occurred only gradually with increase in the flow rate of oxygen. The blue glow was probably due to the β bands of nitric oxide, in accordance with the observation made by Kistiakowsky and Volpi (100).

At low flow rates of oxygen, the condensable products were small amounts of nitrous oxide, nitrogen dioxide and nitric

oxide. These experiments were prolonged for 30 minutes or more, to facilitate analysis of the products. At higher flow rates of oxygen, only ozone and nitrous oxide were obtained in measurable amounts. The duration of these experiments was less than 10 minutes. In both series of experiments, the reaction vessel was poisoned with Na_2HPO_4 and the products were condensed in the trap frozen at -210°C ., (liquid nitrogen at a pressure of about 10 cm).

The presence of nitric oxide and nitrogen dioxide was obvious from the blue colour of the solid nitrogen trioxide formed in the cold trap. The identification of nitrous oxide was made by mass spectroscopic and infra-red analyses, and from its vapour pressure curve, using a LeRoy still. The dark blue solid formed in the cold trap indicated the presence of ozone. A series of experiments was made at a pressure 3.3 mm., with an unheated reaction tube and at 400°C . The results are shown in Tables I and II. Figure 13 indicates the relation between the ozone produced and the oxygen flow rate, for the two temperature conditions.

Various materials were introduced at the end of the reaction tube in an attempt to remove oxygen atoms, or active nitrogen, or both, from the gas stream, and thus to minimize their attack on any oxides of nitrogen that might be formed. Copper wire coated with oxide was found to extinguish the nitrogen afterglow, but it did not cause quantitative re-

TABLE I

PRODUCTION OF OZONE AND OXIDES OF NITROGEN IN THE REACTION
OF ACTIVE NITROGEN WITH OXYGEN

N₂ Pressure : 3.30 mm. Hg.

N₂ Flow Rate : 227.7 x 10⁻⁶ mole/sec.

Reaction Vessel Poisoned with Na₂HPO₄

Unheated Reaction Vessel

O ₂ Flow Rate <u>mole/sec.</u>	O ₃ Produced <u>mole/sec.</u>	NO Produced <u>mole/sec.</u>	NO ₂ Produced <u>mole/sec.</u>	N ₂ O Produced <u>mole/sec.</u>
0.73 x 10 ⁻⁶	-	-	0.44 x 10 ⁻⁸	2.9 x 10 ⁻⁸
2.0	-	0.18 x 10 ⁻⁸	0.40	3.5
4.0	-	0.26	1.0	3.5
5.2	-	-	1.4	3.9
6.4	-	-	1.6	3.9
7.7	0.01 x 10 ⁻⁶	-	-	5.5
9.2	0.09	-	-	3.9
11.7	0.40	-	-	3.9
17.0	0.50	-	-	4.0
18.1	0.42	-	-	4.0
20.5	0.54	-	-	6.0
25.8	0.70	-	-	5.8
29.6	0.95	-	-	5.5
35.4	0.86	-	-	6.0
37.0	1.00	-	-	6.0
38.0	1.01	-	-	6.0
44.2	0.95	-	-	6.7
49.2	1.00	-	-	6.0
55.1	0.98	-	-	6.0
55.4	1.00	-	-	6.0

TABLE II

PRODUCTION OF OZONE AND OXIDES OF NITROGEN IN THE REACTION
OF ACTIVE NITROGEN WITH OXYGEN

N₂ Pressure : 3.30 mm. Hg.

N₂ Flow Rate : 227.7 x 10⁻⁶ mole/sec.

Reaction Vessel Poisoned with Na₂HPO₄

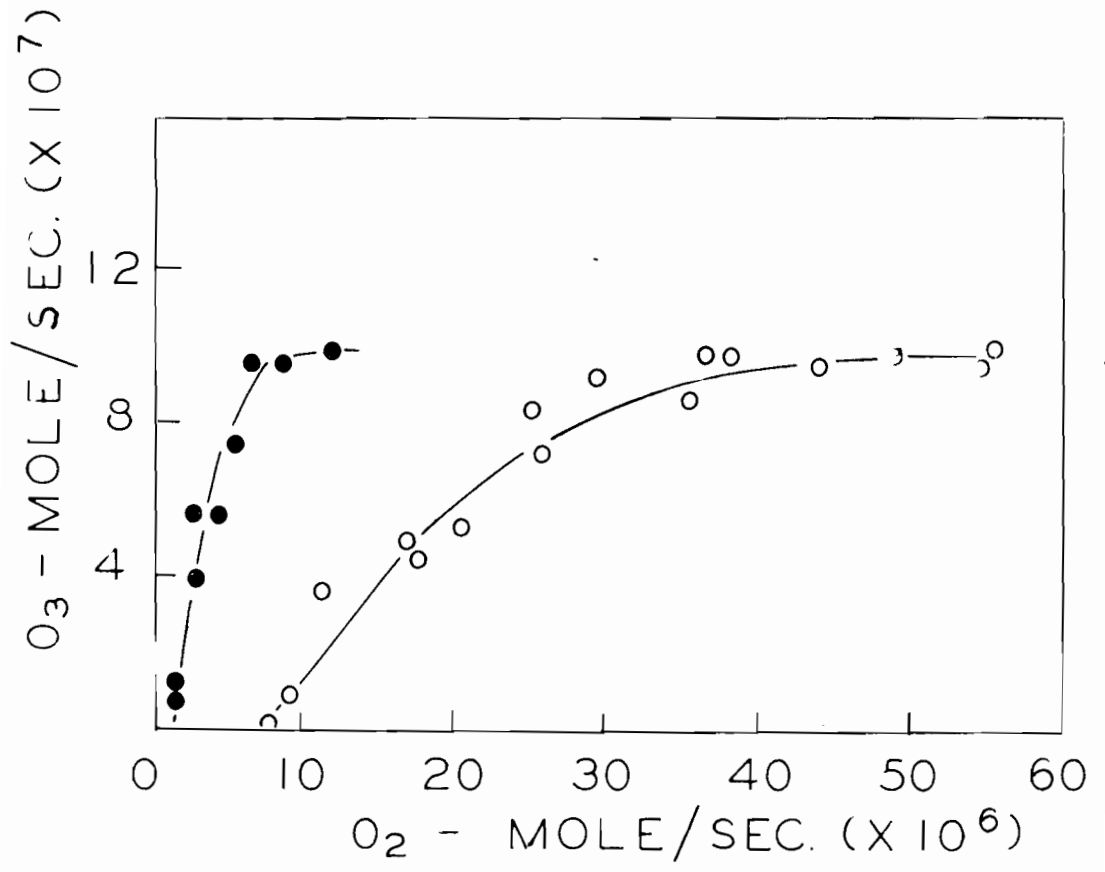
Temperature : 400° C.

O ₂ Flow Rate <u>mole/sec.</u>	O ₃ Produced <u>mole/sec.</u>	NO Produced <u>mole/sec.</u>	NO ₂ Produced <u>mole/sec.</u>	N ₂ O Produced <u>mole/sec.</u>
1.5 x 10 ⁻⁶	0.12 x 10 ⁻⁶	-	-	3.2 x 10 ⁻⁸
1.6	0.08	-	-	3.2
2.5	0.41	-	-	2.7
3.1	0.58	-	-	3.2
4.6	0.58	-	-	3.2
5.1	0.75	-	-	3.2
5.9	0.98	-	-	3.2
8.9	0.97	-	-	3.2
12.0	1.00	-	-	3.2

Figure 13

Plot of Ozone Produced vs Oxygen Flow Rate

- with unheated reaction vessel
- with reaction vessel heated at 400° C.



combination of oxygen atoms. Gold and platinum wires did not quench the nitrogen afterglow completely, and glass wool seemed to be without any effect. Several experiments with the ethylene-active nitrogen reaction in the presence and absence of glass wool yielded identical amounts of hydrogen cyanide. Repetition of the experiments with thoroughly cleaned glass wool gave the same result. The results are shown in Table III and Fig. 14.

Silver wire coated with oxide appeared to remove oxygen atoms completely. This was indicated by the observation that, with the oxide coated wire in place in an unpoisoned reaction tube at 400° C., in the presence of a reaction mixture of active nitrogen with a large excess of oxygen, no nitric oxide was formed by the introduction of excess nitrogen dioxide, with which oxygen atoms should react rapidly to produce nitric oxide (111). The only product trapped in the experiments was a small amount of nitrous oxide (less than 0.1 μ mole/sec), and the same was true when the experiments were repeated without the introduction of the nitrogen dioxide. Apparently nitric oxide did not survive in appreciable amounts, in these experiments, as a product of the active nitrogen-oxygen reaction. This agrees with earlier studies that show its destruction by active nitrogen to be very fast (75), although Clyne and Thrush (103) have concluded from spectroscopic observations that some nitric oxide (less than 10% of the

TABLE III

REACTION OF ACTIVE NITROGEN
WITH ETHYLENE

N₂ Pressure : 4.2 mm. Hg.

Temperature : 400° C.

A. With glass wool

Ethylene Flow Rate <u>mole/cc. x 10⁶</u>	Maximum HCN Production <u>mole/sec. x 10⁶</u>
12.3	1.22
23.8	1.74
29.6	1.66
37.8	1.98
49.1	2.30
53.2	2.12
67.6	2.38
73.2	2.25
85.9	2.35

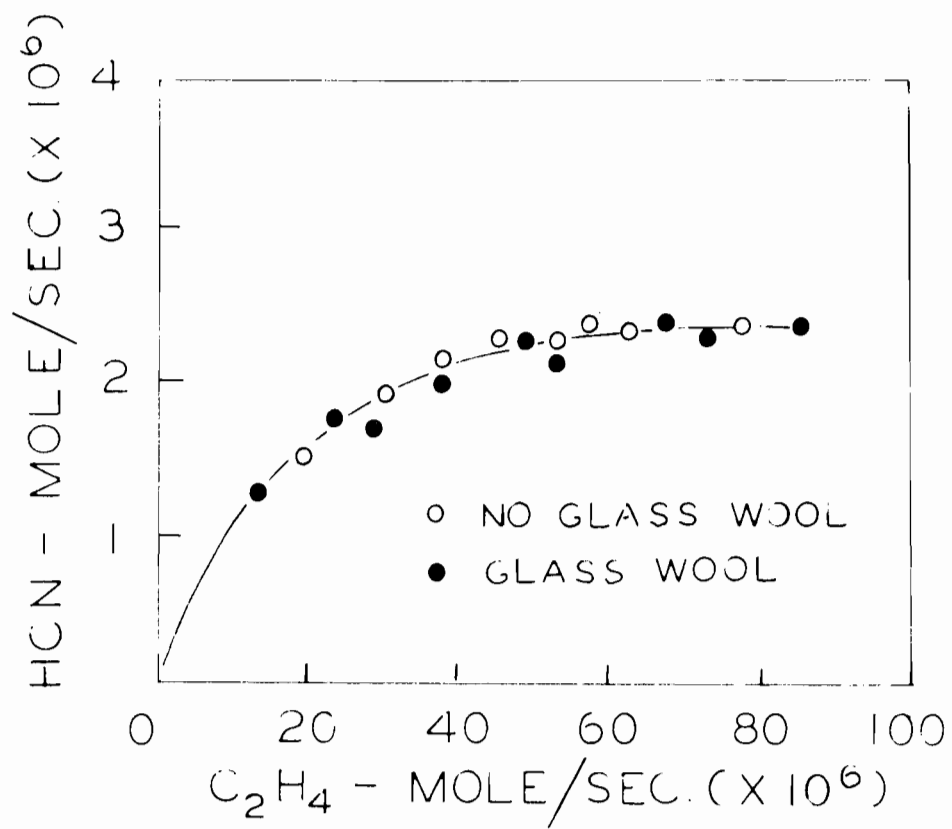
B. No glass wool

19.2	1.53
30.5	1.92
38.0	2.12
45.7	2.30
53.4	2.25
57.5	2.35
62.8	2.30
78.1	2.38

Figure 14

Plot of Maximum Yield of HCN vs Ethylene Flow Rate

- no glass wool
- glass wool



initial nitrogen atom concentration) is present under similar, but not identical conditions.

In an unpoisoned reaction tube, with no silver wire present and with experiments of 100 seconds duration, the addition of excess nitrogen dioxide to reaction mixtures of active nitrogen with excess oxygen yielded no product in measurable amount, other than nitric oxide derived from the reaction of oxygen atoms with the nitrogen dioxide added.

The maximum oxygen atom concentrations were determined, therefore, under such conditions by introducing an excess of pure nitrogen dioxide at the end of the reaction tube (inlet jet 4 in Fig. 12), and trapping the nitric oxide formed as nitrogen trioxide at -192° C. The nitric oxide then was determined as described previously. The maximum oxygen atom concentrations thus determined at 400° C., over the pressure range from 1 mm. to 6 mm. Hg., are shown in Table IV and Fig. 15.

The maximum amounts of hydrogen cyanide formed in the reaction of active nitrogen with ethylene were determined under the same experimental conditions as those that prevailed in the corresponding reaction with molecular oxygen. All determinations were made at 100° C., 150° C., and 400° C., over the pressure range from 1 mm. to 6 mm. Hg. The results are shown in Table IV and Fig. 15. The data recorded represent the average values of many experiments for both reactions.

TABLE IV

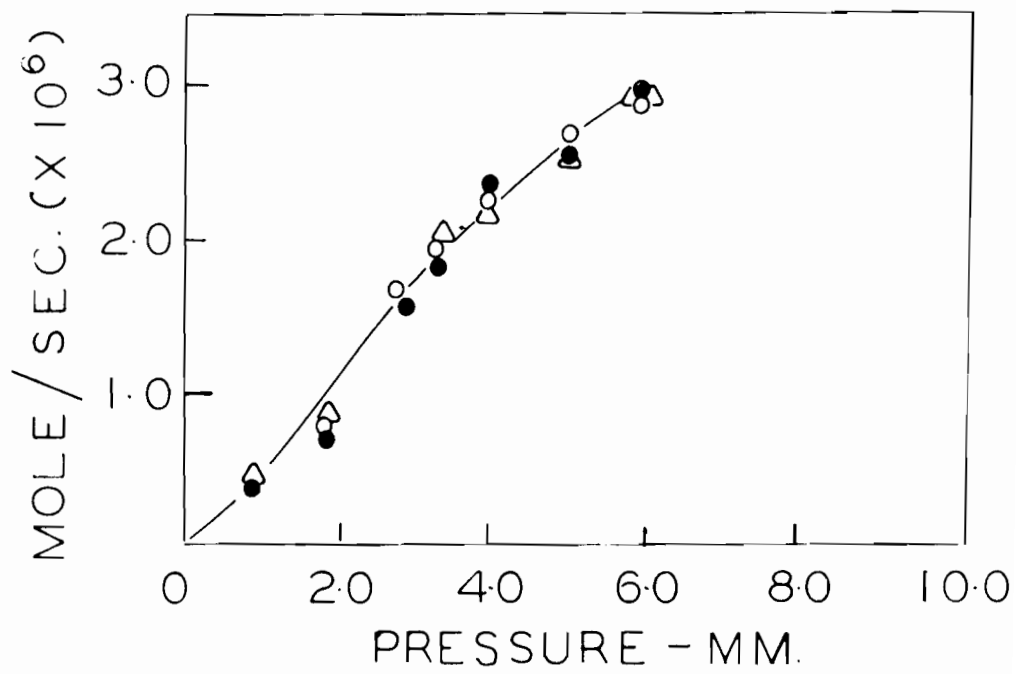
MAXIMUM YIELD OF HCN AND OXYGEN ATOMS FROM THE REACTIONS OF
ACTIVE NITROGEN WITH ETHYLENE AND OXYGEN RESPECTIVELY, AT
VARIOUS TEMPERATURES AND NITROGEN PRESSURES

Unpoisoned Reaction Tube

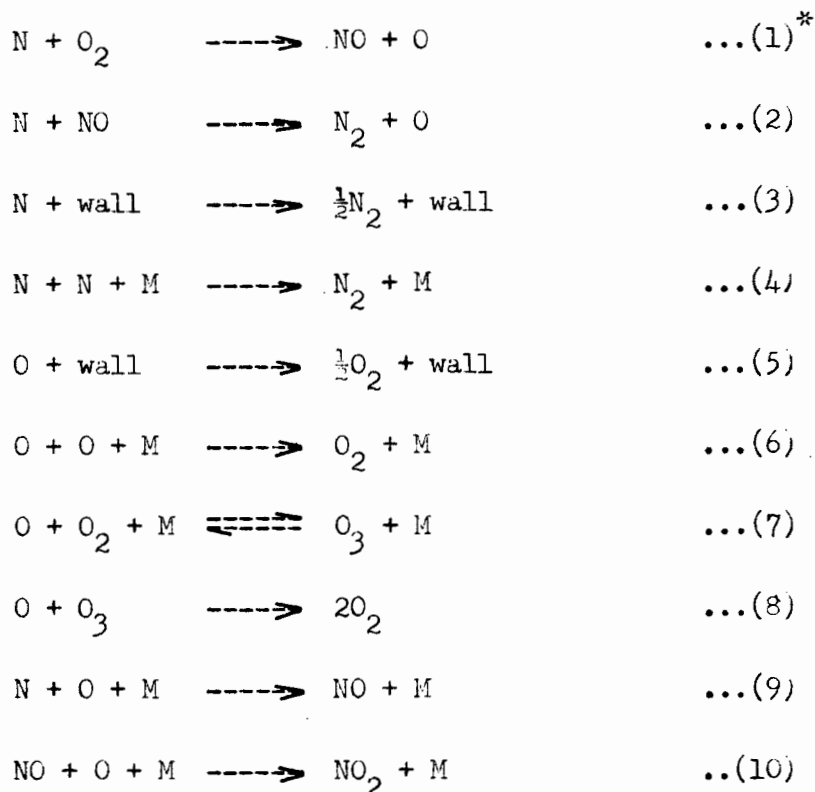
N_2 Total Pressure mm. Hg.	Temp. $^{\circ}C.$	Max. HCN Production mole/sec. $\times 10^6$	Max. Oxygen Atom Production mole/sec. $\times 10^6$
1.0	400	0.40	0.46
2.0	400	0.735	0.88
2.0	150	0.80	
3.3	400	1.86	1.92
3.3	150	1.90	1.92
4.0	400	2.35	2.24
4.0	150	2.25	
5.0	400	2.53	2.56
5.0	150	2.65	
6.0	400	2.94	2.88
6.0	150	2.84	
6.0	100	2.74	

Figure 15
Plot of Maximum Yield of HCN and Oxygen Atoms
from the Reactions of Active Nitrogen with
Ethylene and Oxygen, Respectively, vs Total Pressure

- HCN at 400° C.
- HCN " 150° C.
- △ Oxygen Atoms at 400° C.



The following reactions may be involved, in the gas mixture of active nitrogen with molecular oxygen:



By addition of excess nitrogen dioxide at different positions in the reaction tube (inlet jets 1, 2, 3, 4; Fig. 12), it was possible to show that the maximum production of

* Throughout this manuscript, the following notation has been used: Chemical reactions are indicated by a number in parenthesis, preceded the word reaction, e.g., reaction (1); mathematical equations are identified by a number in square brackets, preceded by the word equation, e.g., equation [1], and references are shown simply by a number in parenthesis, e.g., (1).

oxygen atoms in the unpoisoned tube was independent of temperature (over the range 150°C. to 350°C.), at a given pressure (3.3 mm. or 4.3 mm.) at different points in the reaction tube. The data for the maximum production of oxygen atoms at different temperatures are shown in Table V. Since these maximum values for oxygen atom production are independent of temperature and position in the tube, they have been assumed to correspond to the initial nitrogen atom concentrations, $(N)_0$, and are recorded as such in Table VIII. In none of these experiments was nitrous oxide detected in the reaction products. These data also suggest that, within the experimental errors involved, oxygen and nitrogen atoms do not disappear by the reactions 3-10 to an appreciable extent.

This conclusion agrees with a calculated upper limit of about 5% and 3.5% decay of oxygen and nitrogen atoms in the system respectively, based on available data for the rate constants of the reactions involved (133, 137, 67, 69, 70). Reaction (3) should be of secondary importance at pressures higher than 2.5 mm. (69, 71). The termolecular reactions (9) and (10) may be neglected since neither nitric oxide nor nitrogen dioxide was found to exist in the reaction products, as indicated previously, and they are slower than reactions (1) and (2). Hence, rate constants for the reaction of active nitrogen with oxygen may be obtained from measurements of the oxygen atom concentration resulting from reactions (1)

TABLE V

MAXIMUM OXYGEN ATOM PRODUCTION FROM
THE REACTION OF ACTIVE NITROGEN
WITH OXYGEN, AT VARIOUS TEMPERATURES*

N₂ Pressure : 3.3 mm.

Distance from O₂ inlet jet : 23.5 cm.

Unpoisoned Reaction Tube

<u>O₂</u> <u>Flow Rate</u> <u>mole/sec. x 10⁶</u>	<u>Oxygen Atom</u> <u>Production</u> <u>mole/sec. x 10⁶</u>	<u>Max. Oxygen Atom</u> <u>Production</u> <u>mole/sec. x 10⁶</u>
<u>Temperature 300° C.</u>		
3.25	2.24	
4.05	2.56	
4.55	2.77	
5.20	3.20	
5.85	3.20	
6.50	3.20	
		3.20
<u>Temperature 253° C.</u>		
5.20	2.70	
5.50	3.04	
5.85	3.20	

* A new micro-wave generator was used in these experiments.

Table V (cont'd)

6.17 3.20

6.50 3.20

3.20

Temperature 240° C.

6.50 2.88

7.15 3.20

7.80 3.20

10.4 3.20

3.20

Temperature 225° C.

7.80 3.05

8.45 3.20

8.77 3.20

9.75 3.20

3.20

Temperature 200° C.

9.20 2.56

10.25 2.88

11.00 3.00

11.37 3.20

11.70 3.20

12.35 3.20

3.20

Temperature 175° C.

11.05 2.56

Table V (cont'd)

11.37	2.66
11.70	2.88
12.35	3.20
13.0	3.20
13.52	3.20
14.95	3.20

3.20

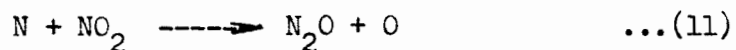
Temperature 150° C.

12.35	2.56
14.00	2.88
15.2	3.20
15.6	3.20
16.57	3.20

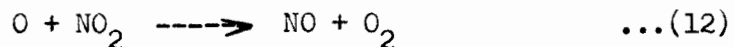
3.20

and (2).

To estimate the oxygen atom concentration under conditions of incomplete consumption of active nitrogen, advantage was taken of the observation that active nitrogen reacts with nitrogen dioxide to produce nitrous oxide (77). A series of experiments was made in which nitrogen dioxide was introduced into active nitrogen. It was found that, with the low nitrogen atom concentration used, the only condensed products were small and equal amounts of nitrous oxide and nitric oxide, which presumably were formed by the reaction sequence,



followed by



The data are shown in Table VI. Since, as above, no measurable nitrous oxide is produced in the reaction of active nitrogen with excess oxygen in the unpoisoned vessel, it was assumed that the same would be true when oxygen was not present in excess. Hence, the oxygen atom concentration, resulting from reactions (1) and (2), could be determined by subtracting the amount of nitrous oxide formed in reaction (11) from the total nitric oxide produced in the attack of nitrogen dioxide by oxygen atoms derived from reactions (1), (2) and (11).

The oxygen atom production from the reaction of active nitrogen

TABLE VI

NITROUS AND NITRIC OXIDE PRODUCED
FROM THE REACTION OF ACTIVE NITROGEN
WITH EXCESS NITROGEN DIOXIDE

N₂ Pressure : 3.3 mm.

Temperature : 240° C.

Unpoisoned Reaction Tube

N ₂ O Produced <u>mole/sec. x 10⁶</u>	NO Produced <u>mole/sec. x 10⁶</u>
0.867	0.88
0.900	0.96
0.867	0.80

with oxygen, and the amount of nitrous oxide produced from reaction (11) at different temperatures, are recorded in Table VII.

Rate constants for the reaction of active nitrogen with oxygen were calculated from data obtained by adding excess nitrogen dioxide at different positions in the reaction tube (inlet jets 1, 2, 3, 4; Fig. 12), for a range of relatively low flow rates of oxygen. All experiments were continued for 100 seconds. On the assumption that reaction (1) is rate determining, rate constants were calculated from the integrated rate equation

$$k_1 = \frac{2.303}{t[(N)_o - 2(O_2)_o]} \log \frac{(O_2)_o}{(N)_o} \times \frac{(N)_o - (O)_t}{(O_2)_o - (O)_t/2}$$

adapted to fast flow system, with complete mixing, to yield the expression

$$k_1 = \frac{2.303 b^2 (RT)^2}{[(N)_o - 2(O_2)_o]VP^2} \log \frac{(O_2)_o}{(N)_o} \times \frac{(N)_o - (O)_t}{(O_2)_o - (O)_t/2}$$

where :

k_1 = second order rate constant

$(N)_o$ = initial nitrogen atom flow rate, from the maximum values of oxygen atom production

TABLE VII

OXYGEN ATOM PRODUCTION FROM THE REACTION
OF ACTIVE NITROGEN WITH OXYGEN
AND NITROUS OXIDE PRODUCED FROM
REACTION (11) AT VARIOUS TEMPERATURES

N₂ Pressure : 3.3 mm.

Distance from O₂ inlet jet : 23.5 cm.

Unpoisoned Reaction Tube

<u>O₂</u> Flow Rate <u>mole/sec. x 10⁶</u>	<u>O + N₂O</u> Produced <u>mole/sec. x 10⁶</u>	<u>N₂O Produced</u> From Reaction (11) <u>mole/sec. x 10⁶</u>	<u>Oxygen Atom</u> Production <u>mole/sec. x 10⁶</u>
<u>Temperature 300° C.</u>			
2.40	1.92	0.32	1.60
3.90	2.42	0.22	2.20
5.40	3.20	-	3.20
6.00	3.20	-	3.20
<u>Temperature 253° C.</u>			
2.60	1.96	0.32	1.64

Table VII (cont'd)

3.25	2.15	0.25	1.90
5.20	2.70	0.14	2.56
5.85	3.20	-	3.20
6.50	3.20	-	3.20

Temperature 240° C.

3.90	1.92	0.32	1.60
5.52	2.24	0.22	2.02
5.85	2.40	0.22	2.18
7.15	3.20	-	3.20
8.50	3.20	-	3.20

Temperature 225° C.

4.87	2.30	0.20	2.10
7.47	2.90	0.12	2.78
8.77	3.20	-	3.20
9.25	3.20	-	3.20

Temperature 200° C.

9.75	2.80	0.14	2.66
11.00	3.00	0.10	2.90
11.70	3.20	-	3.20

Table VII (cont'd)

12.60	3.20	-	3.20
<u>Temperature 175° C.</u>			
8.12	1.92	0.32	1.60
9.10	2.24	0.22	2.02
13.00	3.20	-	3.20
14.00	3.20	-	3.20
14.95	3.20	-	3.20
<u>Temperature 150° C.</u>			
12.35	2.56	0.16	2.40
13.00	2.72	0.10	2.62
14.30	2.90	0.07	2.83
15.60	3.20	-	3.20
16.00	3.20	-	3.20
16.57	3.20	-	3.20

- $(O_2)_o$ = initial flow rate of oxygen added
 $(O)_t$ = flow rate of oxygen atoms at time t
t = reaction time
b = total flow rate
V = volume of the reaction tube
P = total pressure
T = absolute temperature
R = gas constant

The values of the rate constants are given in Table VIII, for various operating conditions. The data yield a satisfactory Arrhenius plot, shown in Fig. 16, from which an activation energy of 5.9 kcal/mole may be estimated, with a pre-exponential factor 2.3×10^{12} cc mole⁻¹ sec⁻¹. Thus, the rate constant may be written

$$k_1 = 2.3 \times 10^{12} \exp(-5,900/RT) \text{ cc mole}^{-1} \text{ sec}^{-1}$$

When $\log k_1$ is plotted against $(\frac{1}{2} \log T - E/2.3RT)$, Fig. 17, the intercept of the best straight line on the ordinate of $\log k_1$ is about 11, i.e., the rate constant may be expressed

$$k_1 = 10^{11} T^{\frac{1}{2}} \exp(-5,900/RT) \text{ cc mole}^{-1} \text{ sec}^{-1}$$

over the range of temperatures used.

$$\text{A pre-exponential factor of } 9.9 \times 10^{12} T^{\frac{1}{2}} \text{ cc mole}^{-1} \text{ sec}^{-1}$$

TABLE VIII

VARIATION OF k_1 AS A FUNCTION OF REACTION TIME, PRESSURE, TEMPERATURE
AND INITIAL REACTANT CONCENTRATIONS

N_2 Pressure: 3.3 mm. Hg., N_2 Flow Rate 212×10^{-6} mole/sec.

N_2 Pressure: 4.3 mm. Hg., N_2 Flow Rate 308×10^{-6} mole/sec.

Unpoisoned Reaction Tube

Distance from O_2 inlet jet (cm.)	Pressure mm. Hg.	$(O_2)_0$ mole/sec. $\times 10^6$	$(N)_0$ mole/sec. $\times 10^6$	Oxygen Atom Production mole/sec. $\times 10^6$	k_1 cc.mole ⁻¹ .sec ⁻¹
Temperature: 350°C.					
3.7	3.3	5.85	3.20	1.58	1.99×10^{10}
3.7	4.3	5.85	3.84	1.24	2.28
7.3	3.3	5.20	3.20	1.80	2.29
7.3	4.3	3.25	3.84	1.25	2.31
14.0	3.3	2.60	3.20	1.50	2.05
14.0	4.3	3.25	3.84	1.70	1.85

Table VIII (cont'd)

23.5	3.3	1.78	3.20	1.50	1.92
23.5	4.3	3.90	3.84	2.66	2.00

Average $k_1 = 2.08 \times 10^{10}$

Linear velocity in the reaction tube at 3.3 mm. pressure: 798.0 cm/sec.
 " " " " " " " " 4.3 mm. pressure: 885.0 cm/sec.

Temperature 300°C.

3.7	3.3	4.87	3.20	0.72	1.26×10^{10}
7.3	3.3	4.22	3.20	1.26	1.46
7.3	4.3	4.55	3.84	1.20	1.25
14.0	3.3	2.60	3.20	1.33	1.40
14.0	4.3	4.22	3.84	1.90	1.35
23.5	4.3	3.90	3.84	2.35	1.29
23.5	4.3	2.60	3.84	1.80	1.33
23.5	3.3	3.25	3.20	2.00	1.30
23.5	3.3	3.90	3.20	2.20	1.27

Average $k_1 = 1.33 \times 10^{10}$

Linear velocity in the reaction tube at 3.3 mm. pressure: 734.0 cm/sec.
 " " " " " " " " 4.3 " " : 814.0 cm/sec.

Table VIII (cont'd)

Temperature: 253°C.

3.7	3.3	7.15	3.20	0.98	0.98×10^{10}
3.7	4.3	7.15	3.84	1.24	1.16
7.3	3.3	5.85	3.20	1.42	0.99
7.3	4.3	5.85	3.84	1.47	1.07
14.0	3.3	2.60	3.20	1.17	0.97
14.0	4.3	5.20	3.84	2.13	1.06
23.5	3.3	5.20	3.20	2.56	1.07
23.5	4.3	3.25	3.84	2.03	1.05

Average $k_1 = 1.04 \times 10^{10}$

Linear velocity in the reaction tube at 3.3 mm. pressure: 674.0 cm/sec.
 " " " " " " " 4.3 " " : 747.0 cm/sec.

Temperature 240°C.

3.7	3.3	7.80	3.20	0.93	7.78×10^9
3.7	4.3	7.15	3.84	0.81	7.63
7.3	3.3	5.85	3.20	1.10	6.93
14.0	3.3	4.55	3.20	1.60	7.88

Table VIII (cont'd)

14.0	4.3	3.90	3.84	1.38	7.36
23.5	3.3	5.85	3.20	2.18	6.16

Average $k_1 = 7.29 \times 10^9$

Linear velocity in the reaction tube at 3.3 mm. pressure: 657.0 cm/sec.
" " " " " " " " 4.3 " " : 729.0 cm/sec.

Temperature 225°C.

3.7	3.3	9.10	3.20	0.93	6.55×10^9
3.7	4.3	8.12	3.84	0.81	6.74
14.0	3.3	5.20	3.20	1.60	6.55
14.0	4.3	5.85	3.84	1.90	6.87
23.5	3.3	7.47	3.20	2.78	7.35
23.5	3.3	4.87	3.20	2.10	6.12

Average $k_1 = 6.70 \times 10^9$

Linear velocity in the reaction tube at 3.3 mm. pressure: 638.0 cm/sec.
" " " " " " " " 4.3 " " : 707.0 cm/sec.

Temperature 200°C.

3.7	3.3	9.42	3.20	0.92	5.30×10^9
-----	-----	------	------	------	--------------------

Table VIII (cont'd)

3.7	4.3	9.10	3.84	0.81	5.08
14.0	3.3	5.62	3.20	1.50	4.75
14.0	4.3	5.85	3.84	1.70	5.10
23.5	3.3	9.75	3.20	2.66	4.60
23.5	4.3	8.45	3.84	2.66	4.49

$$\text{Average } k_1 = 4.90 \times 10^9$$

Linear velocity in the reaction tube at 3.3 mm. pressure: 606.0 cm/sec.
 " " " " " " " " 4.3 " " : 672.0 cm/sec.

Temperature 175°C.

3.7	3.3	12.3	3.20	0.91	3.16×10^9
3.7	4.3	11.7	3.84	0.81	3.14
14.0	3.3	6.5	3.20	1.17	2.70
14.0	4.3	6.5	3.84	1.38	3.12

$$\text{Average } k_1 = 3.03 \times 10^9$$

Linear velocity in the reaction tube at 3.3 mm. pressure: 574.0 cm/sec.
 " " " " " " " " 4.3 mm. " : 636.0 cm/sec.

Temperature 150°C.

3.7	3.3	12.3	3.20	0.92	2.80×10^9
-----	-----	------	------	------	--------------------

Table VIII (cont'd)

14.0	3.3	5.8	3.20	1.17	2.62
14.0	4.3	7.5	3.84	1.38	2.40
23.5	3.3	13.0	3.20	2.62	2.66
23.5	3.3	14.3	3.20	2.83	2.90

Average $k_1 = 2.70 \times 10^9$

Linear velocity in the reaction tube at 3.3 mm. pressure: 543.0 cm/sec.
" " " " " " 4.3 " " : 600.0 cm/sec.

Figure 16
Arrhenius Plot of $\text{Log } k_1$ vs $1/T$

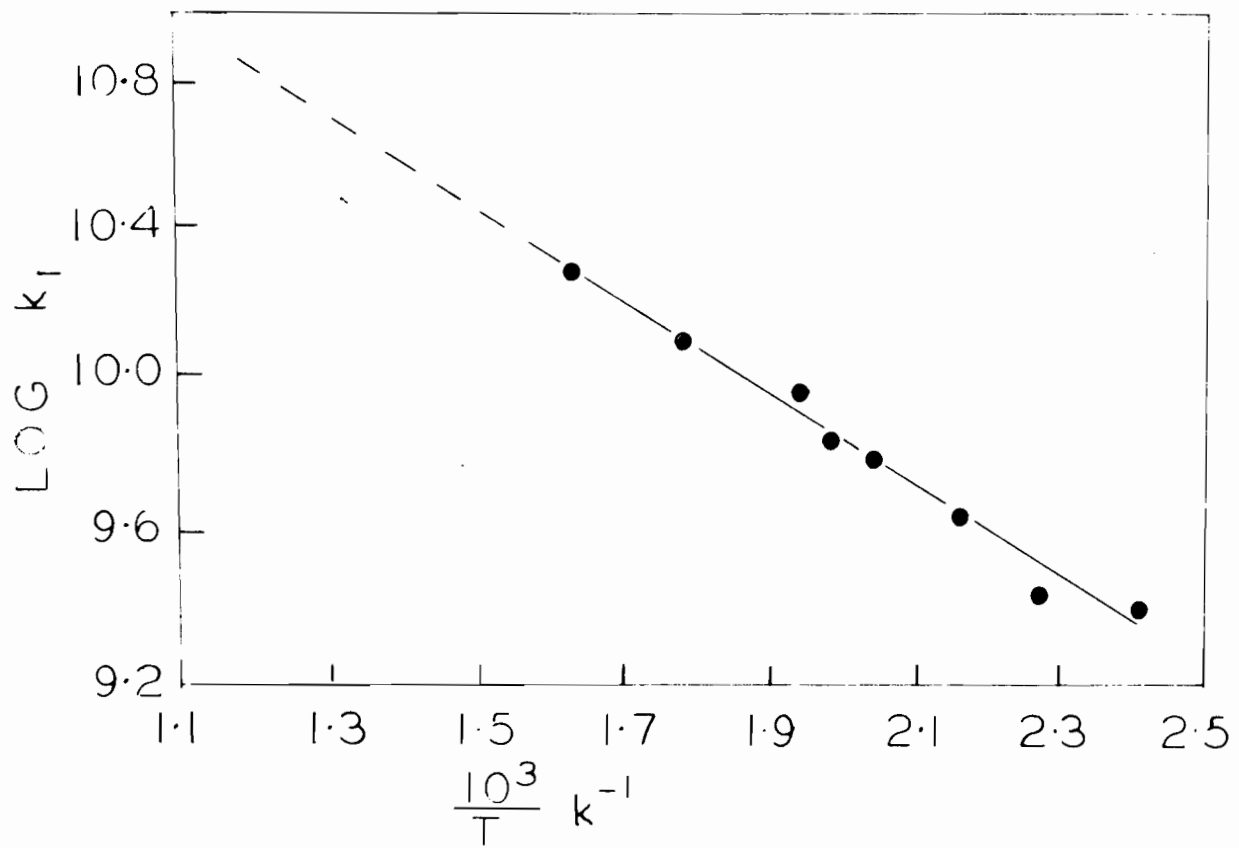
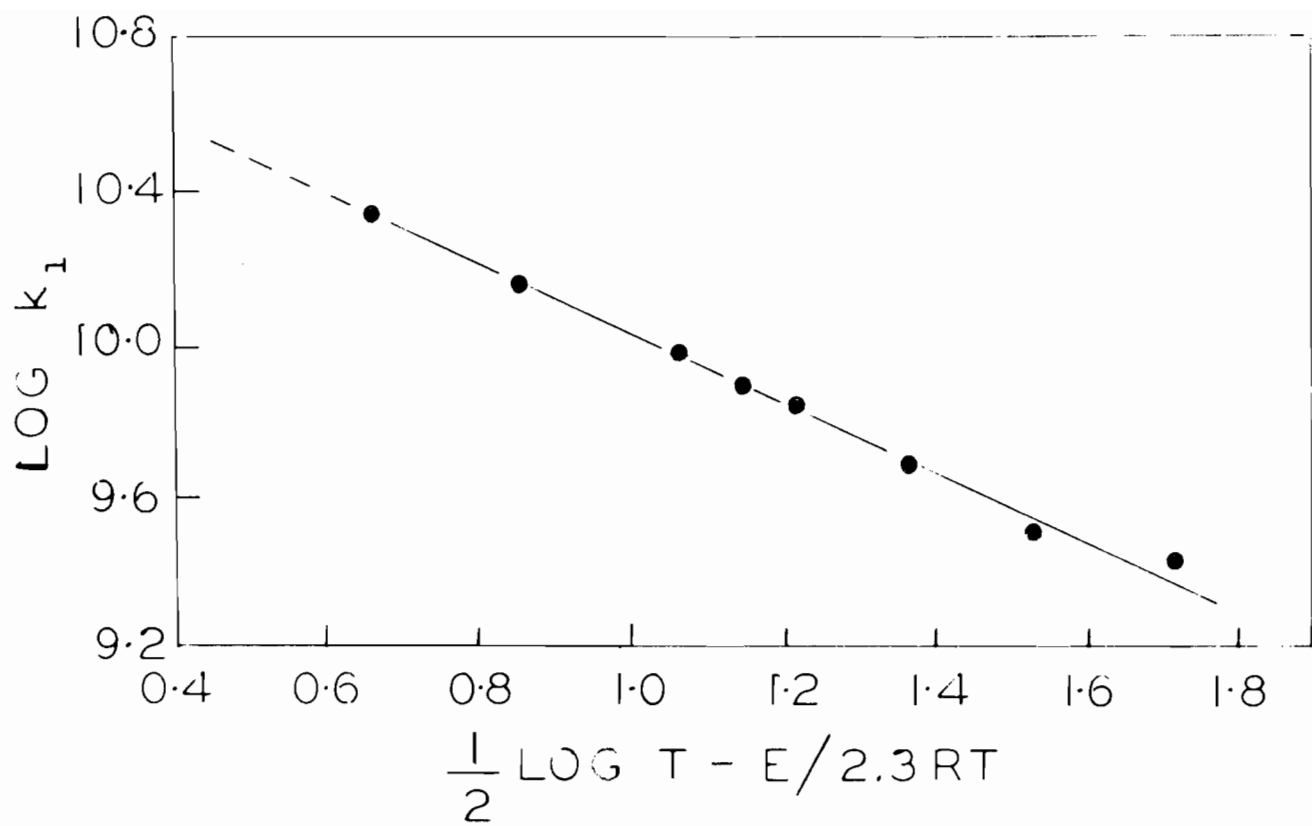


Figure 17

Plot of $\text{Log } k_1$ vs $(\frac{1}{2}\text{Log}T - E/2.3RT)$



was calculated by the hard-sphere collision theory, assuming collisions diameter of 2.98 Å and 3.61 Å for the nitrogen atom and oxygen molecule respectively. Comparison of the calculated and experimental pre-exponential terms gives a probability factor of 10^{-2} .

DISCUSSION

The data in Table IV and Fig. 15 suggest that, at any given total pressure, the maximum production of hydrogen cyanide by the reaction of active nitrogen with ethylene was virtually independent of temperature in the straight reaction tube used in these experiments. This is in marked contrast to the rather large effect of temperature on hydrogen cyanide production in this reaction, and several other active nitrogen-hydrocarbon reactions, when these were studied in spherical vessels (cf. 81, 92). It seems likely that the discrepancy may be attributed to some change in physical characteristics, such as flow pattern, in vessels of different shapes.

It is also apparent from Table IV (Fig. 15) that the maximum production of oxygen atoms in the active nitrogen-oxygen reaction corresponds well with the maximum production of hydrogen cyanide from ethylene under comparable conditions. This presumably means that the same species, probably atomic nitrogen, 4S , is involved in the two reactions. Also, the reaction of active nitrogen with oxygen apparently bears a

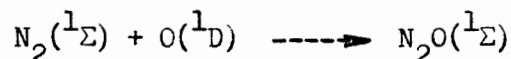
closer resemblance to the active nitrogen-nitrogen dioxide reaction than it does to the corresponding nitric oxide reaction, which suffers a larger maximum extent of reaction (77). The same observation was made in the present study, when active nitrogen flow was estimated by the nitric oxide titration, although Clyne and Thrush (103) have recently reported that nitric oxide and oxygen react with active nitrogen to the same extent. The present study, therefore, appears to strengthen the suggestion that the nitric oxide reaction is exceptional, but the reasons for the apparently exceptional behaviour remain obscure.

The results in Table III and Fig. 14 suggest that no appreciable recombination of nitrogen atoms occurred on the surface of glass wool, in spite of the very large increase in surface area represented. This was an unexpected observation, since nitrogen atoms are known to recombine on the surface of glass (pyrex, quartz), and to smaller extent on surfaces of glass coated with different salts (e.g., Na_2HPO_4 , H_3PO_4). The behaviour might be related to the phenomena observed by Harteck and his co-workers when active nitrogen is allowed to impinge on metal surfaces (c.f. Introduction).

It is interesting, perhaps, that nitrous oxide was present in small, but measurable amounts in the products from a poisoned reaction tube (Table I and II), but seemed to be formed in much smaller amounts, if at all, in an unpoisoned

tube. In the presence of ozone, the amount of nitrous oxide measured may be fictitious because of the carbon dioxide formed by the attack of ozone on stopcock grease.

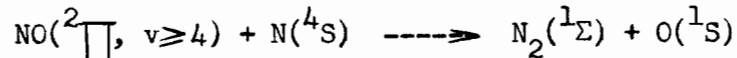
The existence of nitrous oxide in the products of the active nitrogen-oxygen reaction has been observed by Varney (106), but Kistiakowsky and Volpi (100) and Clyne and Thrush (103) have failed to find it. The failure of the last investigations might be due to the small amount of nitrous oxide present in this reaction, and to the experimental techniques used. No satisfactory explanation of this difference can be offered, particularly since the mechanism for the formation of nitrous oxide in the system is not known. It is possible that it results from the fast reaction of active nitrogen with small amounts of nitrogen dioxide that may be formed in the active nitrogen-oxygen reaction (77). Alternatively, it might be produced by the reaction of $O(^1D)$ atoms with nitrogen molecules as postulated by De More and Davidson (184)



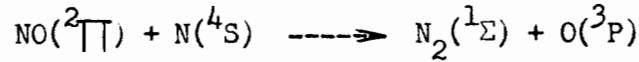
Young and Clark (185) have suggested a mechanism for production of $O(^1D)$ atoms that might be applicable to the present system:



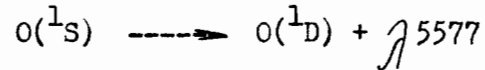
followed by the spin-disallowed reaction



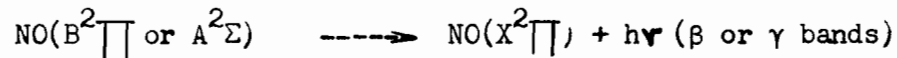
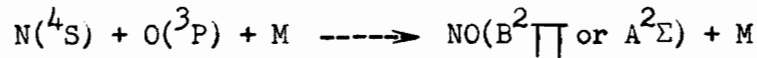
together with the spin-allowed reaction



and



Reaction of $\text{O}({}^3\text{P})$ may produce (101) $\text{NO}({}^2\Pi)$ by



The reaction of active nitrogen with molecular oxygen is undoubtedly



followed by



As indicated earlier, the rate constant k_1 was found to be (Table VIII, Figures 16 and 17)

$$k_1 = 2.3 \times 10^{12} \exp(-5,900/RT) \text{ cc mole}^{-1} \text{ sec}^{-1}$$

or, in the form of

$$k_1 = 10^{11} T^{\frac{1}{2}} \exp(-5,900/RT) \text{ cc mole}^{-1} \text{ sec}^{-1}$$

* Value of ΔH based on data given in ref. (48).

over the range of temperature from 150°C. to 350°C. with a probability or steric factor of 10^{-2} . This may be compared with the values found in other investigations:

$$k_1 = 2 \times 10^{12} \exp(-6,200/RT) \text{ cc mole}^{-1} \text{ sec}^{-1}$$

(Kistiakowsky and Volpi-ref. 100)

$$k_1 = 1.7 \times 10^{13} \exp(-7,500/RT) \text{ cc mole}^{-1} \text{ sec}^{-1}$$

(Kaufman-ref. 107)

$$k_1 = 8.3 \times 10^{12} \exp(-7,100/RT) \text{ cc mole}^{-1} \text{ sec}^{-1}$$

(Clyne and Thrush-ref. 103)

In view of the quite different experimental methods used, the agreement would seem to be satisfactory.

APPROXIMATE CALCULATION OF THE PRE-EXPONENTIAL FACTOR
FOR THE REACTION OF ATOMIC NITROGEN WITH MOLECULAR OXYGEN

To calculate the pre-exponential factor of the rate constant for the reaction $N + O_2$, the configuration and vibration frequencies of the activated complex must be known. The ground state $N(^4S)$ atom contains three unpaired electrons in p orbitals. The normal oxygen molecule is in the $^3\Sigma$ state and contains two unpaired electrons, the two oxygen atoms being held by a single bond and two three-electron bonds (186).

The three unpaired electrons of the nitrogen atom and the two of the oxygen molecule can be paired to yield

activated complexes in either doublet, quartet or sextet states. Their configuration can be either linear (${}^2\Sigma^+$, ${}^4\Sigma^+$, ${}^6\Sigma^+$) or non-linear (${}^2A'$, ${}^4A'$, ${}^6A'$)*. For a non-linear complex, with an uncoupled electron, the structure may be similar to that of nitrogen dioxide, although Walsh (187) claimed that the nitrogen dioxide might be expected to be linear in the excited states.

Some calculations of Magee (188) on a system of two s electrons and one p electron seem to indicate that the directed valence, introduced by the p electron, lowers the activation energy for the formation of the resulting triangular complex below that which is obtained for a linear complex. Approximate estimations of the pre-exponential factor have been made for both a linear and a non-linear activated complex, using the transition state theory.

The specific rate constant, for a linear complex, assuming a transmission coefficient of unity** (since the reaction is spin favourable), is given by

*The prime means that the state concerned is symmetric in respect of reflection in the plane of the molecule.

**The transmission coefficient is defined as the probability that a system which has reached the activated state will continue to the final state. For spin-allowed reactions, its value is close to unity (189).

$$\begin{aligned}
 k_1 &= \frac{kT}{h} K^* \\
 &= \frac{kT}{h} \cdot \frac{g^*}{g_N g_{O_2}} \cdot \frac{\frac{(2\pi m^* kT)^{3/2}}{h^3}}{\frac{(2\pi m_N kT)^{3/2}}{h^3}} \cdot \frac{\frac{8\pi^2 I^* kT}{\sigma^* h^2}}{\frac{(2\pi m_{O_2} kT)^{3/2}}{h^3} \cdot \frac{8\pi^2 I_{O_2} kT}{h^2 \sigma_{O_2}}} \\
 &\quad \cdot \frac{\prod_{i=1}^3 (1 - e^{-h \nu_i^*/kT})^{-1}}{(1 - e^{-h \nu_{O_2}^*/kT})^{-1}} \cdot e^{-E_o/RT} \\
 &= \frac{g^*}{g_N g_{O_2}} \cdot \frac{h^2}{(2\pi)^{3/2} (kT)^{1/2}} \cdot \left(\frac{m^*}{m_N m_{O_2}} \right)^{3/2} \cdot \frac{I^* \sigma_{O_2}}{I_{O_2} \sigma^*} \\
 &\quad \cdot \frac{\prod_{i=1}^3 (1 - e^{-h \nu_i^*/kT})^{-1}}{(1 - e^{-h \nu_{O_2}^*/kT})^{-1}} \cdot e^{-E_o/RT}
 \end{aligned}$$

where:

k_1 = second order rate constant

k = the Boltzmann constant

h = " Planck "

g_N = the electronic statistical weight of the nitrogen atom

g_{O_2} = " " " " " " oxygen molecule

g^* = the electronic statistical weight of the activated complex

σ_{O_2} = the symmetry number of O_2

σ^* = " " " " the activated complex

m_N = the mass of the nitrogen atom

m_{O_2} = " " " " oxygen molecule

m^* = " " " " activated complex

I_{O_2} = the moment of inertia of the oxygen molecule

I^* = " " " " " " activated complex

ν_{O_2} = the vibrational frequency of the oxygen molecule

ν^* = " " " " " " activated complex

π = 3.14

The nuclear spin contributions are omitted, since the reaction is not accompanied by any change in ortho-para ratio. The activated complex contains three atoms, and since there are three ordinary translational degrees of freedom and one degree of translational along the decomposition coordinate, the partition function will contain three vibrational terms. The vibration frequencies of the activated state may be expected to be of the same order as those for an excited NO_2 , and as a rough approximation, they will be assumed to be the same

as for the normal NO_2 .

Normal NO_2 has two stretching vibrations, the symmetric 1617.75 cm^{-1} and the anti-symmetric 1317.0 cm^{-1} , and a symmetric bending 750.6 cm^{-1} (190, 191). For the temperature range of interest i.e., up to 600° K ., only the lowest frequency of 750.6 cm^{-1} is significant, and the other two have been neglected. The vibration frequency of O_2 is high, and its partition function is effectively unity. The moment of inertia of O_2 was taken from spectroscopic data (48), $I_{\text{O}_2} = 19.35 \times 10^{-40} \text{ g. cm}^2$, while that for the activated complex, was calculated from the formula

$$I^* = \frac{1}{m_{\text{O}} + m_{\text{O}} + m_{\text{N}}} [m_{\text{O}}(m_{\text{O}} + m_{\text{N}})r_{\text{N-O}}^2 + 2m_{\text{O}} m_{\text{N}} r_{\text{N-O}} r_{\text{O-O}} + m_{\text{O}}(m_{\text{O}} + m_{\text{N}})r_{\text{O-O}}^2]$$

where: m_{O} and m_{N} are the masses of oxygen and nitrogen atoms respectively and $r_{\text{N-O}}$ and $r_{\text{O-O}}$ are the distances of N and O and of O and O in the activated complex respectively. Assuming an N-O distance of 1.22 \AA (close to the normal), and O-O separation of 5 \AA (by analogy with the H-H separation in the activated state for H_2) (192), I^* takes the value of $I^* = 567.7 \times 10^{-40} \text{ g. cm}^2$. The symmetry numbers are taken to be $\sigma_{\text{O}_2} = 2$, and $\sigma^* = 2$ (for the activated complex could be either N---O---O or O---O---N).

The electronic statistical weights are derived from

spectroscopic measurements. The O_2 is in the $^3\Sigma$ state, but as the three levels are very close together, the corresponding statistical weight may be taken as 3 and that of $N(^4S)$ as 4, whence $g_N g_{O_2} = 4 \times 3$. The products of the reaction are $NO(^2\Pi)$ + $O(^3P)$ with statistical weights:

$$g_{NO} = 2(1 + e^{-343/kT}) = 3.1$$

where the factor of 2 is due to the Λ -type doubling^{**}, and for $O(^3P_2, ^3P_1, ^3P_0)$

$$g_O = 5 + 3 e^{-450/kT} + e^{-640/kT} = 6.76^{***}, \text{ at } T = 300^\circ K$$

It follows, therefore, that g^* may be either 12 (corresponding to $N(^4S) + O_2(^3\Sigma)$) or 21 (corresponding to $NO(^2\Pi) + O(^3P)$). There is also a possibility that the activated state may have the same electronic multiplicity as NO_2 , i.e., 2, in which case $g^*/g_N g_{O_2} = 2/3 \times 4 = 1/6$. However, since it is difficult to say whether the activated state partakes more of the nature of loosely coupled reactants or of a rather stable association

^{**} For states with $\Lambda \neq 0$, i.e., Π, Δ, \dots , the interaction between the rotation of the molecule and the electronic orbital angular momentum produces a splitting of each rotational level into two closely spaced sublevels, the so-called Λ -type doubling.

^{***} $k = 1.986 \text{ cal/mole.degree}$

complex (193), the values of $g^*/g_N g_{O_2} = 1/6, 1/3$ and $1/2$ corresponding to $^2\Sigma, ^4\Sigma$ and $^6\Sigma$ terms of the activated state respectively, will be used in the calculations.

The result for a linear complex is

$$k_1 = \frac{g^*}{g_N g_{O_2}} 1.468 \times 10^{14} \times T^{-\frac{1}{2}} (1 - e^{-1080/T})^{-1} \times e^{-E_o/RT}$$

cc mole⁻¹ sec⁻¹

To compare this with the experimental value, E_o , the activation energy at 0° K., is substituted by

$$E_{\text{exp.}} = RT^2 \frac{\partial \ln k_1}{\partial T} = E_o - \frac{1}{2} RT + \frac{1080R}{e^{1080/T} - 1}$$

and

$$k_1 = \frac{g^*}{g_N g_{O_2}} 8.8 \times 10^{13} \times T^{-\frac{1}{2}} \times \frac{e^{\frac{1080}{T}(e^{1080/T} - 1)}}{1 - e^{-1080/T}} e^{-E_{\text{exp.}}/RT}$$

For a non-linear activated complex, the rate constant is given by

$$k_1 = \frac{kT}{h} \cdot \frac{g^*}{g_N g_{O_2}} \cdot \frac{\frac{(2\pi m^* kT)^{3/2}}{h^3} \cdot \frac{8\pi^2 (8\pi^3 ABC)^{1/2}}{h^3 \sigma^*} (kT)^{3/2}}{\frac{(2\pi m_N kT)^{3/2}}{h^3} \cdot \frac{(2\pi m_{O_2} kT)^{3/2}}{h^3} \cdot \frac{8\pi^2 I_{O_2} kT}{h^2 \sigma_{O_2}}}$$

$$\begin{aligned}
 & \frac{2}{(1 - e^{-h\nu_{O_2}^*/kT})} \cdot e^{-E_0/RT} \\
 & \frac{2}{(1 - e^{-h\nu_{O_2}^*/kT})} \cdot e^{-E_0/RT} \\
 & = \frac{g^*}{g_N g_{O_2}} \cdot \left(\frac{m^*}{m_N m_{O_2}} \right)^{3/2} \cdot \frac{(ABC)^{1/2}}{I_{O_2}} \cdot \frac{\sigma_{O_2}^h}{\sigma^*} \cdot \frac{(1 - e^{-h\nu_{O_2}^*/kT})}{(1 - e^{-h\nu^*/kT})} \\
 & \quad \cdot e^{-E_0/RT}
 \end{aligned}$$

where A, B and C are the three moments of inertia and the remaining symbols are as defined previously. Assuming a structure of the activated complex similar to that of NO₂, the three moments of inertia may be obtained from spectroscopic data (190):

$$A = 3.49 \times 10^{-40}, \quad B = 64.47 \times 10^{-40} \quad \text{and} \quad C = 67.96 \times 10^{-40} \text{ g.cm}^2,$$

and $\sigma^* = \sigma_{NO_2} = 2$. The result is

$$k_1 = \frac{g^*}{g_N g_{O_2}} \times 2.84 \times 10^{12} \cdot \frac{e^{\frac{1080}{T}(e^{1080/T} - 1)}}{1 - e^{-1080/T}} e^{-E_{exp.}/RT}$$

The results, shown in Table IX, indicate a reasonable agreement between the observed and calculated pre-exponential terms, although many uncertainties are involved in the calculations. Also it is very difficult to say which structure

TABLE IX

CALCULATED AND OBSERVED PRE-EXPONENTIAL

FACTORS FOR THE N + O₂ REACTION

Temperature °K	Pre-exponential Factor x 10 ⁻¹² cc mole ⁻¹ sec ⁻¹						Experimental (10 ¹¹ T ^{1/2})
	Calculated			Experimental			
	Linear			Non-linear			
	2 _Σ ⁺	4 _Σ ⁺	6 _Σ ⁺	2 _A [']	4 _A [']	6 _A [']	
373.2	0.90	1.80	2.70	0.57	1.15	1.67	1.93
473.2	0.95	1.89	2.83	0.67	1.34	2.01	2.17
573.2	1.00	2.00	3.00	0.78	1.55	2.32	2.40
673.2	1.05	2.10	3.15	0.88	1.76	2.64	2.60

of the activated complex is more probable.

As indicated previously, the reaction of nitrogen atoms with oxygen molecules produces $\text{NO}(\Sigma^2\Pi)$ in the $v = 6$ vibrational level (185). This corresponds to a vibrational energy $E_v (v = 6) = 33.6$ kcal/mole. Application of Smith's theory of "Participation of Vibration in Exchange Reactions" (194) yields the kinematic factor $\sin^2\beta$, where β is the angle of rotation required to take a coordinate system describing the reactants into one suited to the products. It is given by

$$\tan^2\beta = \frac{m_O}{m_N} + \frac{m_O}{m_N} + \frac{m_O^2}{m_N m_O} = 23/7$$

or

$$\sin^2\beta = 0.77 \quad .$$

Assuming the energy of the reaction to be $-\Delta H = E = 32.8$ kcal/mole*, the predicted vibrational energy is given by

$$E_v(\text{theoretical}) = 32.8 \times 0.77 = 25.25 \text{ kcal/mole}$$

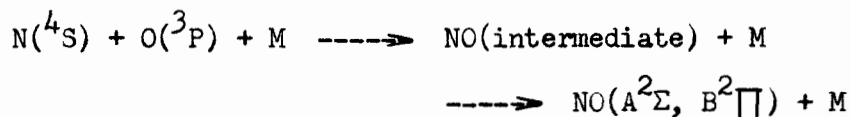
The agreement would seem to be satisfactory, since the difference between the experimental and predicted vibrational energy, 8.4 kcal/mole, could be attributed to the choice of the values used for the derivation of the energy of the reaction.

*Based on data given in ref.(48).

PART II

THE REACTION OF NITROGEN ATOMS WITH OXYGEN ATOMS
IN THE ABSENCE OF OXYGEN MOLECULES
AND THE HOMOGENEOUS AND HETEROGENEOUS RECOMBINATION
OF NITROGEN ATOMS

As mentioned in the introduction, the reaction of nitrogen atoms with oxygen atoms has been found (140, 101) spectroscopically to follow the scheme



No previous study of the kinetics of this reaction has been made.

The homogeneous and heterogeneous recombination of nitrogen atoms has recently been studied in this laboratory (71, 72) as a function of pressure, with the maximum hydrogen cyanide production, resulting from ethylene or ethane, taken as a measure of atomic nitrogen concentrations in a system poisoned with different salts.

A study of the reaction of nitrogen atoms with oxygen atoms in the absence of oxygen molecules was undertaken in an attempt to elucidate the kinetic characteristics of

this reaction. Since homogeneous and heterogeneous recombination of nitrogen atoms is involved in the active nitrogen-oxygen atom reaction, and the heterogeneous recombination depends on the conditions of the walls of the reaction vessel used, a re-investigation of both reactions was undertaken by methods that differ from those used in the previous investigation.

EXPERIMENTAL

MATERIALS

Nitric oxide was obtained from the Matheson Co. Nitrogen dioxide, water and nitrogen were the impurities present. Nitrogen was pumped off while the gas was kept at the temperature of liquid nitrogen. It was then purified by two distillations from a frozen pentane bath at -130° C.

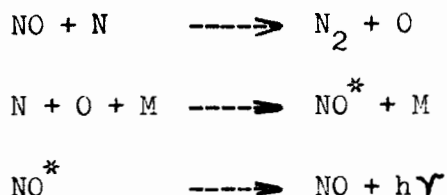
Nitrogen was purified as described previously.

PROCEDURE

The apparatus was the same as that used for the reaction of active nitrogen with molecular oxygen, depicted in Fig. 12.

Nitrogen atom concentrations were determined by a gas phase titration with nitric oxide. This titration method, as described in the introduction, has been developed by Kistiakowsky

and Volpi (100) and Kaufman (101), and consists briefly of the following: Sufficient nitric oxide is added to the active nitrogen to carry to completion, the reactions



However, not enough is added to give the NO + O continuum. The process involves the change of colours from yellow to blue, and then from blue to yellow-green. The change of colour from blue to yellow-green is sharp, and the flow rate of nitric oxide at the end-point corresponds to the nitrogen atom concentration (100, 101).

For the study of the decay of nitrogen atoms, nitrogen entered the reaction tube as described previously, while nitric oxide, from the bulb S, passed through the needle valve V and the flowmeter W, and entered the reaction tube through any one of the inlet jets located along the reaction tube (jets 0, 1, 2, 3, 4; Fig. 12). The flow rate of nitric oxide was determined by the pressure drop, measured by the dibutyl phthalate manometer M_7 , in a calibrated volume after a given time interval. The experiment was started by turning on the nitrogen flow and the microwave discharge. The nitrogen atom concentration along the reaction tube was determined by adding nitric oxide at the different jet positions, and

measuring the pressure, by the manometer M_7 , at which the end-point of the "titration" occurred. Since the system was calibrated, the pressure readings gave the corresponding nitric oxide flow rates.

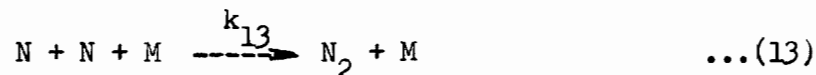
For the active nitrogen-oxygen atom reaction, oxygen atoms were produced by the introduction of nitric oxide to an excess active nitrogen. With the nitrogen flow and the discharge both in operation, nitric oxide, from the bulb P (Fig. 12), passed through the needle valve Q and the flowmeter R, and entered the reaction tube through the jet O. During the experiment, the flow rate of nitric oxide was kept constant by properly adjusting the needle valve Q. The amount of oxygen atoms produced at the point O is then given by the flow rate of NO at this point, since the reaction of active nitrogen with NO is very fast. The disappearance of nitrogen atoms from the excess active nitrogen remaining in the system after jet O was then estimated by titration with nitric oxide at subsequent jet positions (jets 1, 2, 3, 4; Fig. 12) along the reaction tube.

All the experiments were made in the dark to facilitate estimation of the end-point of the titration. The reaction tube was unheated and unpoisoned for the whole series of experiments.

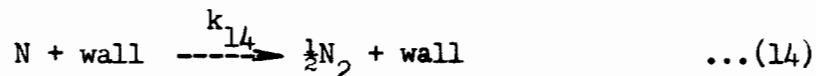
RESULTS AND DISCUSSION

THE DECAY PROCESSES OF NITROGEN ATOMS

The disappearance of nitrogen atoms, due to the recombination process may be attributed to the homogeneous recombination



where M is a third body, and to the heterogeneous or surface reaction



where k_{14} is a pseudo first-order rate constant.

If it is assumed that the only reaction that occurs is the homogeneous recombination of nitrogen atoms (reaction 13)), the rate expression is

$$-\frac{d(N)}{dt} = k_{13}(M)(N)^2$$

and the integrated equation for k_{13} is given by

$$k_{13} = \frac{1}{(M)(t_2 - t_1)} \left[\frac{1}{(N)_{t_2}} - \frac{1}{(N)_{t_1}} \right] \quad [1]$$

where $(N)_{t_1}$, $(N)_{t_2}$ are the respective nitrogen atom concentrations at the reaction times t_1 and t_2 . The results for k_{13} , derived from equation [1], over the range of pressures from 0.5 to 4 mm. are recorded in Table X and a plot of k_{13} against

TABLE X

VARIATION OF k_{13} (from equation [1]) AS A FUNCTION OF PRESSURE,
 REACTION TIME AND INITIAL REACTANT CONCENTRATIONS
 WITH UNHEATED REACTION TUBE

Total Pressure mm. Hg.	Total Flow (mole/sec) $\times 10^6$	(M) (mole/cc) $\times 10^7$	(N) _{t₁} (mole/cc) $\times 10^9$	(N) _{t₂} (mole/cc) $\times 10^9$	t ₁ - t ₂ (sec) $\times 10^2$	k_{13} (cc ² mole ⁻² sec ⁻¹) $\times 10^{-16}$
0.5	17	0.267	0.58	0.51	3.10	24.0
"	"	"	0.64	0.58	3.30	20.5
"	"	"	0.74	0.64	3.80	20.5
"	"	"	0.74	0.58	7.10	20.0
"	"	"	0.74	0.51	10.20	21.8
						Average $k_{13} = 21.3$
1.0	49	0.535	0.70	0.65	2.15	7.80
"	"	"	0.74	0.70	2.25	5.80
"	"	"	0.79	0.74	2.60	6.40

Table X (cont'd)

"	"	"	0.79	0.70	4.85	6.10
"	"	"	0.79	0.65	7.10	7.20
						Average $k_{13} = 6.66$
1.5	83	0.800	1.34	1.24	2.00	4.05
"	"	"	1.50	1.34	2.30	4.30
"	"	"	1.50	1.24	4.30	4.15
"	"	"	1.50	1.10	6.20	4.85
						Average $k_{13} = 4.34$
2.0	135	1.07	1.55	1.44	1.65	2.85
"	"	"	1.72	1.55	1.90	3.15
"	"	"	1.72	1.32	5.10	3.20
"	"	"	1.84	1.44	5.35	2.75
"	"	"	1.84	1.32	6.90	2.95
						Average $k_{13} = 2.98$
2.5	170	1.34	2.95	2.70	1.80	1.25
"	"	"	2.70	2.50	1.90	1.29
"	"	"	2.95	2.50	3.70	1.20
"	"	"	2.95	2.32	5.35	1.26

Table X (cont'd)

"	"	"	2.95	2.20	6.90	1.24
						Average $k_{13} = 1.26$
3.0	210	1.60	3.10	2.85	1.50	1.24
"	"	"	3.40	3.10	1.60	1.00
"	"	"	3.74	3.40	1.82	0.93
"	"	"	3.74	3.10	3.42	0.95
"	"	"	3.74	2.85	4.92	1.05
						Average $k_{13} = 1.00$
3.5	248	1.87	3.38	3.05	1.48	1.12
"	"	"	3.72	3.38	1.57	0.94
"	"	"	4.25	3.72	1.82	1.00
"	"	"	4.25	3.38	3.39	0.96
"	"	"	4.25	3.05	4.87	1.00
						Average $k_{13} = 1.00$
4.0	270	2.15	3.95	3.50	1.50	0.94
"	"	"	4.48	3.95	1.60	0.88
"	"	"	5.20	4.48	1.80	0.86

Table X (cont'd)

"	"	"	4.48	3.50	3.10	0.90
"	"	"	5.20	3.95	3.40	0.86
"	"	"	5.20	3.50	4.90	0.87

Average $k_{13} = 0.90$

pressure is shown in Fig. 18. The data indicate that the value of k_{13} decreases as the pressure is increased to about 2.5 mm., and then remains essentially constant with further increase of pressure. Hence, the surface decay of nitrogen atoms is practically negligible at pressures above about 2.5 mm. A typical plot of $\frac{1}{(N)_t (M)}$ against reaction time at 2.5 mm., pressure yields a straight line (Fig. 19).

Taking into account reaction (14), the over-all rate expression is

$$-\frac{d(N)}{dt} = k_{13}(N)^2(M) + k_{14}(N)$$

This integrates to

$$\ln \frac{(N)_{t_1} [k_{14} + k_{13}(M)(N)_{t_2}]}{(N)_{t_2} [k_{14} + k_{13}(M)(N)_{t_1}]} = k_{14}(t_2 - t_1)$$

which is exponential, and has to be solved graphically.

To separate the homogeneous and surface decay of nitrogen atoms, plots were made of $\ln(N)$ against time. Approximately straight lines were obtained, the slopes of which depended, of course, on (M) . The average slopes of these lines are plotted against (M) in Fig. 20. For pressures of 2.5 mm., and above, an extrapolation of the line passes through zero, indicating again the small effect of the surface decay at these pressures. For pressures lower than 2.5 mm., an extrapolation gives an intersection corresponding to $k_{14} = 2.5 \pm 0.2 \text{ sec}^{-1}$.

Figure 18

Plot of k_{13} calculated from
the Equation [1], vs Total Pressure

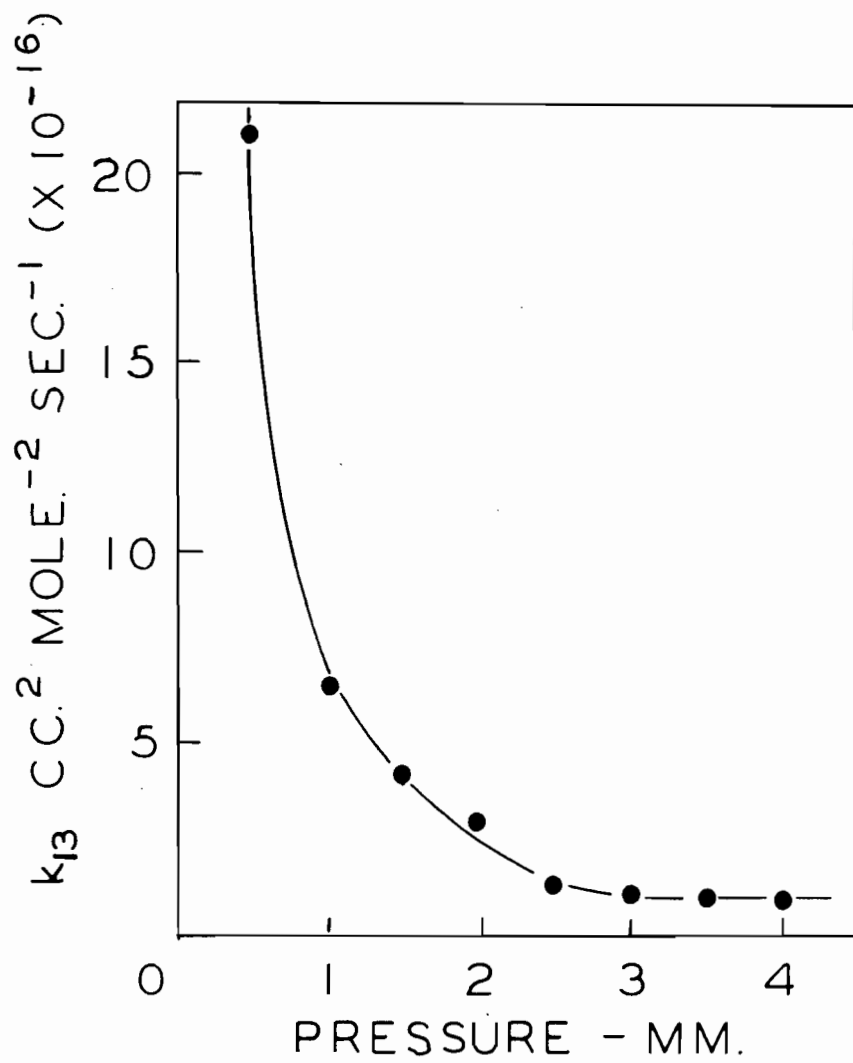


Figure 19

Plot of $\frac{1}{(N)(M)}$ vs Reaction Time

at a Total Pressure of 2.5 mm.

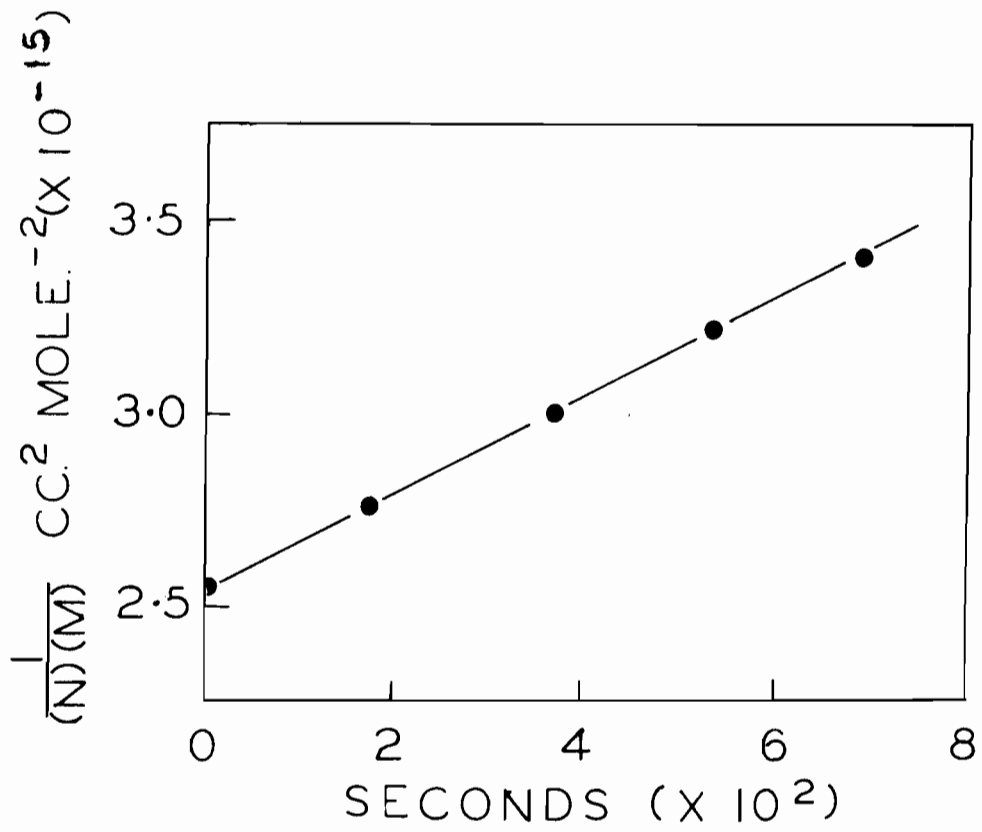
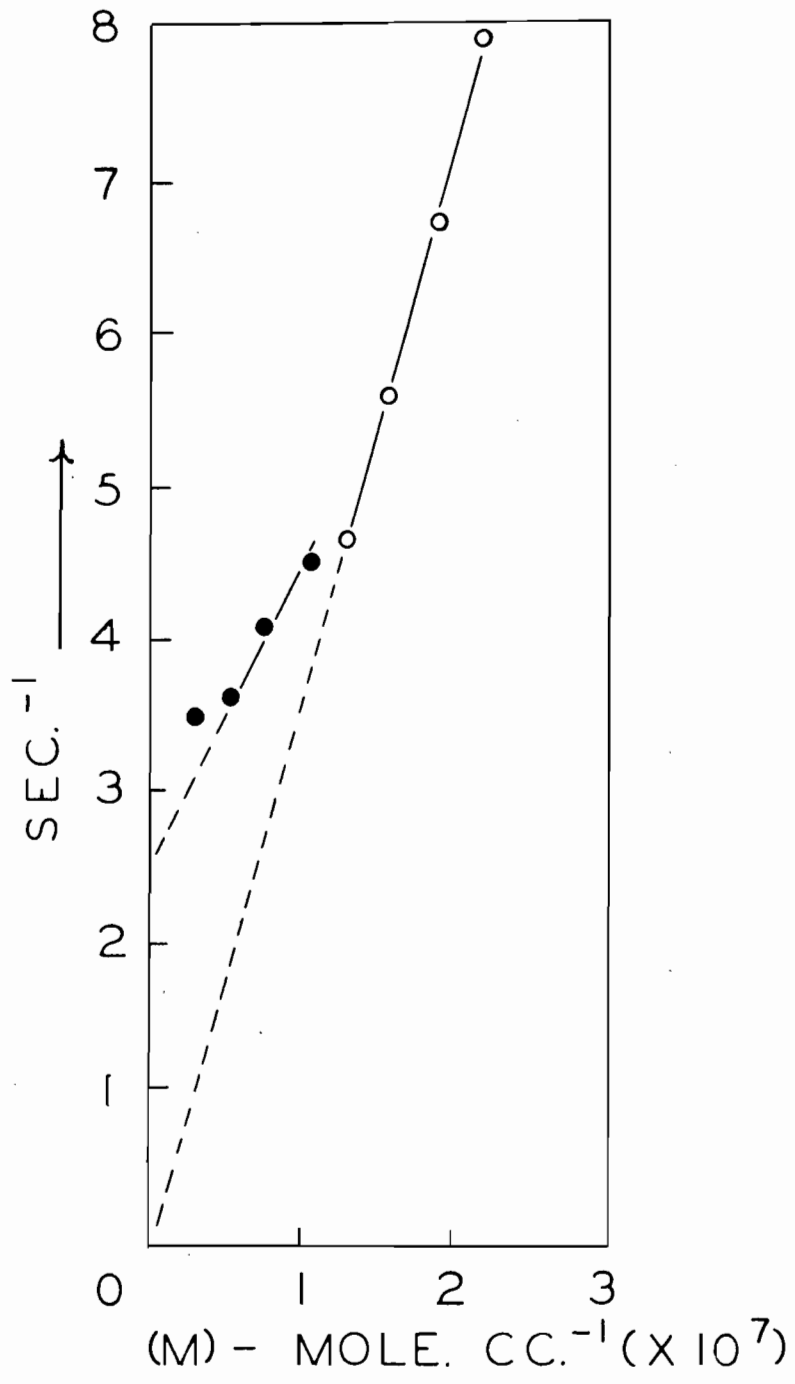


Figure 20

Plot of the Average Slopes (sec^{-1}) vs $(M) \times 10^7 (\text{mole cc}^{-1})$



The surface recombination of atoms has been treated theoretically by Laidler (195) and Laidler and Schuler (161), in terms of the theory of absolute reaction rates. They defined the recombination coefficient γ , the ratio of atoms striking the surface and reacting, to the total number striking the surface, to be equal to

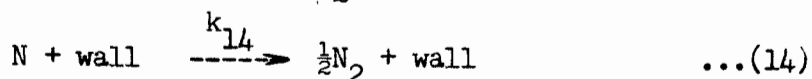
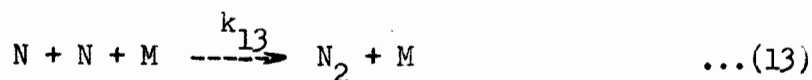
$$\gamma = 2k_{14}r/\bar{c}$$

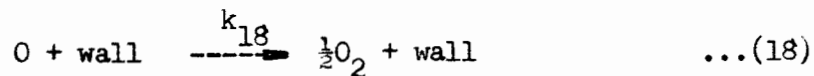
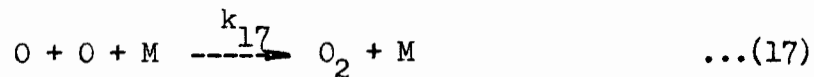
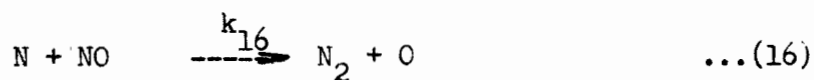
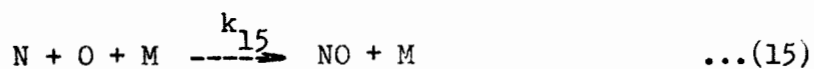
where r is the radius of the reaction vessel, \bar{c} is the root mean square atomic velocity, and k_{14} the pseudo first-order rate constant.

Thus, for $k_{14} = 2.5 \pm 0.2 \text{ sec}^{-1}$, γ takes the value of $\gamma = (7.5 \pm 0.6) \times 10^{-5}$. On the assumption that atoms and molecules are equally efficient as third bodies, a value is obtained for $k_{13} = 1.04 (\pm 0.17) \times 10^{16} \text{ cc}^2 \text{ mole}^{-2} \text{ sec}^{-1}$, corresponding to the disappearance of two nitrogen atoms, essentially constant over the range of pressures from 0.5 to 4mm.

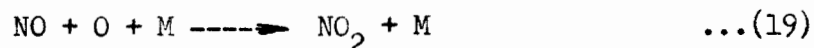
THE REACTION OF NITROGEN ATOMS WITH OXYGEN ATOMS

The following reactions may be involved in the active nitrogen-oxygen atom mixture:





The reaction

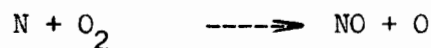


was not taken into account, since NO_2 would react rapidly with oxygen atoms to produce NO (111) and reaction (16) is very fast (75).

Since the system was free from O_2 , except from small amount of O_2 formed by reaction (17) and (18), it was assumed that there would be negligible influence from the reactions



and



Since the reaction of nitrogen atoms with oxygen atoms was studied at pressures of 3, 3.5 and 4 mm., the effect of reaction (14) should be very small, and has been neglected.

The over-all rate expression for the disappearance of nitrogen atoms in reactions (13), (15) and (16) is then

$$-\frac{d(\text{N})}{dt} = 2k_{15}(\text{N})(\text{O})(\text{M}) + k_{13}(\text{N})^2(\text{M})$$

or

$$-\int_0^t \frac{d(N)}{(N)} = 2k_{15}(M) \int_0^t (O)dt + k_{13}(M) \int_0^t (N)dt$$

and

$$\ln \frac{(N)_0}{(N)_t} = 2k_{15}(M) \int_0^t (O)dt + k_{13}(M) \int_0^t (N)dt \quad [2]$$

The integrals in the first and second terms correspond respectively to the disappearance of oxygen and nitrogen atoms, due to their decay processes along the reaction tube. The rate expression, for oxygen atoms in reaction (17) and (18), is given by

$$-\frac{d(O)}{dt} = k_{17}(M)(O)^2 + k_{18}(O)$$

This integrates to

$$\ln \frac{(O)_0}{(O)_t} - \ln \frac{[k_{18} + k_{17}(M)(O)_0]}{[k_{18} + k_{17}(M)(O)_t]} = k_{18}t$$

or

$$(O)_t = \frac{k_{18}}{k_{17}(M)} \frac{1}{\left[\left(1 + \frac{k_{18}}{k_{17}(M)(O)_0} \right) e^{k_{18}t} - 1 \right]}$$

Upon integrating

$$\int_0^t (O)_t dt = \frac{k_{18}}{k_{17}(M)} \int_0^t \frac{dt}{\left[\left(1 + \frac{k_{18}}{k_{17}(M)(O)_0} \right) e^{k_{18}t} - 1 \right]}$$

or

$$\int_0^t (O)_t dt = \frac{1}{k_{17}(M)} \ln \left[1 + \frac{k_{17}(M)(O)_0}{k_{18}} (1 - e^{-k_{18}t}) \right] \quad [3]$$

A similar derivation for the decay of nitrogen atoms in reaction (13) yields

$$\int_0^t (N)_t dt = \frac{1}{k_{13}(M)} \ln [1 + k_{13}(M)(N)_0 t] \quad [4]$$

Substitution of equations [3] and [4] in equation [2], gives

$$\ln \frac{(N)_0}{(N)_t} = \frac{2k_{15}}{k_{17}} \ln \left[1 + \frac{k_{17}(M)(O)_0 (1 - e^{-k_{18}t})}{k_{18}} \right] + \ln [1 + k_{13}(M)(N)_0 t]$$

or rearranging

$$k_{15} = \frac{k_{17}}{2} \frac{\log \frac{(N)_0}{(N)_t} - \log [1 + k_{13}(M)(N)_0 t]}{\log \left[1 + \frac{k_{17}(M)(O)_0 (1 - e^{-k_{18}t})}{k_{18}} \right]} \quad [5]$$

The rate constant for reaction (17) was assumed to be $k_{17} = 3.2 \times 10^{15} \text{ cc}^2 \text{ mole}^{-2} \text{ sec}^{-1}$ with $\gamma = 1.65 \times 10^{-5}$ (137) which, for the conditions used, corresponds to a value of $k_{18} = 0.516 \text{ sec}^{-1}$. The value of $k_{13} = 1.04 \times 10^{16} \text{ cc}^2 \text{ mole}^{-2} \text{ sec}^{-1}$, derived from the present study, was used. The data are recorded in Table XI with an average value of $k_{15} = 1.83 (\pm 0.2) \times 10^{15} \text{ cc}^2 \text{ mole}^{-2} \text{ sec}^{-1}$.

TABLE XI

RATE CONSTANTS FOR THE REACTION OF NITROGEN ATOMS WITH OXYGEN ATOMS
AT VARIOUS PRESSURES WITH UNHEATED REACTION TUBE

Total Pressure <u>mm.</u>	Total Flow (mole/sec) <u>$\times 10^6$</u>	(N) _o (mole/cc) <u>$\times 10^9$</u>	(O) _o (mole/cc) <u>$\times 10^9$</u>	$\log \frac{(N)_o}{(N)_t}$	t (sec) <u>$\times 10^2$</u>	k_{15} (cc ² mole ⁻² sec ⁻¹) <u>$\times 10^{-15}$</u>
3.0	174	1.47	2.30	0.0701	4.35	1.80
"	"	"	"	0.0962	6.30	1.75
"	"	1.22	2.56	0.0375	2.10	1.85
"	"	"	"	0.0632	4.35	1.65
"	"	"	"	0.1239	8.12	2.00
"	"	1.15	2.63	0.0555	4.35	1.70
"	"	"	"	0.0767	6.30	1.60
"	"	"	"	0.0989	8.12	1.52
3.5	202	1.58	2.67	0.0457	2.15	1.92
"	"	"	"	0.0937	4.40	2.03

Table XI (cont'd)

"	"	"	"	0.1335	6.40	2.00
"	"	"	"	0.1659	8.24	1.95
4.0	229	2.60	2.60	0.0681	2.15	1.70
"	"	2.46	2.74	0.0708	2.15	2.15
"	"	"	"	0.1326	4.40	1.80
"	"	"	"	0.1844	6.40	1.75
"	"	"	"	0.2459	8.25	2.05
"	"	0.86	4.34	0.1645	8.25	1.70

$$\text{Average } k_{15} = 1.83 \left(\begin{smallmatrix} + \\ - \end{smallmatrix} 0.2 \right) \times 10^{15} \text{ cc}^2 \text{ mole}^{-2} \text{ sec}^{-1}$$

The rate constant from the present study, for the decay of nitrogen atoms,

$$k_{13} = 5.2 \times 10^{15} \text{ cc}^2 \text{ mole}^{-2} \text{ sec}^{-1}$$

with

$$\gamma = 7.5(^+ 0.6) \times 10^{-5} \text{ (on clean pyrex glass)}$$

may be compared with those found in other investigations:

Harteck, et al.-ref. (67)

$$k_{13} = 6.19 \times 10^{15} \text{ cc}^2 \text{ mole}^{-2} \text{ sec}^{-1}$$

Herron, et al.-ref.(68, 69)

$$k_{13} = 5.7 \times 10^{15} \text{ cc}^2 \text{ mole}^{-2} \text{ sec}^{-1}$$
$$\gamma = 1.6 \times 10^{-5} \text{ (on glass wall partly poisoned with water)}$$

Wentink, et al.-ref.(70)

$$k_{13} = 5.6 \times 10^{15} \text{ cc}^2 \text{ mole}^{-2} \text{ sec}^{-1}$$
$$\gamma = 3 \times 10^{-5} \text{ (on clean pyrex glass)}$$

Kelly and Winkler-ref.(71)

$$k_{13} = 3.83 \times 10^{13} \text{ to } k_{13} = 4.75 \times 10^{15} \text{ cc}^2 \text{ mole}^{-2} \text{ sec}^{-1}$$

(depending on the temperature and whether or not N_2 or N were considered as third bodies)

$$\gamma = 2.75 \times 10^{-4} \text{ (on pyrex glass coated with } Na_2HPO_4)$$

Back and Winkler-ref.(72)

$$k_{13} = 4.21 \times 10^{15} \text{ cc}^2 \text{ mole}^{-2} \text{ sec}^{-1} \text{ (at } 400^\circ \text{ C., and surface poisoned with } Na_2HPO_4),$$

$$\gamma = 1.94 \times 10^{-4}$$

$$k_{13} = 4.28 \times 10^{16} \text{ cc}^2 \text{ mole}^{-2} \text{ sec}^{-1} \text{ (at } 700^\circ\text{C. and surface poisoned with } \text{AlPO}_4\text{)}$$

$$\gamma = 4.4 \times 10^{-4}$$

In view of the quite different experimental methods used, the agreement would seem to be satisfactory with the first three quoted investigations (67, 68, 69, 70). Agreement with previous studies in this laboratory (Refs. 71, 72) is satisfactory only for part of the temperature range used in the earlier studies.

The rate constant for the reaction of nitrogen atoms with oxygen atoms, from the present study, was found to be

$$k_{15} = 1.83 \text{ (}\pm 0.2\text{)} \times 10^{15} \text{ cc}^2 \text{ mole}^{-2} \text{ sec}^{-1}$$

which may be compared with the recently reported values:

Harteck et al.-ref.(196)

$$k_{15} = 1.8 \times 10^{15} \text{ cc}^2 \text{ mole}^{-2} \text{ sec}^{-1}$$

Barth-ref.(197)

$$k_{15} = 5.4 \times 10^{15} \text{ cc}^2 \text{ mole}^{-2} \text{ sec}^{-1}$$

(These values appeared after a paper based on the present study had been accepted for publication in the August number of Canadian Journal of Chemistry).

PART III

THE REACTION OF NITROGEN ATOMS WITH HYDROGEN ATOMS

Much work has been done, in the last five years, on radicals containing hydrogen and nitrogen, which provides evidence for their formation in the gas phase. Most of the radicals such as NH , NH_2 , N_2H_2 , N_2H_3 have been identified spectroscopically from studies on such related substances as hydrozoic acid, hydrazine and ammonia. The failure of many investigators (177, 178, 198) to find NH radicals by mass spectrometry in the dissociation of hydrozoic acid has been attributed to the ability of the NH radical to abstract hydrogen atoms from chemically stable molecules, without the need for any activation energy. Also, the presence of atomic nitrogen and hydrogen in the reaction products has suggested that nitrogen atoms are more or less passive toward bound hydrogen (178). From chemical studies, Winkler and his co-workers (74, 81) have similarly concluded that nitrogen atoms do not abstract hydrogen atoms in their attack on hydrocarbons or ammonia.

The kinetics of the reaction of nitrogen atoms with hydrogen atoms has not been studied. An attempt has been made in the present investigation to establish the kinetics and mechanism of the reaction that occurs in a mixture of nitrogen

and hydrogen atoms.

EXPERIMENTAL

MATERIALS

Hydrogen was obtained from Linde Air Products Co., and dried by passage through a trap surrounded by liquid air.

Hydrogen bromide was obtained from Matheson Company. It was purified by two bulb-to-bulb distillations in which only the middle fraction was retained.

Nitrogen and nitric oxide were purified as described earlier.

PROCEDURE

The apparatus, used previously, was slightly modified for this study and is shown in Fig. 12.

Tank nitrogen passed through the manostat K, the cold trap L, the needle valve Q and the flowmeter R, to enter the discharge tube Y. The stopcock c (Fig. 12) was closed in all these experiments. The discharge tube Y, similar to the tube E described previously, was operated by a second microwave unit as shown in Fig. 12.

Hydrogen, from the cylinder, was passed through the manostat A, the cold trap B, the needle valve C and the

flowmeter D, and entered the discharge tube E. The reaction vessel was "poisoned" with 20% phosphoric acid, to minimize the recombination of hydrogen atoms on the walls.

Before an experiment, the flows of nitrogen and hydrogen were started and adjusted to the desired flow rates. The discharge, Y, for nitrogen, was first turned on, and the experiment then was started by turning on the discharge, E, for hydrogen. The nitrogen atom consumption along the reaction tube was determined, as previously, by addition of nitric oxide at successive jet positions in the reaction tube (jets 1, 2, 3, 4; Fig. 12). Nitric oxide reacts with hydrogen atoms by the termolecular mechanism (167, 168)



followed by



Hence, destruction of nitric oxide should occur only as a result of attack by active nitrogen, which permits the nitric oxide titration to be used for estimation of the nitrogen atom flow rate in the presence of hydrogen atoms.

To make an experiment, the trap T_1 was surrounded by liquid air. With the nitrogen and hydrogen flows, and the nitrogen discharge in operation, the hydrogen discharge was turned on for a measured time. Then both discharges

were shut off, and the nitrogen and hydrogen flow stopped. After evacuation of the system, the product (ammonia) was distilled into a removable absorber containing a known amount of 0.1 N acid frozen in liquid air. On warming, the excess acid was titrated with 0.1 N base.

The hydrogen atom concentration was determined by the method developed by Wiles and Winkler (199). The trap T_1 was surrounded by liquid air, the nitrogen and hydrogen flows were started, and the hydrogen discharge, but not the nitrogen discharge, was turned on. Hydrogen bromide, from the bulb S, was passed through the needle valve, V, and the flowmeter, W, and entered the reaction vessel through the jet O. The experiment was begun when the flow of hydrogen bromide commenced, and was terminated by shutting off the hydrogen bromide flow after a measured time. The system was then evacuated for a few minutes, and the trap T_1 isolated from the pump. The liquid air was removed to permit distillation of the unreacted hydrogen bromide into the removable trap T_3 , containing standard NaOH solution, frozen in liquid air. After warming, the excess alkali was titrated with standard acid.

Hydrogen bromide flow rates were calibrated, in "blank" experiments, by condensing it in a removable trap containing standard NaOH solution, and back titrating the excess alkali with standard acid.

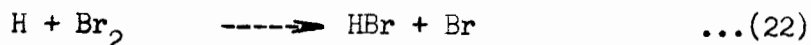
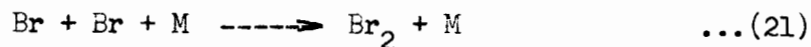
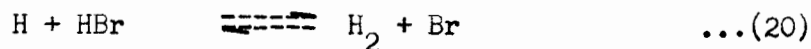
All the experiments were made with an unheated reaction tube, with the one exception that the reaction of active nitrogen with molecular hydrogen was studied at temperatures up to 350° C.

The only product of the reaction between active nitrogen and atomic hydrogen appeared to be traces of ammonia, identified by indicator tests and by titration with standard acid.

RESULTS AND DISCUSSION

THE REACTION OF HYDROGEN ATOMS WITH HYDROGEN BROMIDE

The results of the reaction of hydrogen atoms with hydrogen bromide at hydrogen pressures of 0.5, 0.75 and 1 mm., are shown in Tables XII, XIII, XIV and Fig. 21. The following reactions probably occurred (200, 201):



Reaction (20) and (22) have similar activation energies of about 1 kcal/mole (200), and the ratio $k_{22}/k_{20} = 8.4$, essentially independent of temperature in the range from 0° to 300° C., (202). The value of k_{20} has been found to be 2.2×10^{12} cc mole⁻¹ sec⁻¹ at 821° C., (203). Since the formation of Br₂

TABLE XII

HYDROGEN BROMIDE CONSUMED IN THE REACTION
OF HYDROGEN ATOMS WITH HYDROGEN BROMIDE

Hydrogen Pressure : 0.5 mm.

Hydrogen Flow Rate: 44.5×10^{-6} mole/sec.

Unheated Reaction Tube Poisoned with
Phosphoric Acid

Hydrogen Bromide Flow Rate <u>mole/sec. x 10⁶</u>	Hydrogen Bromide Consumed <u>mole/sec. x 10⁶</u>
66.20	4.15
73.08	4.68
79.38	5.20
80.01	5.16
82.21	5.04
92.61	5.26
93.24	4.95
98.59	5.05
98.91	5.20
99.54	5.40
100.17	5.12

TABLE XIII

HYDROGEN BROMIDE CONSUMED IN THE REACTION
OF HYDROGEN ATOMS WITH HYDROGEN BROMIDE

Hydrogen Pressure : 0.75 mm.

Hydrogen Flow Rate: 74×10^{-6} mole/sec.

Unheated Reaction Tube Poisoned with
Phosphoric Acid

Hydrogen Bromide Flow Rate <u>mole/sec. x 10⁶</u>	Hydrogen Bromide Consumed <u>mole/sec. x 10⁶</u>
73.08	5.94
80.00	6.00
89.46	6.60
92.61	6.82
93.24	6.61
96.39	7.09
97.65	7.05
98.60	7.22
105.52	7.18
117.50	7.10

TABLE XIV

HYDROGEN BROMIDE CONSUMED IN THE REACTION
OF HYDROGEN ATOMS WITH HYDROGEN BROMIDE

Hydrogen Pressure : 1 mm.

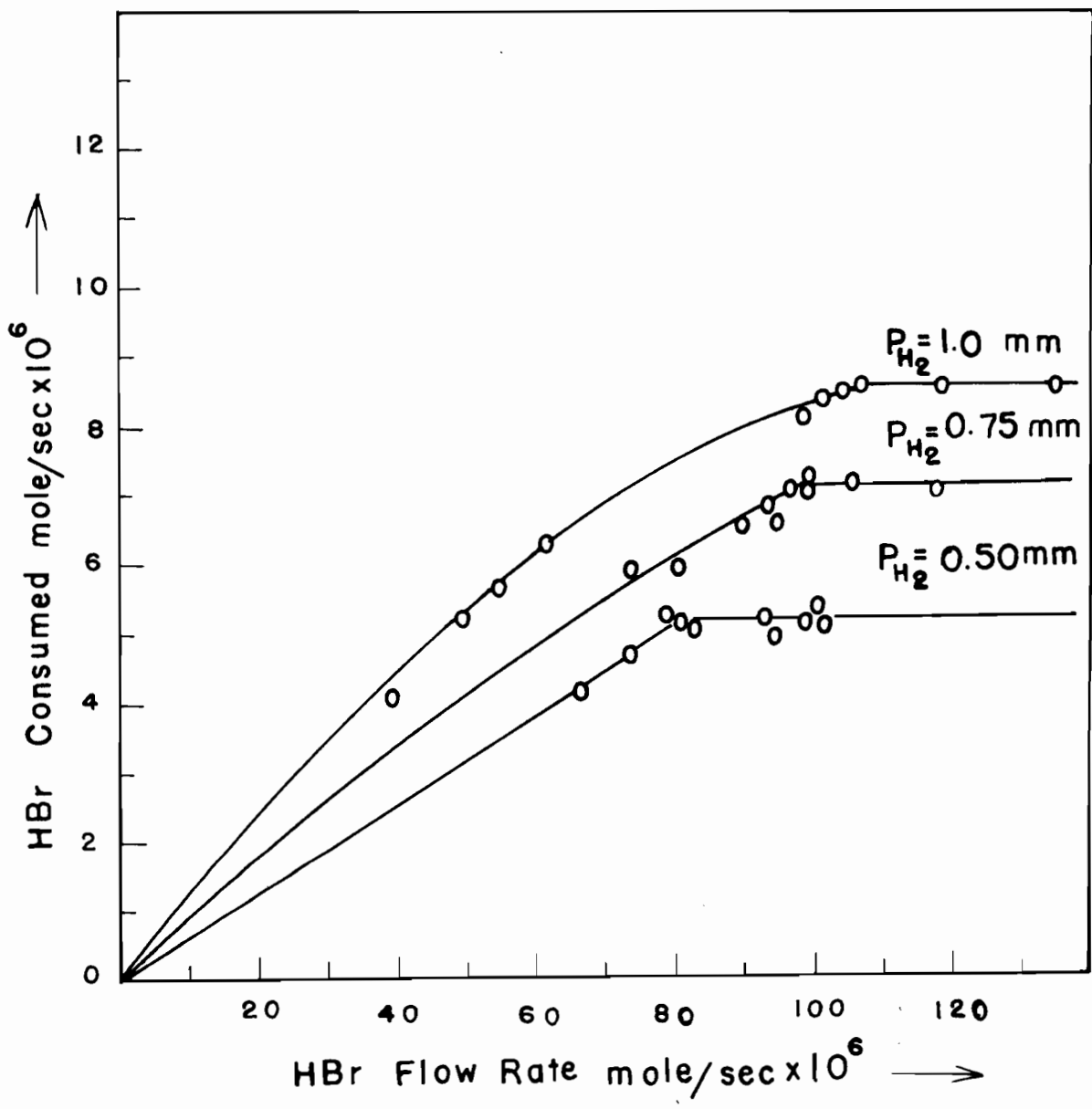
Hydrogen Flow Rate: 95×10^{-6} mole/sec.

Unheated Reaction Tube Poisoned with
Phosphoric Acid

Hydrogen Bromide Flow Rate <u>mole/sec. x 10⁶</u>	Hydrogen Bromide Consumed <u>mole/sec. x 10⁶</u>
38.70	4.01
49.14	5.25
54.18	5.67
61.11	6.29
80.30	6.65
97.90	8.16
100.80	8.40
103.95	8.50
105.20	8.60
118.12	8.60
135.13	8.66

Figure 21

Plot of HBr Consumed vs HBr Flow Rate



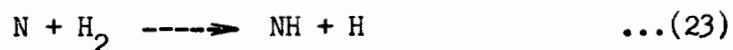
requires termolecular collisions, the use of excess hydrogen bromide should consume virtually all the available hydrogen atoms by reaction (20). The data (Tables XII, XIII, XIV and Fig. 21) indicate that the hydrogen atom consumption was complete and constant when excess hydrogen bromide was added.

Wiles and Winkler (199) found the same extent of reaction when excess of either hydrogen bromide or hydrogen iodide was introduced into a stream of atomic hydrogen. They concluded that the plateau value for the amount of reactant destroyed might be taken as a measure of the flow rate of hydrogen atoms. Hence, in the present study, the plateau values of hydrogen bromide consumed in the reaction of hydrogen bromide with hydrogen atoms have been assumed to represent the hydrogen atom concentrations at the corresponding pressures used.

THE REACTION OF ACTIVE NITROGEN WITH MOLECULAR HYDROGEN

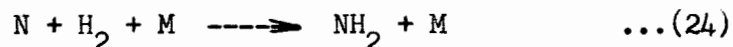
A series of experiments first made in which molecular hydrogen was added to active nitrogen. No product was found from this reaction, and the afterglow intensity was unaffected (except for a possible dilution), even at high flow rates of molecular hydrogen, and at temperatures up to 350° C. This observation is in agreement with that found from earlier studies by Kistiakowsky and Volpi (75) but is contrary to the results of Varney (106), who found small amounts

of ammonia. Steiner (172) attributed the formation of ammonia from the active nitrogen-molecular hydrogen reaction to the diffusion of hydrogen molecules into the nitrogen discharge tube, so that a reaction between nitrogen atoms and hydrogen atoms was probable. According to Kistiakowsky and Volpi (75), the reaction

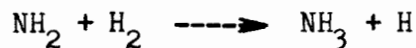


is endothermic to the extent of about 18 ± 12 kcal and must have an activation energy higher than 15 kcal/mole if, at 300°C ., its rate constant is less than $10^8 \text{ cc}^2 \text{ mole}^{-1} \text{ sec}^{-1}$.

The reaction



is about 70 kcal exothermic, and involves a change of spin. If it occurred, it seems reasonable that it should lead to the formation of ammonia, since the reaction



is slightly exothermic (about 1-4 kcal), and spin favourable. Since no ammonia was found, it was concluded that reaction (24) is probably quite slow under the conditions used.

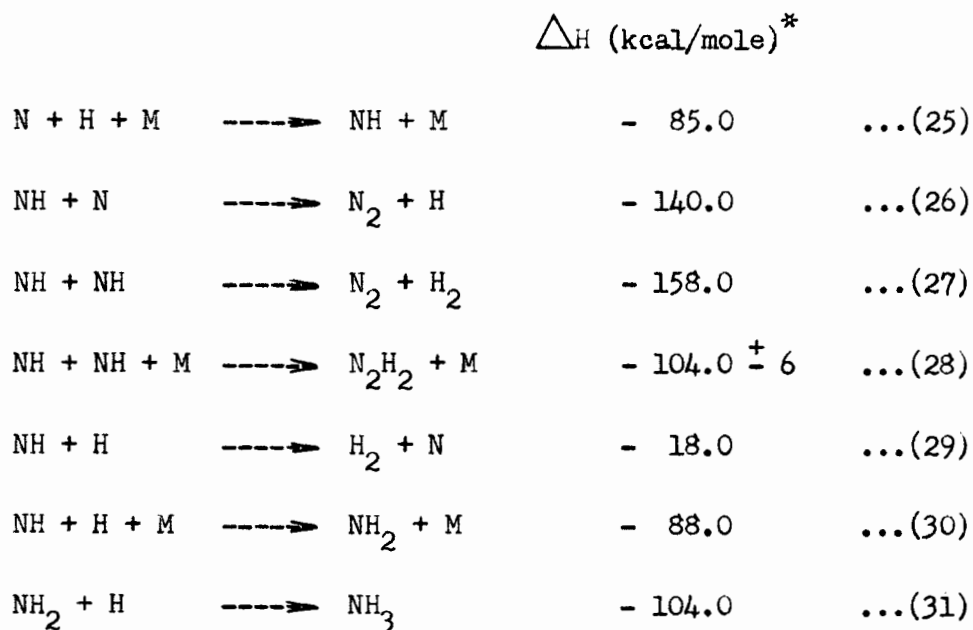
THE REACTION OF NITROGEN ATOMS WITH HYDROGEN ATOMS

The data for the formation of small amounts of ammonia in the reaction of nitrogen atoms with hydrogen atoms,

at various pressures, are shown in Table XV. These are in substantial agreement with earlier observations (174, 179).

No tests for hydrazine were made, since, if it were formed, it should react rapidly with either nitrogen or hydrogen atoms, which were present in excess in the gas stream (204).

The following energetically favourable elementary reactions may be involved in a mixture of nitrogen atoms and hydrogen atoms:



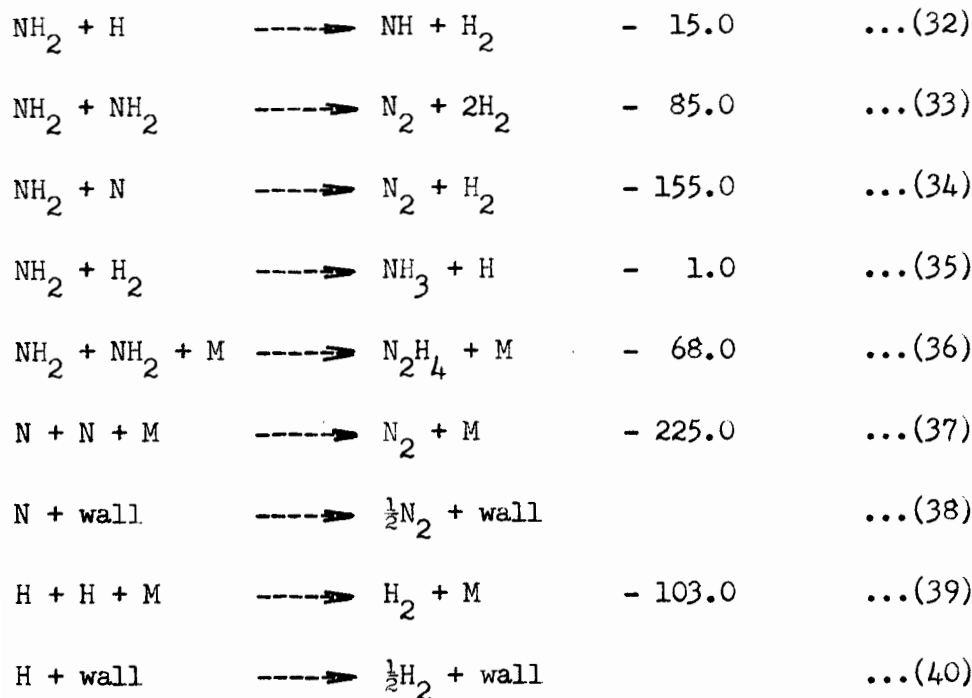
*The heats of reaction are approximate, based on the data:
 $D_{N-N} = 225$ kcal., $D_{H-H} = 103$ kcal., $D_{N-H} = 85$ kcal., (205),
 $D_{H-NH} = 88$ kcal., (206), $D_{H-NH_2} = 104$ kcal., (207), $D_{HN=NH} = 104 \pm 6$ kcal., (178); but they do indicate the energetics of the reactions considered.

TABLE XV

AMMONIA PRODUCED IN THE REACTION OF NITROGEN ATOMS
WITH HYDROGEN ATOMS

Unheated Reaction Tube Poisoned with
Phosphoric Acid

Nitrogen Pressure <u>mm.</u>	Hydrogen Pressure <u>mm.</u>	Total Pressure <u>mm.</u>	Nitrogen Atom Flow Rate <u>mole/sec. x 10⁶</u>	Hydrogen Atom Flow Rate <u>mole/sec. x 10⁶</u>	Ammonia Produced <u>mole/sec. x 10⁶</u>
2.0	0.50	2.50	2.84	5.2	-
2.5	0.50	3.00	3.25	5.2	-
2.0	0.75	2.75	2.84	7.1	0.054
1.5	1.00	2.50	1.60	8.6	0.013
1.0	1.00	2.00	0.73	8.6	0.027
2.0	1.00	3.00	2.84	8.6	0.027
3.0	1.00	4.00	4.34	8.6	0.027
3.5	1.00	4.50	5.29	8.6	0.027



The NH_2 can be formed only by reaction (30) which followed by reactions (31) and (35) would lead to the formation of ammonia. The very small amount of ammonia produced (Table XV) indicates that NH_2 exists in the gaseous mixture in small amounts, in accordance with its formation from ternary collisions (reaction 30). Of course, NH_2 may also be destroyed by the probable reactions (32), (33), (34) and (36), with subsequent reaction of the products with either nitrogen or hydrogen atoms. For kinetic studies, reaction (30), as termolecular, may be neglected in comparison with reactions (26), (27) and (29), which are bimolecular.

Reaction (29) is less exothermic than reactions (26) and (27) and involves change of spin. Reactions involving change of spin are expected to be slow (193), with a probabi-

lity factor less than 10^{-4} . Therefore, reaction (29) might be expected to be slow and, for the present study, has been neglected in comparison with the spin favourable reaction (26). Reactions (27) and (28) are exothermic and spin-allowed, and therefore, possible.

The rate expression, for the disappearance of nitrogen atoms in reactions (25), (26), (37) and (38), is

$$-\frac{d(N)}{dt} = k_{25}(M)(H)(N) + k_{26}(NH)(N) + k_{37}(M)(N)^2 + k_{38}(N) \quad [6]$$

Application of the steady-state approximation for NH yields

$$\frac{d(NH)}{dt} = k_{25}(M)(H)(N) - k_{26}(NH)(N) - k_{27}(NH)^2 - k_{28}(M)(NH)^2 = 0 \quad [7]$$

The NH concentration in the gaseous mixture is expected to be very small owing to the very short half-life of NH radical (about 9×10^{-4} sec (174, 175), compared with a value of approximately 1×10^{-2} sec for the CH and CH_2 radicals). Therefore, terms in $(NH)^2$ should have a little influence in the rate equation [7], and have been neglected. Thus, equation [7] takes the form

$$k_{25}(M)(H)(N) = k_{26}(NH)(N)$$

and then equation [6] becomes

$$-\frac{d(N)}{dt} = 2k_{25}(N)(H)(M) + k_{37}(M)(N)^2 + k_{38}(N) \quad [8]$$

If the wall recombination of nitrogen atoms is neglected, since the reaction of nitrogen atoms with hydrogen atoms has been studied at pressures higher than 2.5 mm., (69, 71, present study), the rate expression is given by

$$-\frac{d(N)}{dt} = 2k_{25}(N)(H)(M) + k_{37}(M)(N)^2$$

Upon integrating

$$\ln \frac{(N)_0}{(N)_t} = 2k_{25}(M) \int_0^t (H)dt + k_{37}(M) \int_0^t (N)dt \quad [9]$$

The rate expression for the decay of hydrogen atoms in reactions (39) and (40) is

$$-\frac{d(H)}{dt} = k_{39}(M)(H)^2 + k_{40}(H)$$

This integrates to

$$\ln \frac{(H)_0}{(H)_t} - \ln \frac{[k_{40} + k_{29}(M)(H)_0]}{[k_{40} + k_{39}(M)(H)_t]} = k_{40}t$$

or

$$(H)_t = \frac{k_{40}}{k_{39}(M)} \frac{1}{\left[\left(1 + \frac{k_{40}}{k_{39}(M)(H)_0} \right) e^{k_{40}t} - 1 \right]}$$

and integrating

$$\int_0^t (H)_t dt = \frac{k_{40}}{k_{39}^{(M)}} \int_0^t \frac{dt}{\left[\left(1 + \frac{k_{40}}{k_{39}^{(M)}(H)_0} \right) e^{k_{40}t} - 1 \right]}$$

$$= \frac{1}{k_{39}^{(M)}} \ln \left[1 + \frac{k_{39}^{(M)}(H)_0}{k_{40}} (1 - e^{-k_{40}t}) \right] \quad [10]$$

Similarly, the nitrogen atom concentration at time t (reaction (37)) is given by

$$(N)_t = \frac{(N)_0}{k_{37}^{(M)}(N)_0 t + 1}$$

and integrating

$$\int_0^t (N)_t dt = \frac{1}{k_{37}^{(M)}} \int_0^t \frac{d[k_{37}^{(M)}(N)_0 t + 1]}{k_{37}^{(M)}(N)_0 t + 1}$$

$$= \frac{1}{k_{37}^{(M)}} \ln [k_{37}^{(M)}(N)_0 t + 1] \quad [11]$$

Substitution of [10] and [11] in equation [9] yields the expression,

$$k_{25} = \frac{k_{39}}{2} \frac{\log \frac{(N)_0}{(N)_t} - \log [1 + k_{37}^{(M)}(N)_0 t]}{\log \left[1 + \frac{k_{39}^{(M)}(H)_0}{k_{40}} (1 - e^{-k_{40}t}) \right]} \quad [12]$$

where:

$(N)_o$ = initial nitrogen atom concentration

$(H)_o$ = initial hydrogen atom concentration

$(N)_t$ = nitrogen concentration at time t

t = reaction time

The rate constant of reaction (39) was taken as

$$k_{39} = 10^{16} \text{ cc}^2 \text{ mole}^{-2} \text{ sec}^{-1} \text{ (155-159)}$$

with $\gamma = 2 \times 10^{-5}$ (160)

which for the conditions used, corresponds to $k_{40} = 2.5 \text{ sec}^{-1}$.

The value of $k_{37} = 1.04 \times 10^{16} \text{ cc}^2 \text{ mole}^{-2} \text{ sec}^{-1}$ was used,

derived from the present study.

Rate constants for the reaction of nitrogen atoms with hydrogen atoms under various conditions, derived from equation [12], on the assumption that atoms and molecules are equally effective as third bodies, are recorded in Table XVI. The average value of k_{25} may be taken as

$$k_{25} = 4.87 (\pm 0.8) \times 10^{14} \text{ cc}^2 \text{ mole}^{-2} \text{ sec}^{-1}$$

over the range of pressures from 2.5 to 4.5 mm., in an unheated reaction tube poisoned with phosphoric acid. Owing to the assumptions made for its derivation, this value may be taken as an upper limit.

TABLE XVI

RATE CONSTANTS FOR THE REACTION OF NITROGEN ATOMS
WITH HYDROGEN ATOMS AS A FUNCTION OF REACTION TIME
PRESSURE AND INITIAL REACTANT CONCENTRATIONS

Unheated Reaction Tube Poisoned with Phosphoric Acid

Nitrogen Pressure mm.	Hydrogen Pressure mm.	Total Pressure mm.	Nitrogen Flow Rate mole/sec. $\times 10^6$	Hydrogen Flow Rate mole/sec. $\times 10^6$	Total Flow Rate mole/sec. $\times 10^6$	M mole/sec. $\times 10^7$	(N) _o mole/cc. $\times 10^9$	(H) _o mole/cc. $\times 10^9$	$\log \frac{(N)_o}{(N)_t}$	t sec. $\times 10^2$	k ₂₅ cc ² mole ⁻² sec ⁻¹ $\times 10^{-14}$
2.0	0.50	2.50	133	44.5	177.5	1.38	2.21	3.91	0.0400	2.69	4.40
"	"	"	"	"	"	"	"	"	0.0659	4.48	5.65
"	"	"	"	"	"	"	"	"	0.0897	6.04	6.30
"	"	"	"	"	"	"	"	"	0.1209	7.50	5.50
Average k ₂₅ = 5.46											
2.0	0.75	2.75	133	74.0	207.0	1.47	2.01	5.04	0.0417	2.54	5.75
"	"	"	"	"	"	"	"	"	0.0641	4.23	4.80

Table XVI (cont'd)

"	"	"	"	"	"	"	"	"	0.0841	5.70	5.00
"	"	"	"	"	"	"	"	"	0.1011	7.09	4.55
Average $k_{25} = 5.02$											
2.0	1.00	3.00	133	95.0	228.0	1.60	2.00	6.03	0.0417	2.52	4.00
"	"	"	"	"	"	"	"	"	0.0659	4.20	3.34
"	"	"	"	"	"	"	"	"	0.0859	5.66	3.90
"	"	"	"	"	"	"	"	"	0.1109	7.03	5.05
Average $k_{25} = 4.08$											
2.5	1.00	3.50	172	95.0	267.0	1.87	2.27	6.03	0.0540	2.51	4.19
"	"	"	"	"	"	"	"	"	0.0854	4.18	4.18
"	"	"	"	"	"	"	"	"	0.1140	5.63	4.62
"	"	"	"	"	"	"	"	"	0.1353	6.99	3.87
Average $k_{25} = 4.22$											
3.0	0.50	3.50	219	44.5	263.5	1.87	3.22	3.69	0.0728	2.54	6.25
"	"	"	"	"	"	"	"	"	0.1143	4.24	5.75
"	"	"	"	"	"	"	"	"	0.1452	5.71	5.15

Table XVI (cont'd)

"	"	"	"	"	"	"	"	"	0.1771	7.09	5.60
Average $k_{25} = 5.67$											
3.0	0.75	3.75	219	74.0	293.0	2.00	3.10	4.84	0.0728	2.45	4.57
"	"	"	"	"	"	"	"	"	0.1143	4.08	4.50
"	"	"	"	"	"	"	"	"	0.1452	5.48	4.10
"	"	"	"	"	"	"	"	"	0.1771	6.81	4.46
Average $k_{25} = 4.41$											
3.0	1.00	4.00	219	95.0	314.0	2.14	2.95	5.85	0.0776	2.44	5.75
"	"	"	"	"	"	"	"	"	0.1256	4.06	6.50
"	"	"	"	"	"	"	"	"	0.1575	5.47	5.65
"	"	"	"	"	"	"	"	"	0.1842	6.79	4.82
Average $k_{25} = 5.68$											
3.5	1.00	4.50	235	95.0	330.0	2.40	3.80	6.25	0.1075	2.61	4.50
"	"	"	"	"	"	"	"	"	0.1577	4.35	4.34
"	"	"	"	"	"	"	"	"	0.2116	5.86	5.35

Table XVI (cont'd)

" " " " " " " " " 0.2435 7.28 3.60

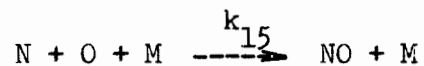
Average $k_{25} = 4.45$

Average $k_{25} = 4.87^{+0.8} \times 10^{14} \text{ cc}^2 \text{ mole}^{-2} \text{ sec}^{-1}$

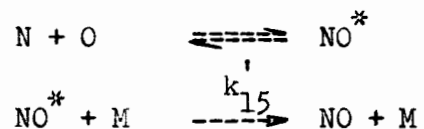
COMPARISON WITH THEORY OF ASSOCIATION REACTIONS

Collision Model

The reaction



may be written as



and the stationary concentration of the binary complex NO^* may be taken approximately as

$$(NO)^* = Z_{N.O} \tau_{NO} (N)(O) \quad [13]$$

where: $Z_{N.O}$ is the collision frequency of N and O, and τ_{NO} is the mean lifetime of the complex NO^* .

The over-all rate expression is then

$$\frac{d(\text{products})}{dt} = k_{15}(N)(O)(M) = k'_{15}(M)(NO)^* \quad [14]$$

Substitution of $(NO)^*$ from equation [13] into equation [14], yields

$$k_{15}(N)(O)(M) = k'_{15} Z_{N.O} \tau_{NO} (N)(O)(M)$$

or

$$k_{15} = k'_{15} Z_{N.O} \tau_{NO}$$

k'_{15} as a bimolecular rate constant, may be expressed as

$$k'_{15} = PZ_{NO.M}^* e^{-E/RT}$$

where P is the probability for the bimolecular collision between NO^* and M. Then k'_{15} becomes

$$k_{15} = PZ_{NO.M}^* Z_{NO} \mathcal{N}_{NO} e^{-E/RT} \quad [14]$$

\mathcal{N}_{NO} is the reciprocal of a unimolecular rate constant and it should be about 10^{-13} sec., if the activation energy is neglected. If there is any activation energy, it may be absorbed in the exponential term. Thus, the frequency of termolecular collisions may be given by

$$Z_{ter.} = Z_{NO.M}^* Z_{N.O} \mathcal{N}_{NO} \quad [15]$$

The bimolecular collision frequencies, $Z_{NO.M}^*$ and $Z_{N.O}$, can be calculated, assuming collision diameters of 3.5, 3.75, 2.95 and 1.8×10^{-8} cm for NO, M = N_2 , N and O respectively. For $T = 300^\circ$ K.

$$Z_{ter.} = 1.65 \times 10^{15} \text{ cc}^2 \text{ mole}^{-2} \text{ sec}^{-1}$$

The calculated value of $Z_{ter.}$ is in good agreement with that given experimentally by $k_{15} = 1.83 \times 10^{15} \text{ cc}^2 \text{ mole}^{-2} \text{ sec}^{-1}$.

Application of the collision model to the gas phase recombination of nitrogen atoms assuming the mechanism



yields

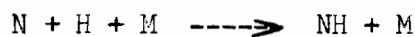
$$Z_{\text{ter.}} = Z_{\text{N}_2^* \text{N}_2} Z_{\text{N.N}} \alpha_{\text{N}_2} \quad [16]$$

For $T = 300^\circ \text{K.}$, and collision diameters $\sigma_{\text{N}} = 2.95 \text{ \AA}$,
 $\sigma_{\text{N}_2} = \sigma_{\text{N}_2^*} = 3.75 \text{ \AA}$, $Z_{\text{ter.}}$ takes the value of

$$Z_{\text{ter.}} = 2.78 \times 10^{15} \text{ cc}^2 \text{ mole}^{-2} \text{ sec}^{-1}$$

The experimental value is $5.2 \times 10^{15} \text{ cc}^2 \text{ mole}^{-2} \text{ sec}^{-1}$, that is, two times higher than the calculated. This may be attributed to the fact that N_2^* is formed in the ${}^5\Sigma_g^+$ state which may have a collision diameter higher than that of the ground state used for the calculation.

For the reaction



the number of termolecular collisions is given by

$$Z_{\text{ter.}} = Z_{\text{NH}} Z_{\text{NH.M}} \alpha_{\text{NH}} \quad [17]$$

which for $T = 300^\circ \text{K.}$, $\text{M} = \text{N}_2$, and collision diameters $\sigma_{\text{H}} = 2.4 \text{ \AA}$, $\sigma_{\text{NH}} = 2.68 \text{ \AA}$, gives

$$Z_{\text{ter.}} = 1.2 \times 10^{16} \text{ cc}^2 \text{ mole}^{-2} \text{ sec}^{-1}$$

and for $\text{M} = \text{H}_2$ and $\sigma_{\text{H}_2} = 2.7 \text{ \AA}$,

$$Z_{\text{ter.}} = 9.2 \times 10^{15} \text{ cc}^2 \text{ mole}^{-2} \text{ sec}^{-1}$$

The experimental value derived from the present study is $4.87 \pm 0.8 \times 10^{14} \text{ cc}^2 \text{ mole}^{-2} \text{ sec}^{-1}$. This indicates that this reaction has a probability of 4×10^{-2} or 5×10^{-2} , depending on whether nitrogen or hydrogen are considered as third bodies.

Wigner's Theory

Wigner (208) has developed an expression which gives an upper limit for the rate of association reactions, by determining the probability of a decrease of the relative energy of two atoms below zero energy, under the influence of a third body. He calculated the recombination rate constant for the atomic reaction



to be given by

$$k' = -2\pi \frac{g_{12}}{g_1 g_2} \left(\frac{2\pi\mu}{kT} \right)^{\frac{1}{2}} \int_{V_0 < 0} V_0 q_{12} [(\alpha_{13}^2 - \alpha_{23}^2)(\alpha_{13/m_1} - \alpha_{23/m_2}) + 2(\alpha_{13/m_1}^2 + \alpha_{23/m_2}^2)q_{12} + (\alpha_{13/m_1} + \alpha_{23/m_2})q_{12}^2] dq_{12}$$

where:

$$k' = \text{termolecular rate constant}$$

k = the Boltzmann constant

V_0 = the relative potential energy of the atoms A_1 and A_2
for infinite separation of A_3

μ = the reduced mass of A_1 and A_2

m_1 = the mass of A_1

m_2 = " " " A_2

g_1 = the statistical weight factor of A_1

g_2 = " " " " " A_2

g_{12} = " " " " " $A_1 A_2$

q_{12} = the separation of the atoms A_1 and A_2

α_{13} = the sum of the collision radii of A_1, A_3

α_{23} = " " " " " " " A_2, A_3

π = 3.14

The term $T^{-\frac{1}{2}}$ will cause a small fall-off in rate with increasing temperature.

The theory was applied to the reaction



For V_0 , the Hulburt-Hirschfelder (209) potential energy curve was used, given by the equation

$$V(r) = 6.609[(1 - e^{-x})^2 + 0.0678 x^3(1 + 2.663x)e^{-2x} - 1] \text{ ev,}$$

where:

$$x = 3.1579 \left(\frac{r - r_e}{r_e} \right), \quad V(\infty) = 0 \text{ and}$$

$r_e = 1.1508 \text{ \AA}$, which according to Vanderslice et al. (210), fits better than a Morse curve for the $X^2\Pi$ state of NO.

The radii were taken to be: 0.89 (211), 1.49 and 1.875 \AA (derived from viscosity data) for O, N and N_2 respectively.

The statistical weights at $T = 300^\circ \text{ K.}$, are:

for $\text{NO}(^2\Pi)$

$$*g_{\text{NO}} = 2(1 + e^{-343/kT}) = 3.13$$

for $\text{O}(^3P_2, ^3P_1, ^3P_0)$

$$**g_{\text{O}} = 5 + 3 e^{-450/kT} + e^{-640/kT} = 6.76$$

for $\text{N}(^4S)$, $g_{\text{N}} = 4$

The final result, for $T = 300^\circ \text{ K.}$, is

$$k' = 3.4 \times 10^{16} \text{ cc}^2 \text{ mole}^{-2} \text{ sec}^{-1}$$

The agreement between the observed ($k' = 1.83 \times 10^{15} \text{ cc}^2 \text{ mole}^{-2} \text{ sec}^{-1}$) and the calculated value might be taken as satisfactory

*The factor of two is due to the Λ -type doubling in the NO molecule.

** $k = 1.986 \text{ cal/degree}$

since this theory gives an upper limit for the rate constant when only atoms are involved as third bodies.

Keck (212, 213) has developed a method of calculating a rigorous upper limit to the rate constant of a termolecular reaction, based on a variational principle. The most important difference between this method and that of Wigner (208) is that it includes explicitly both the effect of the rotational barrier and the Van der Waals force. Application of this method to the recombination of iodine, bromine, oxygen and nitrogen atoms gave results which are in good agreement with the experiment (213). However, the application of this method requires the use of computers for the calculations, and time did not permit this to be done for the thesis.

SUMMARY AND CONTRIBUTIONS TO KNOWLEDGE

1. The reaction of active nitrogen with ethylene was studied in a cylindrical reaction tube at temperatures 100°, 150° and 400° C., in the range of pressures from 1 to 6 mm. The results indicated that the maximum hydrogen cyanide production was independent of temperature.
2. The maximum oxygen atom concentrations, resulting from the reaction of active nitrogen with molecular oxygen, were determined at 400° C., over the pressure range from 1 to 6 mm. It was found that the maximum oxygen concentration was essentially identical with the maximum production of hydrogen cyanide from the active nitrogen-ethylene reaction under the same experimental conditions.
3. Copper wire, coated with oxide, quenched the nitrogen afterglow completely, while gold and platinum were unable to do so. No appreciable recombination of nitrogen atoms was found to occur on the surface of glass wool. Oxygen atoms were recombined quantitatively on silver wire coated with oxide.
4. For the reaction of active nitrogen with molecular oxygen,



followed by



the rate constant k_1 was found to be

$$k_1 = 2.3 \times 10^{12} \exp(-5,900/RT) \text{ cc mole}^{-1} \text{ sec}^{-1}$$

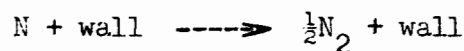
with a probability of 10^{-2} , over the range of temperatures from 150° to 350° C., and at pressures of 3.3 and 4.3 mm.

5. Approximate calculation of the pre-exponential factor for the reaction of nitrogen atoms with molecular oxygen was made in terms of the transition state theory. Values of the pre-exponential factor were estimated for linear and non-linear activated complexes. The results were in reasonable agreement with the observed pre-exponential factors.

6. The homogeneous and heterogeneous recombinations of nitrogen atoms were re-investigated. The rate constant for the gas phase recombination



was found to have the value of $5.2 \times 10^{15} \text{ cc}^2 \text{ mole}^{-2} \text{ sec}^{-1}$ over the range of pressures from 0.5 to 4 mm., in an unheated reaction tube. For the wall reaction



the value of $\gamma = 7.5(\pm 0.6) \times 10^{-5}$, on clean pyrex glass, was

derived and was found to be of secondary importance at pressures above about 2.5 mm.

7. The reaction of nitrogen atoms with oxygen atoms, in the absence of oxygen molecules, was studied at pressures 3, 3.5 and 4 mm., in an unheated reaction tube. The rate constant for the reaction



was determined to have the value of $1.83(^{+} 0.2) \times 10^{15} \text{ cc}^2 \text{ mole}^{-2} \text{ sec}^{-1}$.

8. No reaction between active nitrogen and molecular hydrogen was observed, even at 350°C .

9. The rate constant for the reaction



was found to have the value of

$$4.87(^{+} 0.8) \times 10^{14} \text{ cc}^2 \text{ mole}^{-2} \text{ sec}^{-1}$$

over the range of pressures from 2.5 to 4.5 mm., in an unheated reaction tube, poisoned with phosphoric acid.

10. The observed rate constants for the association reactions were compared with those computed from (a) collision model and (b) Wigner's theory for association reactions. The agreement between the calculated and observed rate constants would seem to be satisfactory.

BIBLIOGRAPHY

1. Warburg, E., Arch. de Gen. 3, 12, 504 (1884).
2. Lewis, P., Astr., Phys. J. 12, 8 (1900).
3. Strutt, R. J., Proc. Roy. Soc. (London) A85, 219 (1911).
 ibid A86, 56 (1912).
 ibid A88, 539 (1913).
 ibid A91, 303 (1915).
 ibid A93, 254 (1917).
4. Mitra, S. K., "Active Nitrogen. A New Theory", Assoc. for
 the Cultivation of Science, Calcutta, 1945.
5. Jennings, K. R., and Linnett, J. W., Quart, Rev. 12, 116 (1958).
6. Edwards, W. J., "Formation and Trapping of Free Radicals"
 Edited by Bass, A. M., and Broida, H. P.,
 (Academic Press, New York 1960).
7. Kenty, C., and Turner, L. A., Phys. Rev. 32, 799 (1928).
8. Stanley, C. R., Proc. Phys. Soc. A67, 821 (1954).
9. Lewis, B., J. Am. Chem. Soc. 51, 654 (1929).
10. Strutt, R. J., Proc. Roy. Soc. A91, 303 (1915).
11. Herzberg, G. H., Z. Physik 46, 878; 49, 512 (1928).
12. Rayleigh, Lord, Proc. Roy. Soc. A180, 123 (1942).
13. Constantinides, P. A., Phys. Rev. 30, 95 (1927).
14. Rayleigh, Lord, Proc. Roy. Soc. A180, 140 (1942).
15. Benson, J. M., J. Appl. Phys. 23, 757 (1952).
16. Strutt, R. J., and Fowler, A., Proc. Roy. Soc. A86, 105 (1911).
17. Willey, E. J. B., and Rideal, E. K., J. Chem. Soc. 669 (1927).
18. Knauss, H. P., Phys. Rev. 32, 417 (1928).

19. Rayleigh, Lord, Proc. Roy. Soc. A87, 179 (1912).
20. Rayleigh, Lord, Proc. Roy. Soc. A176, 16, (1940).
21. Jackson, L. C., and Broadway, L. F., Proc. Roy. Soc. A127, 678 (1930).
22. Herbert, W. S., Herzberg, G. H., and Mills, G. A., Can. J. Res. A15, 35 (1937).
23. Rayleigh, Lord, Proc. Roy. Soc. A102, 453 (1922).
24. Kaplan, J., Nature 122, 771 (1928).
25. McLennan, J. C., Ruedy, R., and Anderson, J. W., Trans. Roy. Soc. Can. 22, 303 (1928).
26. Kaplan, J., Phys. Rev. 33, 189 (1929).
27. Reinecke, L. H., Z. Physik 135, 361 (1953).
28. Herzberg, G. H., Z. Physik 46, 878; 49, 512 (1928).
29. Kistiakowsky, G. B., and Warneck, P., J. Chem. Phys. 27 1417 (1957).
30. LeBlanc, F., Tanaka, Y., and Jursa, A., J. Chem. Phys. 28, 979 (1958).
31. Mulliken, R. S., "The Threshold of Space" (Pergamon Press, New York, 1956), p. 169.
32. Lofthus, A., and Mulliken, R. S., J. Chem. Phys. 26, 1010 (1957).
33. Berkowitz, J., Chupka, W. A., and Kistiakowsky, G. B., J. Chem. Phys. 25, 457 (1956).
34. Herzberg, G. H., "Atomic Spectra and Atomic Structure" Dover Publications 2nd ed. 1944.
35. Spomer, H., Z. Physik 34, 622 (1925).
36. Gaydon, A. G., "Dissociation Energies and Spectra of Diatomic Molecules", Chapman and Hall, London (1947).
37. Wrede, E., Z. Physik 54, 53 (1929).

38. Jackson, D. S., and Schiff, H. I., J. Chem. Phys. 23, 2333 (1955).
39. Moore, C. E., Natl. Bur. Standards (U.S.) Circ. 467-I
40. Reference (6) p. 261.
41. Tanaka, Y., Jursa, A., and LeBlanc, F., "The Threshold of Space"
(M. Zelikoff ed.) p. 89-93. Pergamon Press,
New York (1956).
42. Cario, G., and Kaplan, J., Z. Physik 58, 769 (1920).
43. Worley, R. E., Phys. Rev. 73, 531 (1948).
44. Muschlitz, E. E., and Goodman, L., J. Chem. Phys. 21, 2213 (1953).
45. Lichten, W., J. Chem. Phys. 26, 306 (1957).
46. Rayleigh, Lord, Proc. Roy. Soc. A151, 567 (1935).
47. Mitra, S. K., Phys. Rev. 90, 516 (1953).
48. Herzberg, G. H., "Molecular Spectra and Molecular Structure"
I. Diatomic Molecules Sec. ed. Van Nostrand,
New York (1950).
49. Peyron, M., and Broida, H. P., J. Physique 18, 593 (1957).
50. Gaydon, A. G., Nature 153, 407 (1944).
51. Cario, G., and Reinecke, L. H., Abhandl. braunschweig. wiss.
Ges. 1, 8 (1949).
52. Stanley, C. R., Proc. Roy. Soc. A241, 180 (1957).
53. Bayes, K. D., and Kistiakowsky, G. B., J. Chem. Phys. 29,
949 (1960).
54. Bayes, K. D., and Kistiakowsky, G. B., J. Chem. Phys. 32,
992 (1960).
55. Broida, H. P., and Pellan, J. R., Phys. Rev. 95, 845 (1954).
56. Herzfeld, C. M., and Broida, H. P., Phys. Rev. 101, 606 (1956).
57. Herzfeld, C. M., Phys. Rev. 107, 1239 (1957).
58. Broida, H. P., and Lutes, O. S., J. Chem. Phys. 24, 484 (1956).

59. Minkoff, G. J., Scherber, F. I., and Gallapher, J. S., J. Chem. Phys. 30, 753 (1959).
60. Fontana, B. J., Appl. Phys. 29, 1667 (1958).
61. Fontana, B. J., J. Chem. Phys. 31, 148 (1959).
62. Benrad, A., Ann. Geophys. 3, 63 (1947).
63. Broida, H. P., and Bass, A. M., Phys. Rev. 101, 1740 (1956).
64. Peyron, M., and Broida, H. P., J. Chem. Phys. 30, 139 (1959).
65. Rayleigh, Lord, Proc. Roy. Soc. A176, 1 (1940).
66. Rabinowitch, E., Trans. Farad. Soc. 33, 292 (1937).
67. Harteck, P., Mannella, G., and Reaves, R. R., J. Chem. Phys. 29, 608 (1958).
68. Herron, J., Franklin, D., Bradt, P., and Dibeler, V. H., J. Chem. Phys. 29, 230 (1958).
69. Herron, J., Franklin, D., Bradt, P., J. Chem. Phys. 30, 879 (1959).
70. Wentink, T., Jr., Sullivanand, J., Wray, K. L., J. Chem. Phys. 29, 231 (1958).
71. Kelly, R., and Winkler, C. A., Can. J. Chem. 37, 62 (1959).
72. Back, R. A., and Winkler, C. A., Can. J. Chem. 37, 2059 (1959).
73. Evans, H. G. V., and Winkler, C. A., Can. J. Chem. 34, 1217 (1956).
74. Freeman, G. R., and Winkler, C. A., J. Phys. Chem. 59, 371 (1955).
75. Kistiakowsky, G. B., and Volpi, G. G., J. Chem. Phys. 28, 665 (1958).
76. Kaufman, F., and Kelso, J. R., J. Chem. Phys. 28, 510 (1958).
77. Verbeke, G. J. O., and Winkler C. A., J. Phys. Chem. 64, 319 (1960).
78. Nelson, R., Wright, N. A., and Winkler, C. A., presented at symposium "Some Fundamental Aspects of

Atomic Reactions" held at McGill University,
Sept. 6-7, 1960.

79. Greenblatt, J. H., and Winkler, C. A., Can. J. Res. B27, 721 (1949).
80. Greenblatt, J. H., and Winkler, C. A., Can. J. Res. B27, 732 (1949).
81. Evans, H. G. V., Freeman, G. R., and Winkler, C. A., Can. J. Chem. 34, 1271 (1956).
82. Wrede, E., Z. Physik 54, 53 (1929).
83. Versteeg, J., and Winkler, C. A., Can. J. Chem. 31, 1 (1953).
84. Versteeg, J., and Winkler, C. A., Can. J. Chem. 31, 129 (1953).
85. Trick, G. S., and Winkler, C. A., Can. J. Chem. 30, 915 (1952).
86. Gesser, H., Luner, C., and Winkler, C. A., Can. J. Chem. 31, 346 (1953).
87. Blades, H., and Winkler, C. A., Can. J. Chem. 29, 1022 (1951).
88. Gartaganis, P. A., and Winkler, C. A., Can. J. Chem. 34, 1457 (1956).
89. Onyszchuk, M., Breitman, L., and Winkler, C. A., Can. J. Chem. 32, 351 (1954).
90. Back, R., and Winkler, C. A., Can. J. Chem. 32, 718 (1954).
91. Onyszchuk, M., and Winkler, C. A., J. Phys. Chem. 59, 368 (1955).
92. Forst, W., Evans, H. G. V., and Winkler, C. A., J. Am. Chem. Soc. 61, 320 (1957).
93. Kelly, R., and Winkler, C. A., Thesis, McGill University 1958.
94. Wiles, D. M., and Winkler, C. A., J. Phys. Chem. 61, 902 (1957).
95. Ewart, R. H., and Rodebush, W. H., J. Am. Chem. Soc. 56, 97 (1934).
96. Wiles, D. M., and Winkler, C. A., Can. J. Chem. 35, 1298 (1957).
97. Dunford, H. B., and Melanson, B. E., Can. J. Chem. 37, 641 (1959).

98. Milton, E. R. V., and Dunford, H. B., *J. Chem. Phys.* 34, 51 (1961).
99. Spealman, M. L., and Rodebush, W. H., *J. Am. Chem. Soc.* 57, 1474 (1935).
100. Kistiakowsky, G. B., and Volpi, G. G., *J. Chem. Phys.* 27, 1141 (1957).
101. Kaufman, F., and Kelso, J. R., *J. Chem. Phys.* 27, 1209 (1957).
102. Harteck, P., and Dondes, S., *J. Chem. Phys.* 29, 234 (1958).
103. Clyne, M. A. A., and Thrush, B. A., *Nature* 189, 56 (1961); *Trans. Farad. Soc.* 57, 69 (1961); *Proc. Roy. Soc.* 261, 259 (1961).
104. McCourbey, J. C., and McGrath, W. D., *Quart Revs. (London)* 11, 87 (1957).
105. Lipscomb, F. J., Norrish, R. G. W., and Thrush, B. A., *Proc. Roy. Soc.* A233, 455 (1956).
106. Varney, R. N., *J. Chem. Phys.* 23, 866 (1955).
107. Kaufman, F., and Decker, L. J., *Seventh Symp. "Combustion Insitute"* 57 (Sept. 1958).
108. Harteck, P., and Dondes, S., *J. Chem. Phys.* 24, 619 (1956).
109. Kistiakowsky, G. B., *J. Am. Chem. Soc.* 52, 1868 (1930).
110. Cvetanovic, R., *J. Chem. Phys.* 23, 1203 (1955).
111. Ford, H. W., and Endow, N., *J. Chem. Phys.* 27, 1156 (1957).
112. Ford, H. W., and Endow, N., *J. Chem. Phys.* 27, 1277 (1957).
113. Schumacher, H. J., *Z. Physik Chem.* B10, 7 (1930).
114. Strutt, R. J., *Proc. Phys. Soc.* 23, 66, 147 (1910).
115. Strutt, R. J., *Proc. Roy. Soc. (London)* A85, 219 (1911).
116. Harteck, P., and Kopsch, V., *Z. Physik. Chem.* B12, 327 (1931).
117. McCarthy, R. L., *J. Chem. Phys.* 22, 1360 (1954).
118. Kurt, O. E., and Phipps, I. E., *Phys. Ev.* 34, 1357 (1929).

119. Rawson, E. B., and Beringer, R., Rev. 88, 677 (1952).
120. Rodebush, W. H., and Troxel, S. M., J. Am. Chem. Soc. 52,
3467 (1930).
121. Herron, J. T., and Schiff, H. I., Can. J. Chem. 36, 1159 (1958).
122. Kaplan, J., Nature, 159, 673 (1947).
123. Branscomb, L. M., Phys. Rev. 86, 258 (1952).
124. Broida, H. P., and Gaydon, A. G., Proc. Roy. Soc. (London)
A222, 181 (1954).
125. Foner, S. N., and Hudson, R. L., J. Chem. Phys. 25, 601 (1956).
126. Lennard-Jones, J. E., Trans. Farad. Soc. 25, 668 (1929).
127. Coulson, C. A., "Valence" Oxford University Press, reprint 1959.
128. Geib, K. H., and Harteck, P., Berl. 66, 1815 (1933).
129. Kaufman, F., Geeri, N. O., and Bowman, R. E., J. Chem. Phys.
25, 106 (1956).
130. Kaufman, F., J. Chem. Phys. 28, 352 (1958).
131. Ogryzlo, E., and Schiff, H. I., Can. J. Chem. 37, 1690 (1959).
132. Kistiakowsky, G. B., and Kydd, P. H., J. Am. Chem. Soc. 79,
4825 (1947).
133. Elias, L., Ogryzlo, E. A., and Schiff, H. I., Can. J. Chem.
37, 1680 (1959).
134. Benson, S. W., and Axworthy, A. E., J. Chem. Phys. 26, 1718 (1957).
135. Reeves, R., Mannella, G., and Harteck, P., J. Chem. Phys. 32,
632 (1960).
136. Matthews, D. L., Phys. Fluids 2, 170 (1959).
137. Morgan, J. E., Elias, L., and Schiff, H. I., J. Chem. Phys.
37, 1680 (1959).
138. Linnett, J. W., and Marsden, D. G. H., Proc. Roy. Soc. A234,
489 (1956).

139. Greaves, J. C., and Linnett, J. W., *Trans. Farad. Soc.* 54, 1323 (1958).
140. Barth, A., Schade, W. J., and Kaplan, J., *J. Chem. Phys.* 30, 347 (1959).
141. Reeves, R., Mannella, G., and Harteck, P., *J. Chem. Phys.* 32, 946 (1960).
142. Reeves, R., Mannella, G., and Harteck, P., *J. Chem. Phys.* 33, 636 (1960).
143. Langmuir, I., *J. Am. Chem. Soc.* 37, 417 (1915).
144. Wood, R. W., *Proc. Roy. Soc.* A102, 1 (1922).
145. Finch, G. I., *Proc. Phys. Soc. (London)* A62, 465 (1949).
146. Poole, H. G., *Proc. Roy. Soc.* A163, 415 (1937).
147. Dingle, J. R., and LeRoy, D. J., *J. Chem. Phys.* 18, 1632 (1950).
148. Wittke, J. P., and Dicke, R. H., *Phys. Rev.* 103, 602 (1956).
149. Shaw, T. M., *J. Chem. Phys.* 30, 1366 (1959).
150. Emeleus, K. G., Lunt, R. W., and Meek, C. A., *Proc. Roy. Soc.* A156, 394 (1936).
151. Lunt, R. W., and Meek, C. A., *Proc. Roy. Soc.* A157, 146 (1936).
152. Lunt, R. W., Meek, C. A., and Smith, E. C. W., *Proc. Roy. Soc.* A158, 729 (1937).
153. Smallwood, H. M., *J. Am. Chem. Soc.* 51, 1985 (1929).
154. Senftleben and Riechemair., *Ann. Physik* 6, 105 (1930).
155. Steiner, W., and Wicke, F. W., *Z. Physik Chem. Bodenstein Band*, 817 (1931).
156. Steiner, W., and Wicke, F. W., *T. F. S.* 31, 623 (1935).
157. Amdur, I., *Phys. Rev.* 43, 208 (1933).
158. Amdur, I., and Robinson A. L., *J. Am. Chem. Soc.* 55, 1935 (1933).

159. Amdur, I., J. Am. Chem. Soc. 60, 2347 (1938).
160. Smith, W. V., J. Chem. Phys. 11, 110 (1943).
161. Schuler, K. W., and Laidler, K. J., J. Chem. Phys. 17,
1212 (1949).
162. Dingle, J. R., and LeRoy, D. J., J. Chem. Phys. 18,
1632 (1950).
163. Foner, S. N., and Hudson, R. L., J. Chem. Phys. 21, 1608
(1953); 23, 1364 (1955).
164. Robertson, J. B., Applied Mass Spectroscopy (Institute of
Petroleum, London, England, 1954), p. 112
165. Cashion, J. K., and Polanyi, J. C., J. Chem. Phys. 30,
315 (1959).
166. Charters, P. E., and Polanyi, J. C., presented at the
symposium "Some

Sept. 6-7, 1960.
167. Cashion, J. K., and Polanyi, J. C., J. Chem. Phys. 30,
317 (1959).
168. Hoare, D. E., and Walsh, A. D., T. F. S. 53, 1102 (1957).
169. Rosser, W. A., and Wise, H., J. Chem. Phys. 26, 571 (1957).
170. Rosser, W. A. Jr., and Wise, H., J. Phys. Chem. 65, 532 (1961).
171. Lewis, B., J. Am. Chem. Soc. 50, 27 (1928).
172. Steiner, W., Z. Elektrochem. 36, 807 (1930).
173. Dixon, J. X., and Steiner, W., Z. physik. Chem. B14, 397
(1931); B17, 327 (1932).
174. Rice, F. O., and Frearno, M., J. Am. Chem. Soc. 73, 5529 (1951).
175. Rice, F. O., and Frearno, M., J. Am. Chem. Soc. 75, 548 (1953).
176. Mador, I. L., and Williams, M. C., J. Chem. Phys. 22,
1267 (1954).

177. Becker, E. D., Pimentel, G. C., and Van Thiel, M., J. Chem. Soc. 26, 145 (1957).
178. Foner, S. N., and Hudson, R. L., J. Chem. Phys. 28, 719 (1958); 29, 442 (1958).
179. Ruehrwein, R. A., Hashman, J. S., and Edwards, J. W., Reference 6.
180. Robinson, G. W., and McCarty, M. Jr., Chem. Phys 28, 349 (1958); 28, 350 (1958).
181. Robinson, G. W., and McCarty, M. Jr., J. Chem. Phys. 30, 999 (1959).
182. Mulliken, R. S., Rev. Mod. Phys. 4, 1 (1932).
183. Kolthoff, I. M., and Sandel, E. B., "Textbook of Quantitative Inorganic Analysis", 3rd ed. McMillan, New York (1952).
184. De More, W. B., and Davidson, N., J. Am. Chem. Soc. 81, 5869 (1959).
185. Young, R. A., and Clark, K. C., J. Chem. Phys. 32, 606 (1960).
186. Pauling, L., J. Am. Chem. Soc. 53, 3225 (1931).
187. Walsh, A. D., J. Chem. Soc. 2266 (1953).
188. Magee, J. L., J. Chem. Phys. 8, 687 (1940).
189. Hirschfelder, J. O., and Wigner, E., J. Chem. Phys. 7, 616 (1939).
190. Arakawa, E. T., and Nielsen, A. H., J. of Mol. Spectr. 2, 413 (1958).
191. Keller, F. L., J. Chem. Phys. 24, 636 (1956).
192. Eyring, H., Gershinowitz, H., and Sun, C. E., J. Chem. Phys. 3, 786 (1935).
193. Laidler, K. J., and Schuler, K. E., Chem. Revs. 48, 153 (1951).
194. Smith, F. T., J. Chem. Phys. 31, 1352 (1959).
195. Laidler, K. J., J. Phys. Chem. 53, 712 (1949).
196. Harteck, P., Reeves, R. R., and Mannella, G. G., AFCRC-TR 60-264 (1960).

197. Barth, A., to be published
198. Thrush, B. A., Proc. Roy. Soc. A235, 143 (1956).
199. Wiles, D., Thesis, McGill University, 1957.
200. Morris, J. C., and Pease, R. N., J. Chem. Phys. 3, 796 (1935).
201. Williams, R. R. Jr., and Ogg, R. A., Jr., J. Chem. Phys.
15, 691 (1947).
202. Bodenstein, M., and Jung, Zeits. f. physik Chemie 121, 127 (1926).
203. Steiner, W., Proc. Roy. Soc. (London) A173, 531 (1939).
204. Freeman, G. R., and Winkler, C. A., Can. J. Chem. 33, 692 (1955).
205. Cottrell, T. L., "The Strengths of Chemical Bonds" second
edition, Butterworths Scientific Pub., 1958.
206. Altshuller, A. P., J. Chem. Phys. 22, 1947 (1954).
207. Szwarc, M., Chem. Revs., 47, 75 (1950).
208. Wigner, E., J. Chem. Phys. 5, 720 (1937); 7, 646 (1939);
T. F. S. 34, 29 (1938).
209. Hulburt, H. M., and Hirschfelder, J. O., J. Chem. Phys. 9, 61 (1941).
210. Vanderslice, J. T., Mason, E. A., and Maisch, W. G., J. Chem.
Phys. 31, 738 (1959).
211. Landolt-Bornsteins Tables 1st Ergänzungsband p. 69.
212. Keck, J. C., J. Chem. Phys. 29, 410 (1958).
213. Keck, J. C., Research Report 66, 1959.